

Deflections of Reinforced Concrete Flat Slabs

Estée M. Eigelaar



Thesis presented in partial fulfilment of the requirements for the
degree of Masters of Science of Engineering at
the Stellenbosch University

Supervisor: Professor J.A. Wium

Date of Award: March 2010

DECLARATION

By submitting this thesis electronically, I declare that the entirety of the work contained therein in my own, original work, that I am the owner of the copyright thereof (unless to the extent explicitly otherwise stated) and that I have not previously in this entirety or in part submits it for obtaining any qualification.

Date:

Signature:

SYNOPSIS

It is found that the serviceability limit state often governs the design of slender reinforced concrete members. Slender flexural members often have a percentage tension reinforcement less than 1.0% and an applied bending moment just above the point of first cracking. For such members, the available methods to evaluate the serviceability conditions produce inadequate and unrealistic results. The evaluation of the serviceability of a slender member includes the calculation of the predicted deflection, either by empirical hand-calculation or analysing a finite element model, and the verification using the span-to-effective-depth ratio.

The focus of the study is on flat slab structures. It investigates the different deflection prediction methods and the span-to-effective-depth ratio verifications from various design standards. These design standards include the ACI 318 (2002), the SABS 0100-1 (2000), the EC2 (2004) and the BS 8110 (1997). The background to the methods, as well as the parameters which influences the deflection development for lightly reinforced members, are investigated in order to define the limitations of the methods. As a result of the investigation of the deflection calculation methods, an Alternative Approach is suggested and included in the comparisons of the various methods.

The deflection prediction methods and the span/effective depth verification procedures are accurately formulated to predict the serviceability behaviour of beams. Additional approaches had to be used to apply these methods to a two-dimensional plane such as that of a flat slab structure.

The different deflection prediction methods and the span/effective depth verification methods are calculated and compared to the recorded data of seven experimental flat slab specimens as performed by others. A study by Gilbert and Guo (2005) accurately recorded the flexural behaviour of flat slab specimens under uniformly distributed loads for test periods up to 750 days. The methods to evaluate the serviceability of a slender member were also applied to slab examples designed using South African standards.

The study concludes by suggesting a suitable deflection prediction method for different parameter (limitation) categories with which a slender member can comply to. The typical span/effective depth ratio trend is also presented as the percentage tension reinforcement for a slender member

changes. It is observed that the empirical hand-calculation methods present more reliable results than those of the finite element models. The empirical hand-calculation methods are accurate depending on the precision to which the slab was constructed relative to the actual slab design.

The comparison of the deflection methods with South African case studies identified the role played by construction procedures, material parameters and loading history on slab behaviour.

SINOPSIS

Die diensbaarheidstoestand is in baie gevalle die bepalende factor vir die ontwerp van slank gewapende beton elemente bepaal. Slank elemente, soos lig bewapende buigbare beton elemente, het gewoonlik 'n persentasie trekbewapening van minder as 1.0% en 'n aangewende buigmoment net wat net groter is as die punt waar kinking voorkom. Die metodes beskikbaar om die diensbaarheid van sulke elemente te evalueer gee onvoldoende en onrealistiese resultate. Die evaluering van die elemente in die diensbaarheidstoestand sluit in die bepaling van defleksies deur berekening of die analyse van 'n eindige element model, en die gebruik van die span/effektiewe diepte metode.

Die fokus van die studie is platbladstrukture. Die doel van die studie is om die verskillende metodes vir die berekening van defleksie asook die verifikasie volgens span/effektiewe diepte metodes van die verskillende ontwerp standaarde te ondersoek. Die ontwerp standaarde sluit die ACI 318 (2002), SABS 0100-1 (2000), EC2 (2004) en die BS 8110 (1997) in. Die agtergrond van hierdie metodes is ondersoek asook die parameters wat 'n rol speel, sodat die beperkings van die metodes geïdentifiseer kan word. As 'n gevolg van die ondersoek na die beperkings van die metodes, is 'n Alternatiewe Benadering voorgestel. Die Alternatiewe Benadering is saam met die metodes van die ontwerpstandaarde gebruik om die verskille tussen die metodes te evalueer.

Die defleksievoorspelling en die span/effektiewe diepte verifikasie metodes is korrek geformuleer om die diensbaarheid van balke te evalueer. Ander benaderings was nodig om die diensbaarheid van blad blaai te toets.

Die onderskeie defleksievoorspelling en span/effektiewe diepte metodes is bereken vir sewe eksperimentele plat blaai soos uitgevoer deur ander navorsers. Gilbert and Guo (2005) het 'n studie uitgevoer waar die buigingsgedrag van die sewe plat blaai, met 'n uniforme verspreide las vir 'n toetsperiode van tot 750 dae, akkuraat genoteer is. Die metodes om die diensbaarheid van 'n slank element te toets, was ook op Suid-Afrikaanse blad voorbeelde getoets. Dit was gedoen om die Suid-Afrikaanse ontwerp van ligte bewapende beton elemente te evalueer.

Die gevolgetrekkings stel 'n gepaste defleksie metode vir 'n slank element vir verskillende beperking kategorië voor. Dit is ook verduidelik hoe die tipiese span/effektiewe diepte verhouding met die persentasie trek bewapening vir 'n slank element verander. Dit is bevind dat die imperiese handmetodes om defleksies te bereken, meer betroubaar as die eindige element modelle se resultate is. Die imperiese handberekening metodes is akkuraat relatief tot hoe akkuraat die blad konstruksie tot die blad ontwerp voltooi is.

'n Vergelyking van defleksieberekening met Suid-Afrikaanse gevallestudies het die belangrikheid van konstruksieprosedures, materiaalparamteres and belastingsgeskiedenis geïdentifiseer.

ACKNOWLEDGEMENTS

It was an absolute pleasure to conduct this study. Thank you to all who have supported me through the process.

Thank you to my supervisor, Professor J.A. Wium, for all the endurance and encouraging words. I will always appreciate his inspiration and patience and it was a privilege to have studied under his guidance.

Thank you to our Holy Father for blessing me through this journey. Through Him all things are possible.

NOTATION

$(L/d)_{\text{ACTUAL}}$	-	actual span/effective depth ratio calculated from the dimensions of the flexural member;
$(L/d)_{\text{ALLOWABLE}}$	-	calculated allowable span/effective depth ratio which provides the lower limit of the actual span/effective depth ratio;
Δ_a	-	deflection due to service loads;
Δ_{cp}	-	deflection due to creep;
Δ_{cr}	-	deflection at first cracking;
Δ_{cs}	-	deflection due to shrinkage;
Δ_i	-	short-term (initial) deflection;
$\Delta_{i,\text{add}}$	-	additional deflection due to the additional imposed load not sustained throughout the structure life;
Δ_l	-	long-term deflection;
ΔM	-	change in moment due to the effect of tension stiffening;
Δ_t	-	total (final) deflection for a flexural member at the end the structure life consisting of the sum of the long-term and the shrinkage deflections;
$1/r$	-	curvature of a flexural member at midspan;
$1/r_{cp}$	-	curvature due to creep for a flexural member;
$1/r_{cs}$	-	curvature due to shrinkage for a flexural member;
$1/r_i$	-	initial elastic curvature for a flexural member;
$1/r_{in}$	-	instantaneous curvature due to the non-permanent load;
$1/r_{ip}$	-	instantaneous curvature due to the permanent load;
$1/r_{it}$	-	instantaneous curvature due to the total load;
$1/r_l$	-	long-term curvature;
$1/r_{lp}$	-	long-term curvature due to the permanent load;
A'_s	-	area of compression reinforcement at a Section in a beam;
$A'_{s,\text{prov}}$	-	area compression reinforcing steel provided for the section to resist the moment due to the ultimate loads;

A_c	-	area of concrete at a section in a beam;
A_s	-	area of tension reinforcement at a section in a beam;
$A_{s,prov}$	-	area tension reinforcing steel provided for the Section to resist the moment due to the ultimate loads;
$A_{s,req}$	-	area tension reinforcing steel required for the section to resist the moment due to the ultimate loads;
b	-	width of a section;
b_w	-	web width of a flanged section;
$cov(X,Y)$	-	covariance between random variables X and Y;
COV_A	-	covariance of the %diff of the I_e including the data from all the design standards;
COV_S	-	covariance of the %diff of the I_e including the data from the SABS 0100-1 (2000) and the EC2 (2004);
C_t	-	creep coefficient which is the ratio of the creep strain, ϵ_{cp} to the initial elastic strain, ϵ_i of concrete;
d	-	depth from the compression edge of the section to the centre of the steel reinforcement in tension;
d'	-	the depth from the compression edge of the section to the middle of the steel reinforcement in compression;
E_c	-	modulus of elasticity of concrete;
E_{cr}	-	cracked modulus of elasticity;
E_{eff}	-	effective modulus of elasticity of concrete which is a property dependent on the ultimate creep coefficient, Φ .
E_s	-	modulus of elasticity of reinforcing steel;
f'_c	-	cylinder concrete strength;
f'_s	-	compression strength of reinforcing steel;
f_c	-	cube concrete strength;
f_r	-	tensile strength of concrete obtained from the flexural test known as the modulus of rupture;
f_{re}	-	effective tensile strength of modulus of rupture;

f_{res}	-	concrete tensile strength induced at the extreme tensile strength of concrete due to the shrinkage restraint;
f_s	-	tensile strength of reinforcing steel;
f_t	-	concrete tensile strength;
$f_{t,c}$	-	tensile strength of concrete obtained from the splitting test;
f_{tfl}	-	flexural tensile strength of concrete (similar to the modulus of rupture, f_r);
f_y	-	yield strength of the reinforcing steel;
G	-	shear modulus of concrete;
h	-	height of the section;
h_0	-	ratio of twice the concrete area relative to the perimeter of the part of the cross-section which is exposed to drying;
I_{cr}	-	moment of inertia or second moment of area of a cracked (equivalent) section;
I_e	-	effective moment of inertia of a section;
I_{e1}, I_{e2}	-	effective moment of inertia for a flexural member at the first and second support, respectively;
I_{ea}	-	average effective moment of inertia for a continuous flexural member;
I_{em}	-	effective moment of inertia for a flexural member at midspan;
I_g	-	the moment of inertia or second moment of area of the gross section;
I_u	-	moment of inertia or second moment of area of the uncracked section;
K	-	deflection coefficient dependent on the bending moment diagram for a flexural member;
k_{cr}	-	spring stiffness for the cracked condition;
k_{cs}	-	factor used to determine the shrinkage deflection, Δ_{cs} according to the SABS 0100-1 (2000);
k_e	-	equivalent (effective) spring stiffness for the partially cracked

		condition;
k_g	-	spring stiffness for the uncracked condition;
k_h	-	coefficient depending on the notional size h_0 ;
k_r	-	ratio of initial neutral axis depth, x_i to the neutral axis depth due to creep, x_{cp} ;
K_{sh}	-	shrinkage deflection coefficient dependent on the shrinkage curvature shape;
L	-	span of a member between support centres;
L_n	-	clear span of a member measured face-to-face from the supports in a slab without beams and face-to-face of the beams or other supports in other cases.
M'_{cr}	-	reduced cracking moment due the shrinkage restraint;
M_a	-	moment applied at the Section part of the flexural member due to the service loads;
M_{cr}	-	cracking moment indicating the point of first cracking in a flexural member;
M_p	-	moment due to permanent (sustained) load;
M_r	-	resisting moment;
S_{cr}	-	first moment of area of the reinforcement about the centroid of the cracked section;
S_u	-	first moment of area of the reinforcement about the centroid of the uncracked section;
x	-	distance from the neutral axis to the extreme fibre in compression of a section part of a beam in flexure;
X, Y	-	series of random variables denoted as X and Y;
x_{cp}	-	neutral axis depth due to the effects of creep;
x_{cr}	-	the distance of the neutral axis of the cracked section to the edge in compression;
x_g	-	the centreline through the height of a section;
x_i	-	initial neutral axis depth;

x_u	-	the distance of the neutral axis of the uncracked section to the edge in compression;
y_t	-	distance from the centroidal axis of the concrete section to the extreme fibre in tension;
α	-	deformation parameter and may be strain, curvature or rotation;
α_e	-	modular ratio expressed as the ratio of the modulus of elasticity of steel, E_s to the modulus of elasticity of concrete, E_c ;
α_i, α_{ii}	-	deformation parameter calculated for the uncracked and cracked conditions, respectively;
α_{load}	-	average load factor;
β	-	coefficient accounting for the loss in tension stiffening for the duration of loading or repeated loading;
$\beta_{as}(t)$	-	autogenous shrinkage time coefficient dependent on the age of concrete in days;
β_b	-	ratio of resistance moment at midspan obtained from redistributed maximum moment diagram to that obtained from the maximum moment diagram before redistribution;
$\beta_{ds}(t, t_s)$	-	drying shrinkage time coefficient dependent on the age of the concrete in days;
ϵ'_s	-	steel strain in reinforcement due to compression;
ϵ_c	-	strain of concrete in compression;
ϵ_{ca}	-	autogenous strain of concrete;
$\epsilon_{ca}(\infty)$	-	infinite autogenous strain of concrete dependent on the concrete strength ;
$\epsilon_{ca}(t)$	-	time-dependent autogenous strain of concrete;
ϵ_{cd}	-	drying shrinkage strain of concrete;
$\epsilon_{cd,0}$	-	unrestraint drying shrinkage of concrete;
ϵ_{cp}	-	creep strain of concrete;
ϵ_{cs}	-	free shrinkage strain of concrete;
ϵ_i	-	initial elastic strain of concrete;

ϵ_s	-	steel strain in the reinforcement due to tension;
ζ	-	distribution coefficient allowing for tension stiffening;
η	-	tension stiffening factor;
θ	-	slope of the tangent to a curve;
λ	-	long-term factor used to determine the long-term deflection, Δ_l , according to the SABS 0100-1 (2000);
μ_x, μ_y	-	sum of the values in each series in data set X and Y, respectively;
ρ	-	ratio of tension reinforcement provided relative to the area of the concrete at a section, to resist the moment due to the ultimate (design) loads;
ρ'	-	ratio of compression reinforcement provided relative to the area of the concrete at a section, to resist the moment due to the ultimate (design) loads;
ρ_0	-	reference reinforcement ratio;
σ_i	-	stress induced by permanent (sustained) load;
ν	-	Poisson's Ratio;
Φ	-	ultimate creep coefficient;
Φ'	-	creep factor considering the effect of compression reinforcement;

TABLE OF CONTENTS

DECLARATION	II
SYNOPSIS	III
SINOPSIS	V
ACKNOWLEDGEMENTS	VII
NOTATION	VIII
TABLE OF CONTENTS	XIV
LIST OF ILLUSTRATIONS	XVII
LIST OF TABLES	XX
1 INTRODUCTION	1-1
1.1 IMPORTANCE OF DEFLECTION PREDICTION FOR REINFORCED CONCRETE FLAT SLAB STRUCTURES.....	1-1
1.2 CURRENT LIMITATIONS ON AVAILABLE DEFLECTION CALCULATION METHODS.....	1-2
1.3 PURPOSE OF INVESTIGATION.....	1-3
1.4 OVERVIEW OF CONTENTS OF THE INVESTIGATION.....	1-4
2 FLAT SLAB DESIGN FOR THE SERVICEABILITY LIMIT STATE	2-8
2.1 INTRODUCTION.....	2-8
2.2 FACTORS INFLUENCING REINFORCED FLAT SLAB DEFLECTIONS.....	2-9
2.2.1 <i>Material Properties</i>	2-9
2.2.2 <i>Intrinsic Parameters: Reinforced Flat Slab Behaviour</i>	2-30
2.2.3 <i>Extrinsic Parameters: Loading History and Construction Methods</i>	2-37
2.2.4 <i>Deflection Derivation from Moment–Curvature Theorem</i>	2-40
2.2.5 <i>Boundary Conditions and Deflection Coefficients</i>	2-40
2.2.6 <i>Time-Dependent Deflections</i>	2-42
2.3 DEFLECTION PREDICTION ACCORDING TO THE DESIGN STANDARDS.....	2-46
2.3.1 <i>Deflection Prediction according to the American Concrete Institute (ACI) 318-02</i>	2-46
2.3.2 <i>Deflection Prediction according to the British Standards (BS) 8110: Part 2: 1997</i>	2-51
2.3.3 <i>Deflection Prediction according to the Eurocode 2: Part 1-1</i>	2-56
2.3.4 <i>Deflection Prediction according to the South African Bureau of Standards (SABS) 0100-1</i>	2-62
2.4 SPAN/EFFECTIVE DEPTH RATIO ACCORDING TO DESIGN STANDARDS.....	2-65
2.4.1 <i>Span/Depth Ratio according to the American Concrete Institute (ACI) 318-02</i>	2-66
2.4.2 <i>Span/Depth Ratio according to the British Standards (BS) 8110: Part 2: 1997</i>	2-68

2.4.3	<i>Span/Depth Ratio according to the Eurocode 2: Part 1-1</i>	2-71
2.4.4	<i>Span/Depth Ratio according to the South African Bureau of Standards (SABS) 0100-1</i>	2-74
2.5	METHOD FOR PREDICTING FLAT SLAB DEFLECTIONS: EQUIVALENT FRAME METHOD	2-77
2.6	CONCLUDING SUMMARY	2-80
3	DEFLECTION PREDICTION FOR LIGHTLY REINFORCED CONCRETE SLABS	3-1
3.1	INTRODUCTION.....	3-1
3.2	COMPARISON OF THE EMPIRICAL METHODS FOR SERVICEABILITY EVALUATION.....	3-1
3.2.1	<i>Deflection Prediction Comparison for the Design standard Methods</i>	3-2
3.2.2	<i>Span/Depth Ratio Comparison for the Design standard Methods</i>	3-6
3.3	RELEVANCE OF CRACK DEVELOPMENT AND TENSION STIFFENING	3-10
3.4	INFLUENCE OF PERCENTAGE REINFORCEMENT AND STIFFENING RATIO ON DEFLECTION PREDICTION	3-22
3.5	INFLUENCE OF APPLIED MOMENT TO CRACKING MOMENT RATIO ON DEFLECTION PREDICTION	3-26
3.6	INFLUENCE OF THE GROSS AND UNCRACKED MOMENT OF INERTIA ON DEFLECTION PREDICTION	3-34
3.7	EFFECT OF PATTERN LOADING ON THE FLAT SLABS.....	3-35
3.8	ALTERNATIVE APPROACH TO DEFLECTION CALCULATIONS	3-35
3.9	CONCLUDING SUMMARY	3-40
4	MODELLING APPROACH	4-1
4.1	INTRODUCTION.....	4-1
4.2	MODELLING OF CONCRETE MATERIAL PROPERTIES	4-1
4.3	NONLINEAR MODEL FOR A REINFORCED FLAT SLAB	4-5
4.4	LINEAR MODEL FOR A REINFORCED FLAT SLAB	4-6
4.5	FINAL FINITE ELEMENT MODEL.....	4-10
4.6	CONCLUDING SUMMARY	4-13
5	EXPERIMENTAL TEST SIMULATION	5-1
5.1	INTRODUCTION.....	5-1
5.2	DISCUSSION ON RECORDED EXPERIMENTAL DATA	5-2
5.2.1	<i>Gilbert and Guo's (2005) Experimental Program</i>	5-2
5.3	SIMULATED FINITE ELEMENT MODEL	5-9
5.3.1	<i>Finite Element Model Example: S3</i>	5-10
5.4	PREDICTED DEFLECTION FROM EMPIRICAL AND FINITE ELEMENT MODELS.....	5-18
5.4.1	<i>Empirical Model for Deflection Prediction: Cumulative Crack Development</i>	5-18
5.4.2	<i>Finite Element Model for Deflection Prediction: Cumulative Crack Development</i>	5-20
5.4.3	<i>Deflection Prediction for Experimental Slabs</i>	5-21
5.4.4	<i>Concluding Summary</i>	5-47
5.5	ALLOWABLE SPAN/DEPTH RATIOS FOR EXPERIMENTAL SLABS.....	5-51
5.5.1	<i>Calculated Span/Depth Ratios</i>	5-51

5.6	CONCLUDING SUMMARY	5-54
6	SERVICEABILITY OF SOUTH AFRICAN FLAT SLAB DESIGN	6-1
6.1	INTRODUCTION	6-1
6.2	CURRENT SOUTH AFRICAN FLAT SLAB SERVICEABILITY METHODS	6-1
6.3	FLAT SLAB CASE STUDIES FROM PRACTICE.....	6-2
6.3.1	<i>Example 1: Parking Deck Two-Way Spanning Slab.....</i>	<i>6-2</i>
6.3.2	<i>Example 2: Office Block Two-Way Spanning Slabs</i>	<i>6-7</i>
6.3.3	<i>Example 3: Maritz One-Way Spanning Slabs.....</i>	<i>6-14</i>
6.4	IMPLICATIONS OF THE PREDICTION OF FLAT SLAB DEFLECTIONS ON SOUTH AFRICAN DESIGN	6-19
6.5	CONCLUDING SUMMARY	6-20
7	SUMMARY, CONCLUSIONS AND RECOMMENDATIONS	7-1
7.1	SUMMARY	7-1
7.1.1	<i>Modelling Approach for Predicting Deflections</i>	<i>7-1</i>
7.1.2	<i>Linear Finite Element Model for Flat Slab Serviceability Design</i>	<i>7-2</i>
7.1.3	<i>Methods Available for Predicting Deflections.....</i>	<i>7-3</i>
7.1.4	<i>Methods Available for Calculating Span/Depth Ratios.....</i>	<i>7-4</i>
7.2	CONCLUSIONS	7-5
7.2.1	<i>Different Deflection Prediction Methods Available.....</i>	<i>7-5</i>
7.2.2	<i>Adequacy of the Deflection Prediction Methods for a South African design office</i>	<i>7-6</i>
7.3	RECOMMENDATIONS	7-7
8	REFERENCES	8-1

LIST OF ILLUSTRATIONS

FIGURE 1-1: FLOWCHART OF THE ASPECTS CONSIDERED IN THIS STUDY.....	1-7
FIGURE 2-1: THE REINFORCED CONCRETE SECTION (KONG AND EVANS, 1987).....	2-10
FIGURE 2-2: THE CRACKED REINFORCED CONCRETE SECTION (KONG AND EVANS, 1987).....	2-12
FIGURE 2-3: THE UNCRACKED REINFORCED CONCRETE SECTION (KONG AND EVANS, 1987).....	2-13
FIGURE 2-4: THE PARTIALLY CRACKED REINFORCED CONCRETE SECTION (KONG AND EVANS, 1987).....	2-14
FIGURE 2-5: CREEP CURVATURE IN A FLEXURAL MEMBER (PILLAI AND MENON, 2004).....	2-18
FIGURE 2-6: EFFECTIVE MODULUS OF ELASTICITY UNDER CREEP (PILLAI AND MENON, 2003).....	2-20
FIGURE 2-7: EFFECT OF SHRINKAGE ON FLEXURAL DEFORMATION (DIVAKAR & DILGER, 1988).....	2-23
FIGURE 2-8: THE RELATIONSHIP BETWEEN DIRECT AND INDIRECT TENSILE STRENGTH MEASUREMENTS AND COMPRESSIVE STRENGTH (ILLSTON & DOMONE, 2001)(ROBBERTS & MARSHALL, 2008).....	2-28
FIGURE 2-9: INTERNAL CRACKS AS ESTABLISHED BY GOTO (1971).....	2-32
FIGURE 2-10: DEVELOPMENT OF RESTRAINT STRESSES IN A BEAM (SCANLON & BISCHOFF, 2008).....	2-34
FIGURE 2-11: DEVELOPMENT OF A TYPICAL LOADING HISTORY AND DEFLECTION PREDICTION METHOD TAKING THE LOAD HISTORY INTO ACCOUNT (SCANLON & BISCHOFF, 2008).....	2-38
FIGURE 2-12: LOAD DEFLECTION DIAGRAM (S-CURVE) OF A BEAM (VARGHESE, 2005).....	2-42
FIGURE 2-13: LONG-TERM DEFLECTION OF ACTUAL STRUCTURE ACCORDING TO HEIMAN AND TAYLOR (1977).....	2-44
FIGURE 2-14: ASSUMED SHRINKAGE CURVATURE FOR EMPIRICAL METHODS (BRANSON, 1977).....	2-48
FIGURE 2-15: EFFECT OF TENSION IN CONCRETE ON DEFLECTION ON BEAMS (BS 8110, 1997).....	2-52
FIGURE 2-16: DEFLECTION DUE TO SHRINKAGE (BS 8110, 1997)(KONG & EVANS, 1987).....	2-53
FIGURE 2-17: DEFLECTION OF SLABS: Δ_{Bx} AND Δ_{By} ARE DEFLECTIONS OF MIDDLE STRIPS IN X AND Y DIRECTIONS, RESPECTIVELY (VARGHESE, 2005).....	2-78
FIGURE 3-1: GRAPHICAL COMPARISON OF THE INITIAL CURVATURES FOR THE DESIGN STANDARDS WITH $P = 0.842\%$	3-4
FIGURE 3-2: GRAPHICAL COMPARISON OF THE INITIAL CURVATURES FOR THE DESIGN STANDARDS WITH $P = 0.485\%$	3-4
FIGURE 3-3: GRAPHICAL COMPARISON OF THE INITIAL CURVATURES FOR THE DESIGN STANDARDS WITH $P = 0.203\%$	3-5
FIGURE 3-4: ALLOWABLE SPAN/DEPTH RATIOS FOR THE VARIOUS DESIGN STANDARDS FOR SLAB 1.....	3-8
FIGURE 3-5: ALLOWABLE SPAN/DEPTH RATIOS FOR THE VARIOUS DESIGN STANDARDS FOR SLAB 2.....	3-9
FIGURE 3-6: VARIOUS REGIONS OF STRESS AND CRACKING IN A REINFORCED CONCRETE BEAM CARRYING SERVICE LOADS (BRANSON, 1977).....	3-11
FIGURE 3-7: LIMITING EFFECTIVE SECTIONS FOR A CONTINUOUS BEAM (BRANSON, 1977).....	3-11
FIGURE 3-8: EXPERIMENTAL MOMENT-DEFLECTION CURVE FOR BEAM WITH 0.93 % REINFORCEMENT COMPARED WITH THEORETICAL MOMENT-DEFLECTION CURVES (BRANSON, 1977).....	3-13
FIGURE 3-9: GENERALIZED EFFECTIVE MOMENT OF INERTIA VERSUS BENDING MOMENT RELATION IN THE CRACKING RANGE – I_e/I_g VERSUS M_a/M_{cr} CURVES FOR DIFFERENT VALUES OF I_g/I_{cr} AS COMPUTED BY EQUATION 3-2 (BRANSON, 1977).....	3-14
FIGURE 3-10: EQUIVALENT SPRING MODEL FOR BRANSON’S AND BISCHOFF’S EXPRESSIONS (BISCHOFF, 2007).....	3-16

FIGURE 3-11: THEORETICAL MOMENT CURVATURE RESPONSE AT THE CRITICAL SECTION USING EQUATION 3-5 WITH DIFFERENT TENSION STIFFENING VALUES (BISCHOFF, 2008).	3-17
FIGURE 3-12: DEFLECTION COMPARISON USING BRANSON'S AND BISCHOFF'S EXPRESSIONS FOR I_e (BISCHOFF, 2007).	3-18
FIGURE 3-13: DEGREE OF CRACKING RELATIVE TO VARIOUS PERCENTAGES OF TENSION REINFORCEMENT FOR A SPECIFIC SECTION.	3-23
FIGURE 3-14: STIFFNESS RATIO VERSUS PERCENTAGE TENSION REINFORCEMENT BASED ON THE SECTION DESCRIBED IN TABLE 3-5.	3-24
FIGURE 3-15: MEMBER CURVATURE RESPONSE AT A PERCENTAGE TENSION REINFORCEMENT OF 0.203%.	3-26
FIGURE 3-16: %DIFF VERSUS M_n/M_{cr} FOR A SECTION AT A PERCENTAGE TENSION REINFORCEMENT OF 1.1%.	3-28
FIGURE 3-17: COVARIANCE PEAKS FROM TABLE 3.8.	3-33
FIGURE 3-18: COMPARISON OF I_{cr}/I_u AND I_{cr}/I_g FOR A SECTION AS THE PERCENTAGE TENSION REINFORCEMENT INCREASE.	3-34
FIGURE 4-1: CQ40L LAYERED SHELL ELEMENT AS SUGGESTED BY BAILEY, TOH AND CHAN (2008).	4-2
FIGURE 4-2: MATERIAL STRESS-STRAIN CURVES FOR BOTH THE (A) CONCRETE AND THE (B) REINFORCEMENT (MAADDAWY, SOUDKI AND TOPPER, 2005).	4-3
FIGURE 4-3: THREE-DIMENSIONAL REPRESENTATION OF A COMPOSITE LAYERED ELEMENT FOR A CONTINUOUS BEAM SECTION (STRAND 7, 2005).	4-5
FIGURE 4-4: PROPERTIES FOR EVERY LAYER DEPENDING ON WHETHER THE LAYER IS CONCRETE (QUASI-ISOTROPIC) OR REINFORCEMENT (UNIDIRECTIONAL) (STRAND 7, 2005).	4-5
FIGURE 4-5: APPROXIMATION FOR THE CRACKED MODULUS OF ELASTICITY FOR BEAMS IN FLEXURE (ROBERTS AND MARSHALL, 2008).	4-8
FIGURE 4-6: THREE-DIMENSIONAL FLAT SLAB MODEL WITH ALLOCATED AREAS WHERE THE E_{cr} IS APPLIED.	4-9
FIGURE 4-7: RIGID LINKS BETWEEN BEAMS AND SLAB ELEMENTS.	4-11
FIGURE 4-8: EXAMPLE OF AREAS FOR A CRACKED MODULUS OF ELASTICITY FOR A SLAB.	4-12
FIGURE 5-1: PLAN OF EACH SLAB AND DIAL GAUGE LOCATIONS (NO. 1 TO 16) (GILBERT AND GUO, 2005).	5-2
FIGURE 5-2: SLAB REINFORCEMENT SHOWN IN PLAN FOR SLAB SPECIMENS (GILBERT AND GUO, 2005).	5-6
FIGURE 5-3: SLAB AND COLUMN SECTION 1-1 FOR SLAB SPECIMENS (GILBERT AND GUO, 2005).	5-6
FIGURE 5-4: LOADING HISTORY FOR SLAB S3 (GILBERT AND GUO, 2005).	5-11
FIGURE 5-5: COLUMN AND MIDDLE STRIPS FOR SLAB S3 (GILBERT AND GUO, 2005).	5-12
FIGURE 5-6: ALLOCATING AREAS OF CRACKING ON THE SLAB BY COMPARING THE CRACKING MOMENT, M_{cr} TO THE MOMENT ALONG ..	5-13
FIGURE 5-7: CRACKED FINITE ELEMENT MODEL FOR SLAB S3: PREDICTED CRACK PATTERN.	5-14
FIGURE 5-8: OBSERVED CRACK PATTERN FOR TOP SLAB SURFACE FOR SLAB S3 (GILBERT AND GUO, 2005).	5-14
FIGURE 5-9: VISUAL COMPARISON FOR THE UNCRACKED AND CRACKED FINITE ELEMENT MODELS FOR SLAB S3.	5-16
FIGURE 5-10: ACTUAL AND MATHEMATICAL DEFLECTION BEHAVIOUR.	5-19
FIGURE 5-11: LOADING HISTORY FOR SLAB S1 (GILBERT AND GUO, 2005).	5-22
FIGURE 5-12: LOADING HISTORY FOR SLAB S2 (GILBERT AND GUO, 2005).	5-27
FIGURE 5-13: LOADING HISTORY FOR SLAB S3 (GILBERT AND GUO, 2005).	5-31
FIGURE 5-14: LOADING HISTORY FOR SLAB S4 (GILBERT AND GUO, 2005).	5-35
FIGURE 5-15: LOADING HISTORY FOR SLAB S5 (GILBERT AND GUO, 2005).	5-38

FIGURE 5-16: LOADING HISTORY FOR SLAB S6 (GILBERT AND GUO, 2005).....	5-42
FIGURE 5-17: LOADING HISTORY FOR SLAB S7 (GILBERT AND GUO, 2005).....	5-45
FIGURE 5-18: POSITION OF THE MIDDLE STRIP C7,C8 – C4,C5.....	5-52
FIGURE 5-19: GRAPHICAL REPRESENTATION OF THE ALLOWABLE SPAN/DEPTH RATIOS FOR THE SEVEN EXPERIMENTAL SLABS.	5-53
FIGURE 6-1: PARKING DECK SLAB GRIDLINE LAYOUT.	6-3
FIGURE 6-2: PANEL LAYOUT FOR THE PARKING DECK.....	6-4
FIGURE 6-3: DIMENSIONING DETAILS FOR PANEL 3 FOR THE PARKING DECK.	6-4
FIGURE 6-4: PROCESS TO OBTAIN MID-PANEL DEFLECTION: Δ_{MID}	6-6
FIGURE 6-5: GRAPHICAL REPRESENTATION OF THE PREDICTED DEFLECTION FOR THE PARKING DECK FOR THE VARIOUS DESIGN STANDARDS.	6-6
FIGURE 6-6: OFFICE BLOCK SLAB GRIDLINE LAYOUT.	6-8
FIGURE 6-7: THE TWO SLAB PANELS, PART OF THE OFFICE BLOCK SLAB, WHICH HAVE EXPERIENCED EXCESSIVE DEFLECTIONS.....	6-8
FIGURE 6-8: COLUMN AND MIDDLE STRIP DIMENSIONS FOR THE TWO PANELS PART OF THE OFFICE BLOCK SLAB.....	6-10
FIGURE 6-9: GRAPHICAL REPRESENTATION OF THE PREDICTED DEFLECTIONS FOR THE FIRST OFFICE BLOCK PANEL FOR THE VARIOUS DESIGN STANDARDS.	6-12
FIGURE 6-10: GRAPHICAL REPRESENTATION OF THE PREDICTED DEFLECTION FOR THE SECOND OFFICE BLOCK PANEL FOR THE VARIOUS DESIGN STANDARDS.	6-12
FIGURE 6-11: EXPERIMENTAL SETUP AND LOAD APPLICATION (MARITZ, 2009).....	6-15

LIST OF TABLES

TABLE 1-1: TYPES OF FLOOR (ROBBERTS AND MARSHALL, 2008).....	1-5
TABLE 2-1: EQUATIONS FOR THE UNCRACKED CONDITION ACCORDING TO THE VARIOUS DESIGN STANDARDS.	2-15
TABLE 2-2: EQUATIONS FOR THE CRACKED SECTION ACCORDING TO THE VARIOUS DESIGN STANDARDS.	2-16
TABLE 2-3: NUMERICAL COMPARISON OF THE EQUATIONS FROM TABLE 2-2.....	2-17
TABLE 2-4: SUMMARY OF VARIABLES ACCOUNTED FOR BY THE CREEP PREDICTION MODELS (FANOURAKIS AND BALLIM, 2003)(BARR, HOWELLS AND LARK, 2004).	2-21
TABLE 2-5: SUMMARY OF THE EQUATIONS USED TO CALCULATE THE SHRINKAGE CURVATURE AND FREE SHRINKAGE STRAIN ACCORDING TO THE DESIGN STANDARDS.....	2-25
TABLE 2-6: VARIOUS EQUATIONS ON HOW THE DESIGN STANDARDS INCORPORATE THE TENSILE STRENGTH IN DEFLECTION PREDICTION.	2-29
TABLE 2-7: DISTINCTION BETWEEN SHORT- AND LONG-TERM DEFLECTIONS CONCERNING THE CRACKING MOMENT AND B FACTOR (VOLLUM, 2002).	2-37
TABLE 2-8: REFERENCES FOR DEFLECTION COEFFICIENTS K FROM DESIGN STANDARDS.	2-41
TABLE 2-9: VARIOUS SHRINKAGE DEFLECTION COEFFICIENTS FOR SUPPORT CONDITIONS (BRANSON, 1977).....	2-41
TABLE 2-10: SUMMARY OF INITIAL CURVATURE CRITERIA FOR BS 8110 (1997).	2-53
TABLE 2-11: DISTRIBUTION COEFFICIENT Z, FOR THE UNCRACKED AND CRACKED SECTION ACCORDING TO CLAUSE 7.4.3 IN EC2 (2004).....	2-60
TABLE 2-12: SHRINKAGE DEFLECTION COEFFICIENT K_{sh} ACCORDING TO THE SABS 0100-1 (2000).....	2-63
TABLE 2-13: MINIMUM THICKNESS OF NONPRESTRESSED BEAMS OR ONE-WAY SLABS AS IN TABLE 9.5 (A) IN THE ACI 318 (2002).	2-67
TABLE 2-14: MINIMUM THICKNESS OF SLABS WITHOUT INTERIOR BEAMS ACCORDING TO TABLE 9.5 (C) IN ACI 318 (2002).....	2-67
TABLE 2-15: BASIC SPAN/EFFECTIVE DEPTH RATIOS (BS 8110: CLAUSE 3.4.6.3, 1997).	2-68
TABLE 2-16: MODIFICATION FACTOR FOR TENSION REINFORCEMENT (BS 8110: CLAUSE 3.4.6.5, 1997).	2-69
TABLE 2-17: MODIFICATION FACTOR FOR COMPRESSION REINFORCEMENT (BS 8110: CLAUSE 3.4.6.6, 1997).....	2-70
TABLE 2-18: BASIC RATIOS OF SPAN/EFFECTIVE DEPTH FOR REINFORCED CONCRETE MEMBERS WITHOUT AXIAL COMPRESSION AS SHOWN IN TABLE 7.4N IN EC2 (2004).	2-73
TABLE 2-19: BASIC SPAN/DEPTH RATIOS FOR BEAMS AS IN SABS 0100-1 (2000).	2-74
TABLE 3-1: SECTIONAL PROPERTIES OF THE GILBERT (2007) SLABS.	3-3
TABLE 3-2: SECTIONAL PROPERTIES TWO SECTIONS FOR THE PURPOSE OF THE SPAN/DEPTH COMPARISON.....	3-7
TABLE 3-3: SUMMARY OF THE DIFFERENT MODEL OF I_e FOR THE VARIOUS DESIGN STANDARDS.....	3-19
TABLE 3-4: SUMMARY OF THE RESULTS AS RECORDED FROM GILBERT (2007).....	3-21
TABLE 3-5: SLAB PROPERTIES FOR A SIMPLY-SUPPORTED ONE-WAY SLAB.	3-22
TABLE 3-6: ONE-WAY SLAB SECTIONAL DIMENSIONS AND PROPERTIES.	3-27
TABLE 3-7: %DIFF OF I_e VERSUS M_d/M_{cr} WITH REFERENCE TO I_g FOR A RANGE OF PERCENTAGE TENSION REINFORCEMENT.	3-30
TABLE 3-8: COVARIANCE VERSUS M_d/M_{cr} FOR A RANGE OF PERCENTAGE TENSION REINFORCEMENTS OF $0.18\% \leq P \leq 1.50\%$	3-32

TABLE 3-9: ALTERNATIVE EQUATIONS FOR THE SHORT-TERM DEFLECTION (SECTION 2.2.2).....	3-37
TABLE 3-10: ALTERNATIVE EQUATIONS FOR THE SHRINKAGE DEFLECTION (EC2, 2004)(SECTION 2.2.2).....	3-38
TABLE 3-11: ALTERNATIVE EQUATIONS FOR THE LONG-TERM DEFLECTION (SECTIONS 2.2.2 AND 2.2.3).....	3-39
TABLE 5-1: DETAILS FOR EACH SLAB SPECIMEN AS DESIGNATED BY GILBERT AND GUO (2005).....	5-4
TABLE 5-2: CONCRETE PROPERTIES AT 14 AND 28 DAYS FOR EXPERIMENTAL SLABS (GILBERT AND GUO, 2005).....	5-8
TABLE 5-3: CREEP COEFFICIENT AND SHRINKAGE STRAIN ($\times 10^{-6}$) OVER TIME FOR EXPERIMENTAL SLAB (GILBERT AND GUO, 2005).....	5-9
TABLE 5-4: CALCULATED CRACKED MODULUS OF ELASTICITY, E_{cr} FOR SLAB S3.....	5-16
TABLE 5-5: CRACKED FINITE ELEMENT MODEL FOR SLAB S1 AT DAY 169.....	5-23
TABLE 5-6: PREDICTED DEFLECTION COMPARISON RELATIVE TO THE EXPERIMENTAL DEFLECTIONS FOR SLAB S1.....	5-24
TABLE 5-7: DEFLECTION RATIOS RELATIVE TO THE EXPERIMENTAL DEFLECTIONS FOR SLAB S1.....	5-26
TABLE 5-8: CRACKED FINITE ELEMENT MODEL FOR SLAB S2 AT DAY 14.....	5-28
TABLE 5-9: PREDICTED DEFLECTION COMPARISON RELATIVE TO THE EXPERIMENTAL DEFLECTIONS FOR SLAB S2.....	5-29
TABLE 5-10: DEFLECTION RATIOS RELATIVE TO THE EXPERIMENTAL DEFLECTIONS FOR SLAB S2.....	5-29
TABLE 5-11: CRACKED FINITE ELEMENT MODEL FOR SLAB S3 AT DAY 28.....	5-32
TABLE 5-12: PREDICTED DEFLECTION COMPARISON RELATIVE TO THE EXPERIMENTAL DEFLECTION FOR SLAB S3.....	5-33
TABLE 5-13: DEFLECTION RATIOS RELATIVE TO THE EXPERIMENTAL DEFLECTIONS FOR SLAB S3.....	5-34
TABLE 5-14: CRACKED FINITE ELEMENT MODEL FOR SLAB S4 AT DAY 15.....	5-36
TABLE 5-15: PREDICTED DEFLECTION COMPARISON RELATIVE TO THE EXPERIMENTAL DEFLECTIONS FOR SLAB S4.....	5-36
TABLE 5-16: DEFLECTION RATIOS RELATIVE TO THE EXPERIMENTAL DEFLECTIONS FOR SLAB S4.....	5-37
TABLE 5-17: CRACKED FINITE ELEMENT MODEL FOR SLAB S5 AT DAY 15.....	5-39
TABLE 5-18: PREDICTED DEFLECTION COMPARISON RELATIVE TO THE EXPERIMENTAL DEFLECTIONS FOR SLAB S5.....	5-40
TABLE 5-19: DEFLECTION RATIOS RELATIVE TO THE EXPERIMENTAL DEFLECTIONS FOR SLAB S5.....	5-40
TABLE 5-20: RACKED FINITE ELEMENT MODEL FOR SLAB S6 AT DAY 14.....	5-43
TABLE 5-21: PREDICTED DEFLECTION COMPARISON RELATIVE TO THE EXPERIMENTAL DEFLECTIONS FOR SLAB S6.....	5-43
TABLE 5-22: DEFLECTION RATIOS RELATIVE TO THE EXPERIMENTAL DEFLECTIONS FOR SLAB S6.....	5-44
TABLE 5-23: CRACKED FINITE ELEMENT MODEL FOR SLAB S7 AT DAY 14.....	5-45
TABLE 5-24: PARTIALLY CRACKED FINITE ELEMENT MODEL FOR SLAB S7 AT DAY 14.....	5-46
TABLE 5-25: DEFLECTION RATIOS RELATIVE TO THE EXPERIMENTAL DEFLECTIONS FOR SLAB S7.....	5-47
TABLE 5-26: SUMMARY OF THE ACCURACY OF THE RESULTS FOR THE DEFLECTION PREDICTION METHODS.....	5-50
TABLE 5-27: THE ACTUAL AND ALLOWABLE SPAN/DEPTH RATIOS FOR THE SEVEN EXPERIMENTAL SLABS.....	5-53
TABLE 6-1: SLAB CHARACTERISTICS FOR THE PARKING DECK.....	6-3
TABLE 6-2: SPAN/DEPTH RATIOS FROM THE VARIOUS DESIGN STANDARDS AS CALCULATED FOR THE PARKING DECK.....	6-5
TABLE 6-3: SLAB CHARACTERISTICS FOR OFFICE BLOCK SLAB.....	6-9
TABLE 6-4: SPAN/DEPTH RATIOS FROM THE VARIOUS DESIGN STANDARDS AS CALCULATED FOR THE OFFICE BLOCK SLAB.....	6-10
TABLE 6-5: DIMENSIONS AND PROPERTIES OF THE NINE SLAB SPECIMENS FROM MARITZ (2009).....	6-14
TABLE 6-6: RECORDED SHORT-TERM DEFLECTION RESULTS FROM THE EXPERIMENTAL SLAB SPECIMENS (MARITZ, 2009).....	6-15
TABLE 6-7: SHORT-TERM DEFLECTION COMPARISON FOR SLAB SPECIMENS AT 0.39 % TENSION REINFORCEMENT.....	6-16

TABLE 6-8: SHORT-TERM DEFLECTION COMPARISON FOR SLAB SPECIMENS AT 0.79 % TENSION REINFORCEMENT.....6-17

TABLE 6-9: SHORT-TERM DEFLECTION COMPARISON FOR SLAB SPECIMENS AT 1.13 % TENSION REINFORCEMENT.....6-18

1 INTRODUCTION

1.1 IMPORTANCE OF DEFLECTION PREDICTION FOR REINFORCED CONCRETE FLAT SLAB STRUCTURES

A flat slab is a structure composed of a solid concrete slab supported only on columns. The slab is very thin relative to the span length therefore deflection of the structure is an important design consideration. Flat slab floor systems have grown to be one of the most popular forms of construction due to their low cost and ease of construction. For this reason engineers strive to find ways to produce efficient flat slabs with ever increasing spans (Jones and Morrison, 2005). The present-day use of higher-strength concrete and reinforcing steel, the strength or load-factor method of design, and the resulting shallower Sections have resulted in the problem of predicting and controlling deflections of reinforced concrete flexural members since the 1950s (Branson, 1997).

There are a number of reasons for the occurrence of serviceability problems, including (Webster and Brooker, 2006):

- The increase in reinforcement strength leading to less reinforcement being required for the ultimate limit state and resulting in higher service stresses in the reinforcement.
- Increase in concrete strength resulting from the need to improve both durability and construction time, and leading to concrete that is stiffer and with higher service stresses.
- A greater understanding of structural behaviour and the ability to analyse that behaviour faster by computer.
- The requirement to produce economic designs for slabs with a thickness that is typically determined by the serviceability limit state.
- Client requirements for longer spans and greater operational flexibility from their structures.

Several methods are available for flat slab design including the equivalent frame method, design by yield line and finite element methods. These methods are discussed by Jones and Morrison (2005) with specific comments on the finite element approach. The finite element method is a powerful way to analyse structures but caution is required, especially when used by engineers who do not

have a grasp of the rationale behind the method. Most finite element programs are based on elastic moment distributions and materials that obey Hooke's Law. Using this assumption for reinforced concrete is not entirely accurate, because the reinforced concrete is an elasto-plastic material and once it cracks its behaviour becomes non-linear. As a consequence, in an elastic analysis the support moments tend to be overestimated and the deflection of the slab is underestimated. It is also stated that the calculation of slab deflection is an inexact science due to the variation of the elastic modulus and tensile strength of concrete, the load applied and the duration of the load (Jones and Morrison, 2006). There is always pressure on engineers to use thinner slabs and faster construction programmes and the results from an elastic finite element analysis of a flat slab, which does not take cracking into account, produces unrealistic results (Jones and Morrison, 2006).

The alternative method for complying with the code requirements is to use the deemed-to-satisfy span-to-effective-depth ratios, which are appropriate and economic for the vast majority of designs. However, there are some situations where direct calculation of deflection is necessary, as listed below (Brooker and Webster, 2006):

- When an estimate of the deflection is required.
- When deflection limits of span/250 for quasi-permanent actions or span/500 for partition and/or cladding loads are not appropriate.
- When the design requires a particularly shallow member, direct calculation of deflection may provide a more economic solution.
- To determine the effect on deflection of early striking of formwork or of temporary loading during construction.

The effects of excessive deflection on structures range from an impaired performance of the structure to unsightly crack openings within the walls and roofs.

1.2 CURRENT LIMITATIONS ON AVAILABLE DEFLECTION CALCULATION METHODS

The methods of predicting or calculating deflections are deterministic in nature. However, the actual behaviour is a decidedly probabilistic phenomenon, requiring statistical approaches for a rational

analysis. Even with the most sophisticated methods of analysis using experimentally determined material properties, the range of variation between measured and computed results for a short-term as well as long-term deflection is high. Studies have shown that the coefficient of variation for such deflections is of the order of 15% to 20% and higher (Branson, 1977). In addition, the difficulty is compounded when applied to actual structures and conditions instead of laboratory specimens, since the only property of the concrete usually known at the calculation stage is the specified characteristic compressive strength.

Because of the variability of deflections, it would appear to be not only feasible but essential that relatively simple procedures be used so that engineers will guard against placing undue reliance on the computed or predicted results (Branson, 1977).

1.3 PURPOSE OF INVESTIGATION

The different aspects of deflection prediction in slender flexural members cover large variety of topics. This large scope of factors influencing deflection prediction, range from a molecular level to the global behaviour of the structure in itself. It was therefore seen fit to identify specific objectives to stay within a specific scope of variables. It was important to mathematically quantify these variables as far as possible. The objectives for this study include:

- Investigate the main variables influencing short- and long-term deflection prediction.
- Investigate the current deflection methods available from chosen design standards.
- Identify the limitations of the methods available for accurate deflection prediction.
- Suggest a suitable finite element model and suitable analysis procedure for time-dependent deflection prediction.
- Propose an effective mathematical procedure and finite element model that best reflect actual deflection occurrence.

It was decided to include the methods from the following design standards in this investigation:

- The American Concrete Institute (ACI) 318-02 (2002)
- The British Standards (BS) 8110: Part 2: 1997 (1997)

- EN 1992 -1-1 Eurocode 2: Part 1-1 (EC2, 2004)
- South African Bureau of Standards (SABS) 0100-1 (2000)

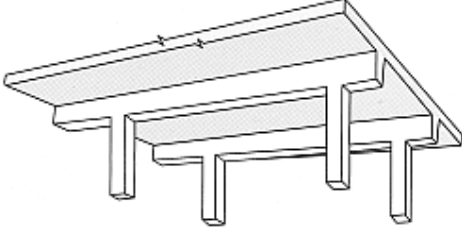
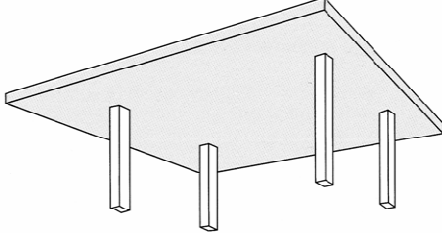
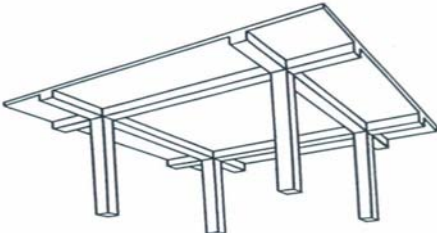
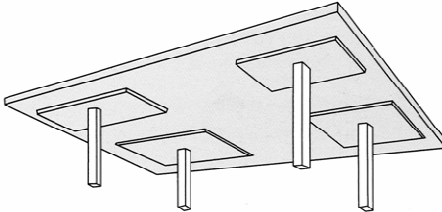
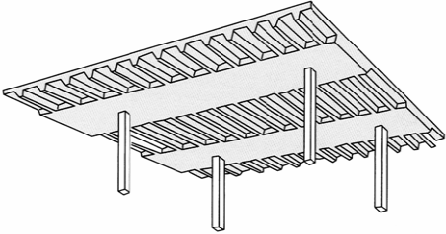
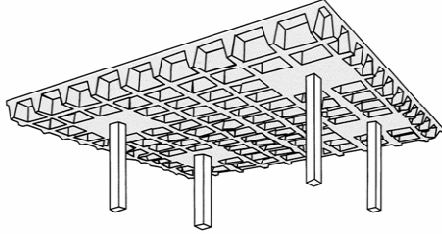
The SABS 0100-1 is under review to be revised based on the recent Eurocode Standard (EC2, 2004). Also, the BS 8110 is to be declared obsolete in March 2010, according to reports by the British Standards Institute (Update to specifiers regarding BS 8110, Eurocode 2 and Building Regulations). Many of the principles concerning deflection prediction in the SABS 0100 are based on the principles discussed in the BS 8110. This study is therefore aimed to provide clarity on the subject of deflection prediction to allow a future South African standard to reflect the best practice from the available research.

1.4 OVERVIEW OF CONTENTS OF THE INVESTIGATION

The contents of this study are aimed at providing the necessary solutions and answers as stated in the objectives in Section 1.3.

The term 'flat slab' has acquired a slightly different meaning in various countries according to Jones and Morrison (2006). In Australia it can mean any combination of flat slab and broad beam panels. In the United Kingdom flat slabs can be solid or of coffer construction, with or without column head or drops panels. Branson (1977) refers to the simple flat slab as either a flat slab or flat plate. Branson (1977) also distinguishes between the flat slab and the two-way spanning slab. Table 1-1 shows the range of forms that come under the heading of flat slab. This study only focuses on the flat slab as defined in Table 1-1. Some references are made to the one-way spanning slab for simplified comparisons, but essentially most attention is turned towards the flat slab structure.

Table 1-1: Types of Floor (Robberts and Marshall, 2008).

Edge Supported Slabs	Slabs Supported by Columns
<p data-bbox="451 323 594 352">One-Way Slab</p> 	<p data-bbox="1052 323 1143 352">Flat Slab</p> 
<p data-bbox="399 716 646 745">Two-Way Spanning Slab</p> 	<p data-bbox="964 716 1230 745">Flat Slab with Drop Panels</p> 
<p data-bbox="354 1085 691 1115">One-Way Spanning Coffered Slab</p> 	<p data-bbox="1008 1085 1190 1115">Coffered Flat Slab</p> 

The approach to investigate the occurrence of deflections, specifically for the flat slab structure, was divided into two parts. The basic approach for these two parts is presented in Figure 1-1. The basic approach for this study was done first to consider the simplest form of a slab, the one-way spanning slab. Most of the deflection prediction methods available apply to a normal beam Section, therefore to consider a relatively simple one-way slab Section, would be appropriate. Chapters 2 and 3 discuss, identify and quantify the deflection prediction limitations. Any trends identified for the two-dimensional problem may then be taken into consideration for the three-dimensional problem. The

limits are concerned with the numerical limits due to the Equations from the design standards, as well as the limits as experienced using finite element software. The software packages considered in this study include PROKON (2008) and STRAND 7 (2005).

Chapter 4 fully discusses the capabilities and limits concerning finite element simulation of a flat slab system. The empirical and finite element results are compared with experimental data as published by Gilbert and Guo (2005). The comparisons for the various results including empirical, finite element and experimental results are discussed in Chapter 5.

The final step to be completed within the scope of the study is to predict the deflection for slabs that were built and designed under South African conditions. Chapter 6 discusses three examples of lightly reinforced members that have been designed using South African standards.

The final Chapter, Chapter 7 summarizes the conclusions and findings for the study and present recommendations for future investigations.

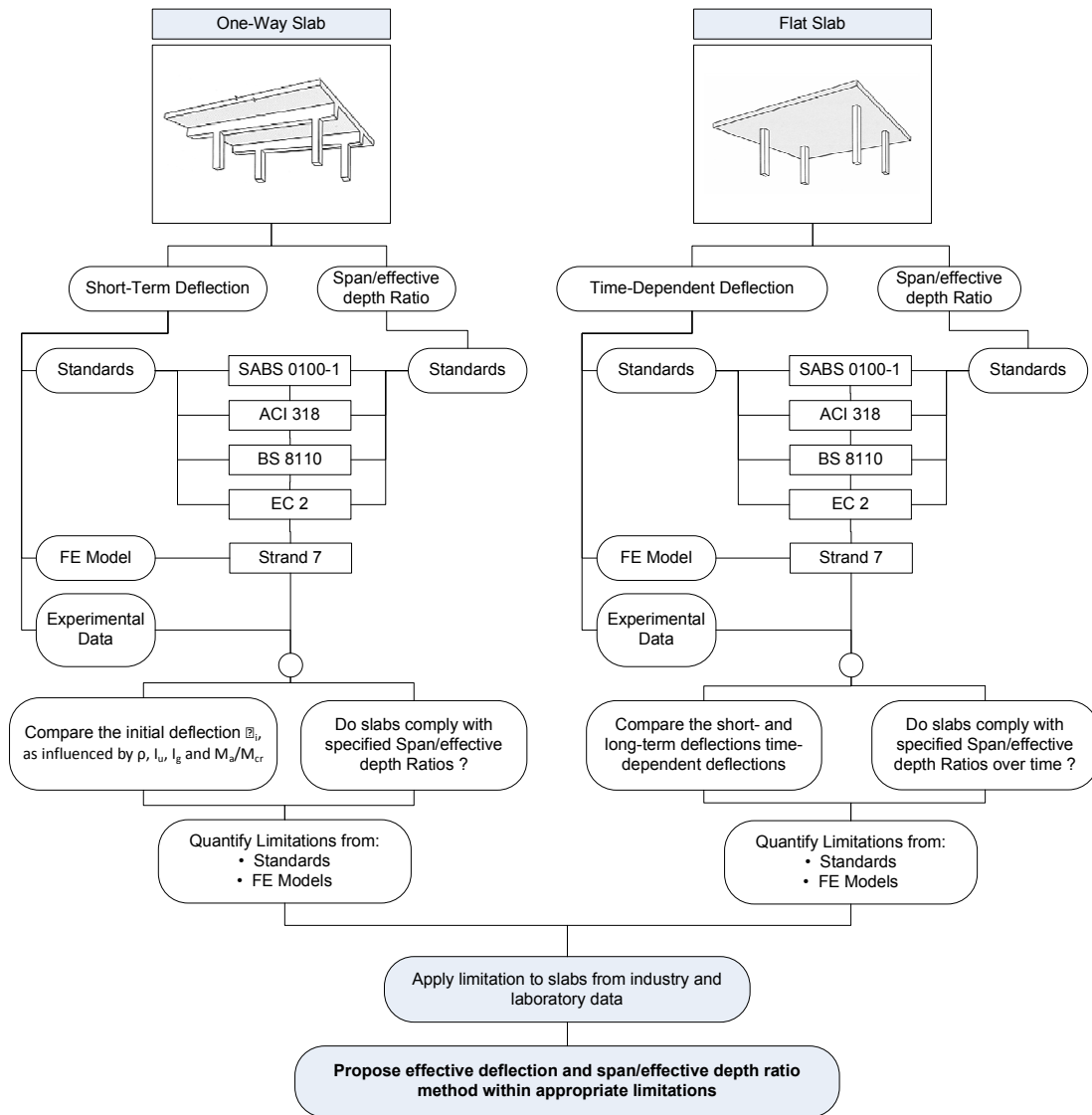


Figure 1-1: Flowchart of the aspects considered in this study.

2 FLAT SLAB DESIGN FOR THE SERVICEABILITY LIMIT STATE

2.1 INTRODUCTION

The deflections or cracking of a structure must not adversely affect the appearance, durability or efficiency of the structure (Kong & Evans, 1987). Of the serviceability limit states, those of excessive flexural deflection and of excessive flexural cracking are the most prominent in building design. Practically, the serviceability limit state requirements are met with the following two procedures:

- Deflections are controlled by limiting the span/effective depth ratios
- Crack widths are controlled by limiting the maximum spacing of the tension reinforcement (not focused on in this study)

Even though the span/effective depth ratio evaluations for the deflection check have proven to be effective, some discrepancies may arise when the calculated ratios border onto to the limiting value. In such cases, it might be necessary to calculate the expected deflection (Kong & Evans, 1987).

In this Chapter, the factors influencing flexural deflections are discussed. These range from the material properties to the intrinsic and extrinsic influences and are presented, in Section 2.2. Section 2.2 also elaborates on the derivation of the deflection prediction expression using the moment-curvature theorem, and the deflection coefficient K which is a variable part of the deflection prediction expression. At the end of Section 2.2, after the discussions from the factors influencing the deflection, a discussion on the deflection process is also presented. Understanding the influences on deflection improves the understanding on how the analytical methods are derived for each design standard. Section 2.3 discusses the deflection prediction method presented by the various design standards. The Chapter also discusses some of the different span/effective depth methods available from the various design standards, in Section 2.4. Finally, the Chapter concludes by explaining the methodology recommended for calculating the deflections for a three-dimensional flat slab structure.

2.2 FACTORS INFLUENCING REINFORCED FLAT SLAB DEFLECTIONS

2.2.1 Material Properties

The principal aspects of material behaviour related to the deflection of concrete structures are normally identified as elastic, cracking, creep, shrinkage, temperature, and relaxation effects. The corresponding parameters most commonly used to define these effects on properties are the modulus of elasticity of concrete and steel, Poisson's ratio, modulus of rupture and direct tensile strength of concrete, concrete creep coefficient or specific creep strain, shrinkage strain, thermal coefficient, and steel relaxation stress or percentage. The general quality of the concrete and the influence of the time-dependent hydration process are important functions of concrete deformation primarily as they relate to the above properties. Additional factors such as the environment conditions, member size and shape, stress history, concrete mix, etc., effect the deformation behaviour of concrete structures as well (Branson, 1977).

Not much attention is paid to the temperature and relaxation effects. These parameters are not often recorded and for the purpose of this study, it is assumed to have minor effects on the final deformation (deflection) of the structure.

Elastic Theory: Cracked, Uncracked and Partially Cracked Sections

The elasticity theory is described in the following Section for three different types of reinforced concrete Sections under different states of cracking. After concrete structures are cast, set and shuttering removed, the concrete changes from an uncracked to a partially cracked state. Using the theory of elasticity, expressions for the different states of cracking are derived empirically using certain assumptions (Kong and Evans, 1987). An understanding of the elasticity deflection theory is important to know which material properties are necessary to account for the phenomenon of cracking. Kong and Evans (1987) fully describe the three states of cracking for a typical concrete Section undergoing flexure. The following paragraphs provide an explanation as presented by Kong and Evans (1987).

CASE 1: The Cracked Section

Figure 2-1 shows the cross-section of a beam subjected to a bending moment M . The following simplifying assumptions are made:

- Plane sections remain plane during bending. Quantifying this it is assumed that the strains vary linearly with their distances from the neutral axis.
- Stresses in the steel and concrete are proportional to the strains.
- The concrete is cracked up to the neutral axis, and no tensile stress exists in the concrete below it, therefore it is known as a *Cracked Section*.

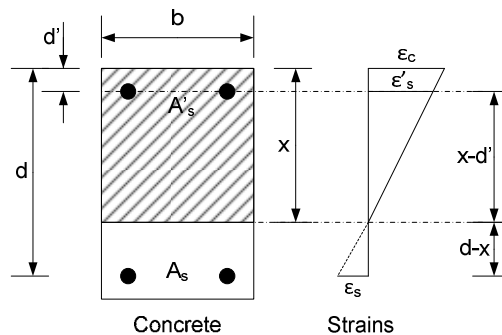


Figure 2-1: The Reinforced Concrete Section (Kong and Evans, 1987).

From the first assumption, the steel strains can be expressed in terms of the concrete strain ϵ_c on the compression face:

$$\epsilon'_s = \frac{x-d'}{x} \epsilon_c \quad (2-1)$$

$$\epsilon_s = \frac{d-x}{x} \epsilon_c \quad (2-2)$$

The variables include ϵ'_s , the steel strain in the reinforcement due to compression, x , the distance from the neutral axis to the extreme fibre in compression, d' the depth from the compression edge of the section to the middle of the steel reinforcement in compression, ϵ_s , the steel strain in the reinforcement due to tension and d , the depth from the compression edge of the section to the centre of the steel reinforcement in tension.

From the second assumption (as long as the steel and concrete remains in the elastic range), the concrete stress f_c on the compression face, the tension steel stress f_s and the compression steel stress f'_s are

$$f_c = E_c \varepsilon_c \quad (2-3)$$

$$f'_s = E_s \varepsilon'_s = \alpha_e E_s \varepsilon'_s \quad (2-4)$$

$$f_s = E_s \varepsilon_s = \alpha_e E_s \varepsilon_s \quad (2-5)$$

$$\alpha_e = \frac{E_s}{E_c} \quad (2-6)$$

where E_c is the modulus of elasticity of concrete, E_s is the modulus of elasticity of the reinforcing steel and α_e is the modular ratio. Since the concrete strength below the neutral axis is to be ignored as in the third assumption, the effective cross-section is that of Figure 2-2. From the condition of equilibrium of forces

$$\frac{1}{2} A_c f_c + A'_s f'_s = A_s f_s \quad (2-7)$$

where A_c is the area of the concrete in compression and A'_s and A_s are respectively the area of the compression steel and that of the tension steel. Using Equations 2-1 and 2-2 to express all stresses in terms of ε_c , we have

$$\frac{1}{2} A_c E_c \varepsilon_c + A'_s \alpha_e E_c \frac{x-d'}{x} \varepsilon_c = A_s \alpha_e E_c \frac{d-x}{x} \varepsilon_c \quad (2-8)$$

which simplifies to:

$$\frac{1}{2} A_c (x) + (A'_s \alpha_e)(x - d') = (A_s \alpha_e)(d - x) \quad (2-9)$$

Equation 2-9 shows that the neutral axis of the cracked section passes through the centroid of the equivalent section, obtained by replacing the areas A'_s and A_s by their respective equivalent concrete areas $\alpha_e A'_s$ and $\alpha_e A_s$. In Figure 2-2, the areas of concrete displaced by the compression bars are indicated by voids. The effects of the voids are included by writing $\alpha_e A'_s$ as $(\alpha_e - 1)A'_s$ in Equation 2-9.

The concrete compression area A_c is taken as the nominal area bx , where b is the section width. The resulting quadratic Equation 2-10 is shown below.

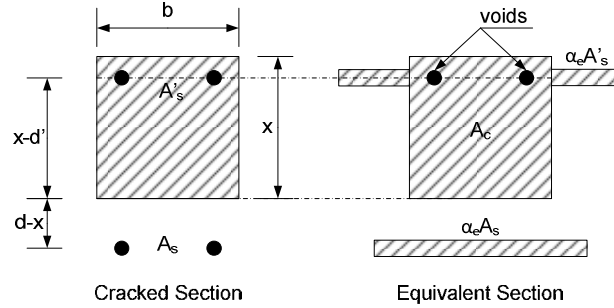


Figure 2-2: The Cracked Reinforced Concrete Section (Kong and Evans, 1987).

$$\frac{1}{2}bx^2 + (A'_s(\alpha_e - 1) + A_s\alpha_e)x - (A'_s(\alpha_e - 1)d' + A_s\alpha_e d) = 0 \quad (2-10)$$

The solution to quadratic Equation 2-10, produces an equation to calculate the neutral axis of a cracked section, x_{cr} .

$$x_{cr} = \{[\omega^2 + 2b(A'_s(\alpha_e - 1)d' + A_s\alpha_e d)]^{0.5} - \omega\}/b \quad (2-11)$$

$$\text{where } \omega = A'_s(\alpha_e - 1) + A_s\alpha_e$$

Referring to Figure 2-2, the moment of inertia for a cracked section can be derived.

$$I_{cr} = \frac{1}{3}bx_{cr}^3 + (\alpha_e - 1)A'_s(x_{cr} - d')^2 + \alpha_e A_s(d - x_{cr})^2 \quad (2-12)$$

where I_{cr} is the second moment of area of the cracked equivalent section.

CASE 2: The Uncracked Section

When the applied moment M is small enough for the maximum concrete tensile stress not to exceed the tensile strength or the modulus of rupture of the concrete, an analysis based on an uncracked

section becomes relevant. The effective concrete section is then the full section width (b) times the height (h) and the equivalent section changes to what is shown in Figure 2-3.

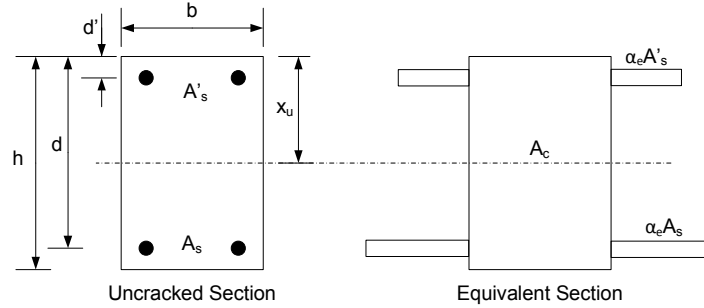


Figure 2-3: The Uncracked Reinforced Concrete Section (Kong and Evans, 1987).

As in Equation 2-9, the neutral axis of the uncracked section passes through the centroid of the equivalent section, the neutral axis depth x_u is therefore given by

$$A_c \left(x_u - \frac{h}{2} \right) + (\alpha_e - 1) A'_s (x_u - d') = (\alpha_e - 1) A_s (d - x_u) \quad (2-13)$$

where A_c is now the entire area bh . The equation for x_u (Equation 2-14) reduces to

$$x_u = \frac{\frac{bh^2}{2} + (\alpha_e - 1)(A_s d + A'_s d')}{bh + (\alpha_e - 1)(A_s + A'_s)} \quad (2-14)$$

Referring to the equivalent section in Figure 2-3, the moment of inertia of an uncracked section is

$$I_u = \frac{1}{12} bh^3 + bh \left(x - \frac{h}{2} \right)^2 + (\alpha_e - 1) [A'_s (x - d')^2 + A_s (d - x)^2] \quad (2-15)$$

CASE 3: The Partially Cracked Section

Figure 2-4 shows a beam section in which strains are assumed to be linearly distributed. However, in the tension zone some concrete tension still exists as represented by the triangular stress distribution shown in Figure 2-4. The concept where the concrete between developed cracks in a

flexural member still retains some of its concrete tensile strength is known as tension stiffening. To accommodate for the effect of tension stiffening an assumption is made on the level of the concrete in tension. The concrete tensile stress has a specified value f_t at the level of tension reinforcement. The concrete stresses above the neutral axis and the reinforcement stresses are related to the strains by the usual equations:

$$f_c = E_c \epsilon_c; \quad f_c = E_s \epsilon_c; \quad f_s = E_s \epsilon_s \quad (2-16)$$

Below the neutral axis, the concrete tensile stresses are not to be determined from the strain diagram, but from a specified value f_t .

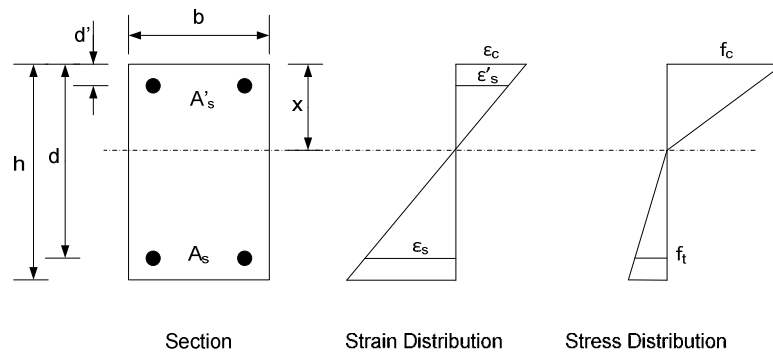


Figure 2-4: The Partially Cracked Reinforced Concrete Section (Kong and Evans, 1987).

The partially cracked Section is an important application in deflection calculations. The different design standards apply the partially cracked section theory differently. More detail is presented in Section 2.3.

The equations used to account for a cracked and uncracked section as proposed by the design standards, are summarised in the Tables 2-1 and 2-2. Even though these equations differ, the result from each is roughly similar. The fact that the sectional characteristic of a slender flexural member is dependent on the cross-sectional dimensions of the section and is only partially influenced by the presence of tension and compression reinforcement, allows the differences to be insignificant.

Table 2-1: Equations for the Uncracked Condition according to the various design standards.

Design standard	Uncracked Condition	
	Uncracked Neutral Axis	Uncracked Moment of Inertia
ACI 318 (2002)	$x_g = h/2$	$I_g = bh^3/12$
BS 8110 (1997)	$x_u = \frac{\frac{bh^2}{2} + \alpha_e(A_s d + A'_s d')}{bh + \alpha_e(A_s + A'_s)}$	$I_u = \frac{bh^3}{12} + bh\left(\frac{h}{2} - x_u\right)^2 + \alpha_e[A_s(d - x_u)^2 + A'_s(x_u - d')^2]$
EC2 (2004)	$x_u = \frac{\frac{bh^2}{2} + (\alpha_e - 1)(A_s d + A'_s d')}{bh + (\alpha_e - 1)(A_s + A'_s)}$	$I_u = \frac{bh^3}{12} + bh\left(\frac{h}{2} - x_u\right)^2 + (\alpha_e - 1)[A_s(d - x_u)^2 + A'_s(x_u - d')^2]$
SABS 0100-1 (2000)	$x_g = h/2$	$I_g = bh^3/12$

The variables include h as the total depth of the section, b as the width of the section, A_s as the area of tension reinforcement in the section, A'_s as the area compression reinforcement in the section, d as the effective depth of the section and d' as the total height less the effective depth of the section. The modular ratio, α_e , is simply the ratio of the modulus of elasticity of steel to the modulus of elasticity of the concrete.

The BS 8110 (1997) refers to using equations for the uncracked condition taking the effect of both the tension reinforcement ($\alpha_e A_s$) and compression reinforcement ($\alpha_e A'_s$) into account. The EC2 (2004) strictly refers to using the equations for the uncracked condition and also accounting for the effects of the reinforcement. The EC2 (2004) specifies the use of $\alpha_e A_s$ to account for the tension reinforcement and $(\alpha_e - 1)A'_s$ for the compression reinforcement, where α_e is defined as the modular ratio. The ACI 318 (2002) and the SABS 0100-1 (2000) refer to the gross cross-sectional properties. The equations used to calculate the gross cross-sectional properties do not take the effect of reinforcement into account. The equations for the uncracked condition produce more accurate results, but the equations to obtain the gross cross-sectional properties are assumed to produce a satisfactory approximation.

The equations used to calculate the values for the cracked cross-section are presented in Table 2-2. These equations also differ as was discussed for the equations for Table 2-1. As was explained for the equations in Table 2-1, the BS 8110 (1997) and the EC2 (2004) account for the reinforcement in compression differently. However, all the equations from the four different design standards take the effect of tension reinforcement into account in a similar way.

Table 2-2: Equations for the cracked section according to the various design standards.

Design standard	Cracked Condition	
	Cracked Neutral Axis	Cracked Moment of Inertia
ACI 318 (2002)	$\omega = A_s \alpha_e + A'_s (\alpha_e - 1)$ $x_{cr} = \frac{\left\{ \left[\omega^2 + 2b(A_s d \alpha_e + A'_s d' (\alpha_e - 1)) \right]^{0.5} - \omega \right\}}{b}$	$I_{cr} = \frac{bx_{cr}^3}{3} + \alpha_e A_s (d - x_{cr})^2 + (\alpha_e - 1) A'_s (d' - x_{cr})^2$
BS 8110 (1997)	$\frac{x_{cr}}{d} = -\alpha_e (\rho - \rho')$ $+ \sqrt{\left\{ \alpha_e^2 (\rho - \rho')^2 + 2\alpha_e \left(\rho - \frac{d'}{d} \rho' \right) \right\}}$ <p>where $\rho = A_s / bd$ and $\rho' = A'_s / bd$</p>	$\frac{I_{cr}}{bd^3} = \frac{1}{3} \left(\frac{x_{cr}}{d} \right)^3 + \alpha_e \rho \left(1 - \frac{x_{cr}}{d} \right)^2 + \alpha_e \rho' \left(\frac{x_{cr}}{d} - \frac{d'}{d} \right)^2$ <p>where $\rho = A_s / bd$ and $\rho' = A'_s / bd$</p>
EC2 (2004)	$\omega = A_s \alpha_e + A'_s (\alpha_e - 1)$ $x_{cr} = \frac{\left\{ \left[\omega^2 + 2b(A_s d \alpha_e + A'_s d' (\alpha_e - 1)) \right]^{0.5} - \omega \right\}}{b}$	$I_{cr} = \frac{bx_{cr}^3}{3} + \alpha_e A_s (d - x_{cr})^2 + (\alpha_e - 1) A'_s (d' - x_{cr})^2$
SABS 0100-1 (2000)	$x_{cr,1} = \frac{\frac{1}{2} x_{cr,2}^2 b + A_s d \alpha_e}{x_{cr,2} b + A_s \alpha_e}$ <p>where $x_{cr,1} = x_{cr,2}$</p>	$I_{cr} = \frac{1}{3} b x_{cr}^3 + A_s (d - x_{cr})^2 \alpha_e$

The variables include A_s as the area tension reinforcement in the section, A'_s as the area of the compression reinforcement in the section, b is the width of the section, d is the effective depth of the section and the modular ratio as α_e . The modular ratio is the ratio of the modulus of elasticity of reinforcing steel to the modulus of elasticity of concrete.

FLAT SLAB DESIGN FOR THE SERVICEABILITY LIMIT STATE

Applying the equations from Table 2-2 to a section of a width of 850.0 mm, height of a 100.0 mm and an effective depth of 79.0 mm, a numerical comparison may be made between the different equations. The values for the cracked neutral axis and the cracked modulus of elasticity are presented in Table 2-3. The percentage tension reinforcement for the section is increased to observe how the results change as the tension reinforcement of the section is increased. No compression reinforcement is included in the section. By examining the values within Table 2-3, it is noted that the values calculated for x_{cr} and I_{cr} using the equations from Table 2-2 are the same for each design standard. It is therefore insignificant which equations from Table 2-2 are more distinctive.

Table 2-3: Numerical comparison of the equations from Table 2-2.

ρ [%]	SABS 0100		EC2		BS 8110		ACI 318		Average	
	x_{er} [mm]	I_{cr} [mm ⁴]	x_{er} [mm]	I_{cr} [mm ⁴]	x_{er} [mm]	I_{cr} [mm ⁴]	x_{er} [mm]	I_{cr} [mm ⁴]	x_{er} [mm]	I_{cr} [mm ⁴]
0.18	11.2	4.0E+06	11.2	4.0E+06	11.2	4.0E+06	11.2	4.0E+06	11.2	4.0E+06
0.30	14.2	6.4E+06	14.2	6.4E+06	14.2	6.4E+06	14.2	6.4E+06	14.2	6.4E+06
0.49	17.6	9.6E+06	17.6	9.6E+06	17.6	9.6E+06	17.6	9.6E+06	17.6	9.6E+06
0.70	20.6	1.3E+07	20.6	1.3E+07	20.6	1.3E+07	20.6	1.3E+07	20.6	1.3E+07
0.84	22.3	1.5E+07	22.3	1.5E+07	22.3	1.5E+07	22.3	1.5E+07	22.3	1.5E+07
1.10	24.8	1.9E+07	24.8	1.9E+07	24.8	1.9E+07	24.8	1.9E+07	24.8	1.9E+07
1.30	26.6	2.1E+07	26.6	2.1E+07	26.6	2.1E+07	26.6	2.1E+07	26.6	2.1E+07
1.50	28.1	2.3E+07	28.1	2.3E+07	28.1	2.3E+07	28.1	2.3E+07	28.1	2.3E+07
1.70	29.5	2.6E+07	29.5	2.6E+07	29.5	2.6E+07	29.5	2.6E+07	29.5	2.6E+07
1.90	30.8	2.8E+07	30.8	2.8E+07	30.8	2.8E+07	30.8	2.8E+07	30.8	2.8E+07
2.10	32.0	3.0E+07	32.0	3.0E+07	32.0	3.0E+07	32.0	3.0E+07	32.0	3.0E+07
2.30	33.1	3.2E+07	33.1	3.2E+07	33.1	3.2E+07	33.1	3.2E+07	33.1	3.2E+07
2.50	34.1	3.3E+07	34.1	3.3E+07	34.1	3.3E+07	34.1	3.3E+07	34.1	3.3E+07
2.70	35.1	3.5E+07	35.1	3.5E+07	35.1	3.5E+07	35.1	3.5E+07	35.1	3.5E+07
2.90	36.0	3.7E+07	36.0	3.7E+07	36.0	3.7E+07	36.0	3.7E+07	36.0	3.7E+07
3.10	36.8	3.8E+07	36.8	3.8E+07	36.8	3.8E+07	36.8	3.8E+07	36.8	3.8E+07

Creep: Concrete Creep Coefficient

The difference between the uncracked and cracked conditions for a flexural member under loading has been discussed. The next aspect influencing deflection development is creep. This method is

only useable in statically determinable cases as for indeterminable cases the moments will be redistributed due to creep.

Under sustained loading, compressive strains in concrete keep increasing nonlinearly with time, owing to the phenomenon called creep, according to Pillai and Menon (2004). The variation of creep strain with time for concrete under uniaxial compression is shown in Figure 2-5.

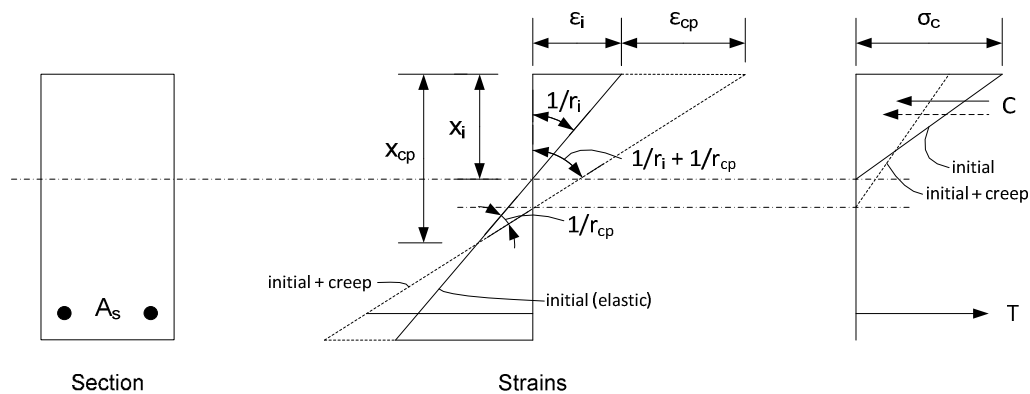


Figure 2-5: Creep curvature in a flexural member (Pillai and Menon, 2004).

The creep coefficient, C_t , defined as the ratio of the creep strain, ϵ_{cp} , to the initial elastic strain, ϵ_i , provides a measure of creep in concrete at any given time. The maximum value of C_t , called the ultimate creep coefficient is required for predicting the maximum deflection of a flexural member due to creep.

In a flexural member, the distribution of creep strains across the depth at any cross-section is non-uniform, with a practically linear variation similar to that produced by the applied loading. This linear variation of creep strains results in a creep curvature, $1/r_{cp}$, which is additive to the initial elastic curvature, $1/r_i$, and is similar in effect to the shrinkage curvature, $1/r_{cs}$ described below. It may be noted that although the creep effect is primarily related to increased strains in concrete under compression, there is also a small increase in the tensile strain in the steel as shown in Figure 2-5. The steel itself is not subjected to creep. However, due to creep in concrete, there is a slight increase in the depth of neutral axis, with a consequent reduction in the internal lever arm. Then, to maintain static equilibrium with the applied moment at the section, there has to be a slight increase in the steel stress, and the steel strain.

Within the range of service loads, creep curvature $1/r_{cp}$ may be assumed to be proportional to the initial elastic curvature $1/r_i$. With reference to Figure 2-5,

$$\frac{1/r_{cp}}{1/r_i} = \frac{\varepsilon_{cp}/x_{cp}}{\varepsilon_i/x_i} = k_r C_t \quad (2-17)$$

where $C_t = \varepsilon_{cp} / \varepsilon_i$ is the creep coefficient, and $k_r = x_i / x_{cp}$ is the ratio of the initial neutral axis depth to the neutral depth due to creep. As $x_i < x_{cp}$, the coefficient k_r is less than unity. For singly reinforced flexural members, $k_r \approx 0.85$ (Branson, 1977). This is, however, a function of the material specific creep characteristics.

The variation of creep curvature $1/r_{cp}$ along the span of the flexural member may be assumed to be identical to the variation of $1/r_i$. Hence, it follows that:

$$\frac{\Delta_{cp}}{\Delta_i} = \frac{1/r_{cp}}{1/r_i} = k_r C_t \quad (2-18)$$

where Δ_i and Δ_{cp} denote respectively the maximum initial elastic deflection and the additional deflection due to creep. For estimating maximum deflection due to creep, the ultimate creep coefficient Φ should be used with C_t . Accordingly,

$$\Delta_{cp} = (k_r \cdot \Phi) \Delta_i \quad (2-19)$$

where Δ_i is to be taken as the initial displacement due to the permanently applied loads. It may be noted that although transient live loads are excluded in the computation of Δ_i , the possibility of a reduced flexural stiffness on account of prior cracking due to such live loads should be considered. Hence, the calculation of Δ_i should be based on stiffness considering the total dead and live load.

The deflection due to creep may also be labelled as the long-term deflection due to permanent load, Δ_l , since the deflection is composed of the initial deflection over time. The effect of time is included using the creep coefficient and k_r .

$$\Delta_l = \Delta_{cp} = (k_r \cdot \phi) \Delta_i \quad (2-20)$$

When calculating the deflection due to permanent load and creep, an effective modulus of elasticity of concrete, E_{eff} is used to account for the long-term effects of creep within the stiffness variable. The formulation of E_{eff} is based on the assumption that the total strain in concrete ε_{i+cp} (initial strain plus creep strain) is directly proportional to the stress σ_i induced by the permanent loads (Pillai and Menon, 2003).

$$\varepsilon_{i+cp} = \varepsilon_i + \varepsilon_{cp} = \varepsilon_i(1 + \phi)$$

then
$$E_{eff} = \frac{\sigma_i}{\varepsilon_{i+cp}} = \frac{\sigma_i}{\varepsilon_i} \cdot \frac{1}{1+\phi} = \frac{E_c}{1+\phi} \quad (2-21)$$

where $E_c = \sigma_i / \varepsilon_i$

Figure 2-6 explains this principle graphically.

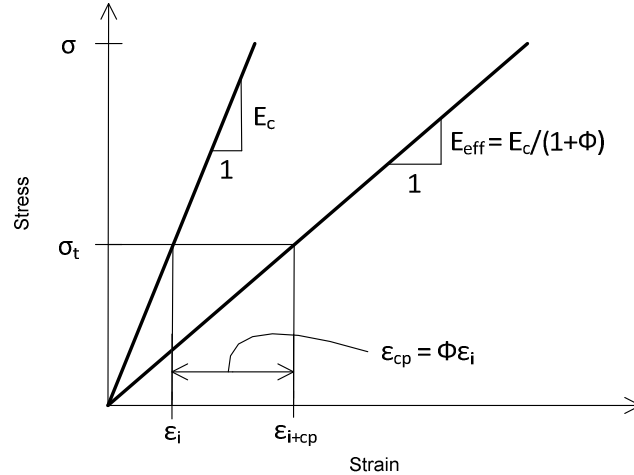


Figure 2-6: Effective modulus of elasticity under creep (Pillai and Menon, 2003).

The magnitude of creep can be estimated at various levels. The choice of level depends on the type of structure and the quality of the data available for the design. In a case where only a rough estimate of the creep is required, which is suitable only for approximate calculations, an estimate can be made on the basis of a few parameters such as relative humidity, age of concrete and

member dimensions. On the other extreme, in the case of deflection-sensitive structures, estimates are based on comprehensive laboratory testing and mathematical and computer analyses. Ideally, a compromise has to be sought between the simplicity of the prediction procedure and the accuracy of results obtained (Fanourakis & Ballim, 2003).

At the design stage, when often the only information available is the compressive strength of the concrete, the general environmental conditions for exposure and the member sizes, the designer has to rely on a design code model to estimate the extent and rate of creep strains. Given their nature, these models are not able to account for the full range of factors that are known to influence the creep deformation in concrete and simplicity of application is usually demanded by the users of the model. Nevertheless, the users of the model require some confidence as to the accuracy of the prediction as well as the range of error of the prediction (Bangash, 1989).

In an investigation done by Fanourakis and Ballim (2003) the factors accounted for by the creep prediction models for the various design standards, are summarized. Fanourakis and Ballim (2003) included the SABS 0100-1 (2000), BS 8110 (1997) and the ACI 209 in their comparison. A study by Barr, Howells and Lark (2004) included the influences on the creep prediction model by the EC2 (2004). Table 2-4 combine the available information from the two sources.

Table 2-4: Summary of variables accounted for by the creep prediction models (Fanourakis and Ballim, 2003)(Barr, Howells and Lark, 2004).

Factor	SABS 0100-1 (2000)	BS 8110 (1997)	ACI 209	EC2 (2004)
Humidity	√	√	√	√
Temperature				√
Age at Loading	√	√	√	√
Slump			√	
28-day Strength			√	√
Elastic Modulus	√	√	√	√
w/c Ratio				
Cement Content				
Cement Type				√
Curing Regime				
Aggregate Type	√			
Shape				

The SABS 0100-1 (2000) has adopted the BS 8110 (1997) method for predicting creep. However, the SABS 0100-1 uses specific values for the elastic modulus of the aggregate type as explained by Fanourakis and Ballim (2003).

The comparative study by Fanourakis and Ballim (2006) yielded the following comments concerning the accuracy and reliability of the creep prediction models available. The creep prediction models included in their study consider the value of a predicted modulus of elasticity of concrete in the calculation of creep prediction. When comparing predicted creep results over a period of time with experimental creep results, the ACI 209 model showed the largest under-prediction. The BS 8110 model, which is the simplest of the models and containing the least number of variables (Table 2-4) yielded the second most accurate predictions. This model proved to be more accurate than the SABS 0100-1 (2000), which account for the aggregate type. The EC2 (2004) model also under-predicted the results when compared with the experimental data. The level of dependability (i.e. the reliability to accurately predict creep realistically) of the EC2 (2004) model, lies near the dependability of the SABS 0100-1 (2000) model. Fanourakis and Ballim (2006) also concluded that the accuracy of the predictions did not increase with the complexity of the method applied or with increasing number of variables accounted for in the method. It is thus suggested here that the simpler model from the BS 8110 is to be considered for creep prediction where initial estimates are needed.

Shrinkage: Specific Creep Strain and Shrinkage Strain

There are different aspects of the material properties that influence deflection prediction for flexural members. The elastic theory, used to predict the properties for whether the section is in an uncracked or cracked state, has been discussed. The concept of creep prediction has also been discussed. The aspect under discussion in this next section includes the phenomenon of shrinkage and how the shrinkage deflection should be determined.

Concrete shrinkage in both statistically determinate and indeterminate reinforced concrete structures induces compressive stress in the steel which is balanced by the tensile stress in the concrete. When the reinforcement is unsymmetrical, the resulting non-uniform strain distribution and accompanying curvature cause deflections in the same direction as those caused by the loads for which the structure was designed and reinforced (Branson, 1977)(Divakar & Dilger, 1988).

The concrete shrinkage stress can have an effect on cracking although the extent of which is uncertain. Firstly, much of the shrinkage may occur before the application of the design live load and cracking. Secondly, even though a section is cracked on the tension side under load, the separate effect of shrinkage curvature may only be nominally influenced by such cracks, since the shrinkage shortening on the compression side occurs in a zone that is uncracked by loads. To put it in another way, shrinkage forces are axial in nature and cause some tension on the compression side of the member. Furthermore, shrinkage forces and loads are not resisted in the same way by a cracked section (Branson, 1977).

In both the cracked and uncracked states, shrinkage is independent on the load level and creates a parallel shift of the moment curvature diagram as shown in Figure 2-7 (Divakar & Dilger, 1988).

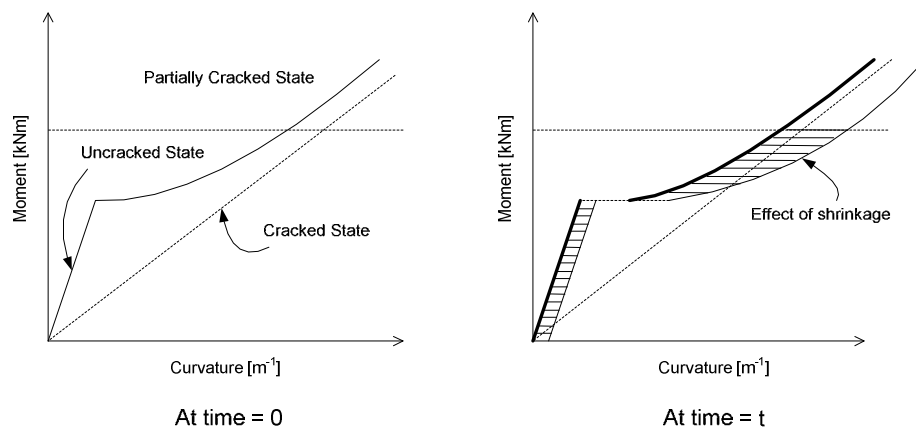


Figure 2-7: Effect of shrinkage on flexural deformation (Divakar & Dilger, 1988).

Compression steel has only a minor effect on short-term deflections, as reflected in the uncracked or cracked equivalent section moment of inertia. However, for both shrinkage and creep effects, compression steel has the effect of significantly reducing deflections (Branson, 1977). By providing restraint at the top section, in addition to the restraint at the bottom, the eccentricity of the resultant tension in the concrete is reduced and, consequently, so is the shrinkage curvature. An uncracked, symmetrically reinforced section will suffer no shrinkage curvature. Shrinkage will however induce a uniform tensile stress which when added to the tension caused by external loading may cause time-dependent cracking (Gilbert, 2001).

It is important from the outset to distinguish between plastic shrinkage, chemical shrinkage and drying shrinkage. Some high strength concretes are prone to plastic shrinkage, which occurs in the wet concrete, and may result in significant cracking during the setting process. This cracking occurs due to capillary tension in the pore water. Since the bond between the plastic concrete and the reinforcement has not yet developed, the steel is ineffective in controlling such cracks. This problem may be severe in the case of low water content, silica fume concrete. The use of such concrete in a slab element with large exposed surfaces is not recommended (Gilbert, 2001).

Drying shrinkage is the reduction in volume caused principally by the loss of water during the drying process. Chemical (or autogenous) shrinkage results from various chemical reactions within the cement paste and includes hydration shrinkage, which is related to the degree of hydration of the binder in a sealed specimen. Concrete shrinkage strain, which is usually considered to be the sum of the drying and chemical shrinkage components, continues to increase with time at a decreasing rate (Gilbert, 2001).

Drying shrinkage is greatest at the surfaces exposed to drying and decreases towards the interior of a concrete member. This nonlinear strain causes internal stresses to develop across the cross-section of the element. These stresses occur in all concrete structures and are tensile near the drying surfaces and compressive in the interior of the member. Because the shrinkage-induced stresses near the drying surfaces often overcome the tensile strength of the immature concrete and result in surface cracking, soon after the commencement of drying. Moist curing delays the commencement of drying and may provide the concrete time to develop sufficient tensile strength to avoid unsightly surface cracking (Gilbert, 2001).

Shrinkage is assumed to approach a final value, ϵ_{cs} , as time approaches infinity and is dependent on all the factors which affect the drying of concrete, including the relative humidity and temperature, the mix characteristics (in particular, the type and quantity of the binder, the water content and water-to-cement ratio, the ratio of fine to coarse aggregate, and the type of aggregate) and the size and shape of the member.

Shrinkage of concrete significantly contributes to overall deformations of concrete structures. The different design standards approach the calculation of the free shrinkage strain and the shrinkage curvature differently. Table 2-5 summarizes the applicable equations.

Table 2-5: Summary of the equations used to calculate the shrinkage curvature and free shrinkage strain according to the design standards.

Design Standard	Shrinkage Curvature, $1/r_{cs}$	Free Shrinkage Strain, ϵ_{cs}
<p>ACI 318 (2002), as proposed by Branson (1977)</p>	$\frac{1}{r_{cs}} = 0.7 \frac{\epsilon_{cs}}{h} (\rho - \rho')^{1/3} \left[\frac{\rho - \rho'}{\rho} \right]^{1/2}$ <p>for $\rho - \rho' \leq 3.0\%$</p> <p>The empirical derivation relate the shrinkage curvature or slope of the strain diagram as a direct function of the free shrinkage and steel content, and an inverse function of the depth of the section (Branson, 1977).</p>	<p>The free shrinkage strain, ϵ_{cs} is determined from recorded experimental results. Branson (1977) published tables for various curing conditions.</p>
<p>BS 8110 (1997) (clause 3.6)</p>	$\frac{1}{r_{cs}} = \frac{\epsilon_{cs} \alpha_e S_{cr}}{I_{cr}}$	<p>An estimate of the free shrinkage strain, ϵ_{cs} of plain concrete may be obtained from Figure 7.2 in BS 8110 (1997).</p>
<p>EC 2 (2004) (clause 7.4.3)</p>	$\frac{1}{r_{cs}} = \zeta \epsilon_{cs} \alpha_e \frac{S_u}{I_u} + (1 - \zeta) \epsilon_{cs} \alpha_e \frac{S_{cr}}{I_{cr}}$ <p>where $\epsilon_{cs} = \epsilon_{cd} + \epsilon_{ca}$ while $\epsilon_{cd}(t) = \beta_{ds}(t, t_s) \cdot k_h \cdot \epsilon_{cd,0}$ and $\epsilon_{ca}(t) = \beta_{as}(t) \cdot \epsilon_{ca}(\infty)$</p>	<p>The total shrinkage strain, ϵ_{cs} is composed of two components, the drying shrinkage strain, ϵ_{cd} and the autogenous strain, ϵ_{ca} (EC2, 2004).</p>
<p>SABS 0100-1 (2000) (clause A.2.2.5)</p>	$\frac{1}{r_{cs}} = k_{cs} \frac{\epsilon_{cs}}{h}$ <p>where $k_{cs} = 0.7 \sqrt{\rho \left(1 - \frac{\rho'}{\rho}\right)}$ for uncracked members where $0 \leq k_{cs} \leq 1.0$ or $k_{cs} = 1 - \frac{\rho'}{\rho} [1 - 0.11(3 - \rho)^2]$ for cracked members where $0.3 \leq k_{cs} \leq 1.0$ limited by $\rho \leq 3.0$ and $\rho'/\rho \leq 1.0$</p>	<p>An estimate of the free shrinkage strain, ϵ_{cs} of plain concrete may be obtained from Figure C.2 in SABS 0100-1 (2000). The figure presented in SABS 0100-1 is the same as the Figure in BS 8110 (1997).</p>

The variables are defined as h for the depth of the section, $\rho = 100A_s/bd$ and $\rho' = 100A'_s/bd$. The area tension reinforcement is noted as A_s , b is the width of the section, d the effective depth and A'_s as the compression reinforcement for the section. α_e is the modular ratio, S_{cr} represents the first moment of area of the reinforcement about the centroid of the cracked section and I_{cr} represents the moment of inertia of the cracked section. ζ is noted as the distribution coefficient and defined in section 2.3.3, S_u represents the first moment of area of the reinforcement about the centroid of the uncracked section and I_u represents the moment of inertia of the uncracked section.

The variables used in the Equations for calculating the drying shrinkage, ϵ_{cd} and the autogenous shrinkage ϵ_{ca} , according to EC2 (2004) are explained as follows:

The development of the drying strain, ϵ_{cd} in time follows from

$$\epsilon_{cd}(t) = \beta_{ds}(t, t_s) \cdot k_h \cdot \epsilon_{cd,0} \quad (2-22)$$

where the nominal unrestraint drying shrinkage strains, $\epsilon_{cd,0}$ for concrete with cement CEM Class N is given in Table 3.2 in EC2 (2004). $\epsilon_{cd,0}$ is dependent on the concrete strength and the relative humidity of the environment during drying. k_h is a coefficient depending on the notional size h_0 according to Table 3.3 in EC 2 and $h_0 = 2A_c/u$. A_c is the concrete cross-sectional area and u is the perimeter of that part of the cross-section which is exposed to drying. Equation 2-23 for $\beta_{ds}(t, t_s)$ is as follows:

$$\beta_{ds}(t, t_s) = \frac{(t-t_s)}{(t-t_s) + 0.04\sqrt{h_0^3}} \quad (2-23)$$

In Equation 2-23 t is the age (days) of the concrete at the moment considered and t_s is the age (days) of the concrete at the beginning of drying shrinkage. Normally this age (days) is at the end of curing.

The autogenous shrinkage strain, ϵ_{ca} in time follows from:

$$\epsilon_{ca}(t) = \beta_{as}(t) \cdot \epsilon_{ca}(\infty) \quad (2-24)$$

$$\text{where } \varepsilon_{ca}(\infty) = 2.5(f'_c - 10)10^{-6} \quad (2-25)$$

$$\text{and } \beta_{as}(t) = 1 - \exp(-0.2t^{0.5}) \quad (2-26)$$

f'_c refers to the concrete cylinder strength and t refers to the age (days) of the concrete at the time considered.

From experimental results performed by Divakar and Dilger (1988), to analyse the shrinkage in concrete structures, it was found that shrinkage deformations were significantly different in cracked and uncracked states. For accurate estimation of long-term deflections due to shrinkage, it becomes necessary to account for this difference. It is interesting to note that the EC2 (2004) approach for determining the shrinkage curvature $1/r_{cs}$, is the only method presented which accounts for the differences between the cracked and uncracked states.

Direct Tensile Strength of Concrete and Cracking Moment

The material properties that influence the deflection prediction for a flexural member have included the elastic theory, to determine the amount of cracking for a section, the effect of creep to reduce the modulus of elasticity and the effect of shrinkage strain that increases the final time-dependent deflection. The next aspect concerning the material properties, include the tensile strength of concrete.

The direct testing of concrete in uniaxial tension is more difficult than for steel or timber. Relatively large cross-sections are required to be representative of the concrete, and, because the concrete is brittle, it is difficult to grip and align. Eccentric loading and failure at or in the grips is then difficult to avoid, thus more indirect tests are preferred according to Illston and Domone (2001). These tests include the splitting test and the flexural test. The tensile strength due the splitting strength is denoted $f_{t,c}$ and the tensile strength due to the flexural test is known as the modulus of rupture, f_r .

Tensile strengths determined from the different methods will differ because of differences in stress distribution. A comparison is made in Figure 2-8 which also shows that the tensile strength increases for an increase in concrete strength, but not at the same rate (Robberts & Marshall, 2008)(Illston & Domone, 2001).

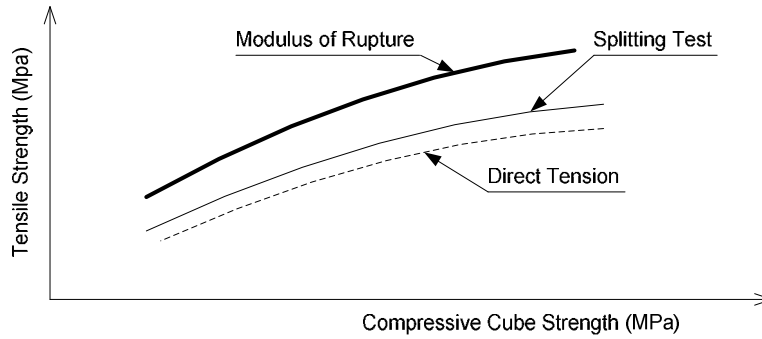


Figure 2-8: The relationship between direct and indirect tensile strength measurements and compressive strength (Illston & Domone, 2001)(Robberts & Marshall, 2008).

The tensile strength of concrete is an important property because the slab will crack when the tensile stress in the extreme fibre is exceeded. The degree of restraint to shrinkage movements will influence the effective tensile strength of the concrete (Webster & Brooker, 2006), as will be explained in Section 2.2.2.

The tensile strength of concrete is approached differently from each design standard. Table 2-6 shows the approach by the various design standards under consideration.

Table 2-6: Various equations on how the design standards incorporate the tensile strength in deflection prediction.

Design Standard	Tensile Strength	Cracking Moment, M_{cr}
<p>ACI 318 (2002) (clause 9.5.2.3) The modulus of rupture is a function of the compressive cylinder strength of concrete.</p>	$f_r = 0.623\sqrt{f'_c} \text{ [MPa]}$ for normal-weight concrete	$M_{cr} = \frac{f_r I_g}{y_t} \text{ [kNm]}$
<p>BS 8110 (1997) (Figure 3.1) It is the assumed maximum tensile strength of the concrete between the cracks (tension stiffening), that is fixed for all concrete strengths.</p>	$f_t = 1.0 \text{ MPa} \text{ (short-term)}$ $f_t = 0.55 \text{ MPa} \text{ (long-term)}$	No equation for the cracking moment exists. Applied moment is reduced due to concrete in tension between the cracks (tension stiffening) determined by the f_t value.
<p>EC 2 (2004) (Table 3.1) Tensile strength is obtained as a function of the compressive cylinder strength of concrete.</p>	$f_t = 0.3f'_c{}^{(2/3)}$ for $\leq C50/60$ $f_t = 2.12 \ln(1 + (f'_c + 8)/10)$ for $> C50/60$ [MPa]	$M_{cr} = \frac{f_t I_u}{h - x_u} \text{ [kNm]}$
<p>SABS 0100-1 (2000) (clause A.2.4.1.1) The modulus of rupture is a function of the compressive cube strength of concrete.</p>	$f_r = 0.65\sqrt{f_c} \text{ [MPa]}$ for unrestraint beams and slabs $f_r = 0.30\sqrt{f_c} \text{ [MPa]}$ for restraint beams and slabs	$M_{cr} = \frac{f_r I_g}{y_t} \text{ [kNm]}$

The variables used in the Table 2-6 include:

- f_r is the modulus of rupture;
- f'_c is the compressive cylinder concrete strength;
- M_{cr} is the cracking moment of the element;
- I_g is the gross moment of inertia of the element's cross-section;
- y_t is the distance from the centroidal axis of the concrete section, to extreme fibre in tension;
- f_t is the tensile strength of concrete;

- I_u is the moment of inertia of an uncracked section taking the effect of tension and compression steel into consideration;
- x_u is the neutral axis of an uncracked section taking the effect of tension and compression steel into consideration;
- h is the total depth of the section; and
- f_c is the compressive cube concrete strength.

Deflections depend on the concrete tensile strength in the slab at loading that can be estimated from tensile tests on control specimens or from the concrete compressive strength, as seen from Table 2-6. It is evident that there is little consensus on the magnitude of concrete tensile strength that should be used in deflection calculations (Vollumn, 2002).

Poisson's Ratio

The Poisson's Ratio effect, defined simply as the ratio of lateral strain to longitudinal strain, is normally neglected in practical concrete deformation calculations. This is due to its relatively small elastic value to begin with, the fact that creep Poisson's Ratio tend to be even smaller, and such structures as slabs are relatively insensitive to the effect, which is given by $(1-\nu^2)$ (Branson, 1977). Elastic values of Poisson's Ratio normally range from 0.15 to 0.25 (Robberts & Marshall, 2008), with a typical value for design taken as

$$\nu = 0.2 \quad (2-27)$$

The shear modulus, G , of concrete may be calculated using the Poisson's Ratio and the modulus of elasticity, E_c .

$$G = \frac{E_c}{2(1+\nu)} \quad (2-28)$$

2.2.2 Intrinsic Parameters: Reinforced Flat Slab Behaviour

Intrinsic parameters are related to local phenomena that contribute to cracking and shrinkage restraint, and increase the stiffness of a flexural member (tension stiffening). The topics discussed in

this section include tension stiffening, the effect of shrinkage restraint on the modulus of rupture and the consequences due to these effects. This parameters' explanation aims to discuss the complex behaviour of flat slab structures relative to normal beams and how these phenomena are to be taken into account with mathematical expressions and factors.

Tension Stiffening

An understanding of the interaction of reinforcement and the surrounding concrete is fundamental to the understanding of the behaviour of reinforced concrete. These include an understanding of bond behaviour, of cracking behaviour and of the related problem of tension stiffening. Traditionally, it is assumed in the design of reinforced concrete that concrete carries no tension. Based on this assumption, and assuming elastic behaviour of the steel and the concrete in compression, it is possible to calculate the stresses and strains in the concrete and the reinforcement and hence the deformations of the member. In practice, it is found that this procedure over-estimates the deformations because the concrete in tension surrounding the reinforcement does, on average, carry some stress, even after cracking. This reduction in deformation or increase in stiffness is referred to as tension stiffening (Beeby & Scott, 2006). Tension stiffening only has a relatively minor effect on the deformation of heavily reinforced members but is highly significant in lightly reinforced members such as slabs (Scott & Beeby, 2005). A principal finding of the research, according to Beeby and Scott (2006), has been that tension stiffening decays rapidly and will reach its long-term value of approximately half the short-term value in a period less than 30 days and generally less than 20 days.

There are a number of mechanisms which lead to a reduction in tension stiffening. These include creep, extension of internal cracks, shrinkage restraint, the formation of new surface cracks and sudden internal events (Beeby & Scott, 2006).

Creep

Since the concrete surrounding the reinforcement is supporting tensile stresses, some degree of creep will occur. This can differ significantly from creep in compression and the differences appear to depend on the nature of the curing regime. In practice, it is commonly assumed that creep in tension and compression is the same. In the case of tension stiffening, the problem is not straightforward since the strain in the reinforcement, and the strain imposed on the concrete, does

no change greatly and therefore the issue is more one of relaxation than creep. These are adherent concepts of the same phenomenon. It should be noted that, while the compressive stresses in the compression zones of beams or slabs tend to be fairly high, the average tensile stresses in the concrete surrounding the reinforcement are low (commonly in the order of 1.0 MPa in the short-term). Since creep is proportional to stress, the creep is relatively small. The stress will reduce from the tensile strength of the concrete at initial cracking to a much lower level as cracking develops; the creep might be in a creep recovery mode and could be very small or even negative, depending on the rate of loading. Creep can be expected to be greater in members loaded at a level only just above the cracking load because the tensile stresses will be higher levels. Overall, the effects of creep are likely to be small and difficult to predict (Beeby & Scott, 2006).

Extension of Internal Cracks

Goto (1971) carried out tests on tension specimens which showed that internal cracks develop from the ribs on the deformed bar. The tests suggest that the cracks are the longest near the face of the concrete and reduce in length more or less linearly with increasing distance from the face. This led Beeby and Scott (2006) to suggest that, on the formation of a primary crack, internal cracks formed as shown in Figure 2-9. Since the steel strain is greater than the tensile strain capacity of the concrete over the whole transfer length (S_0), it was suggested by Beeby and Scott (2006) that the internal cracking formed over the whole of S_0 almost instantaneously on the formation of the major surface cracks. With time, it seems likely that, although few new internal cracks should form, the existing internal cracks could lengthen, thus decreasing the stiffness of the connection between the bars and the surrounding concrete and hence decreasing the stress transferred to the concrete over the transfer length.

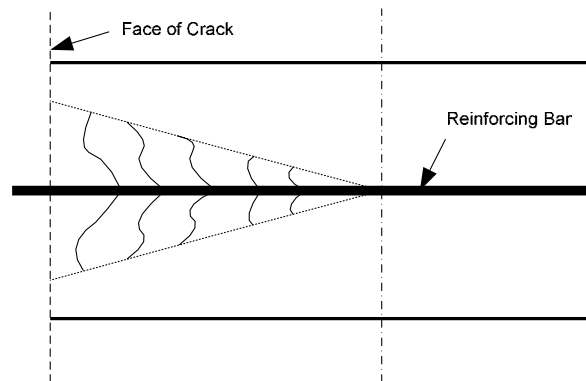


Figure 2-9: Internal cracks as established by Goto (1971).

Shrinkage Restraint

The effect of shrinkage restraint on deformation (deflection) is discussed in the Section that follows.

It has been suggested by Beeby and Scott (2006) that the major cause of the decrease in tension stiffening with time is an increase in cumulative damage. To some extent this is caused by the formation of further surface cracks but to a larger extent, this seems likely to be the result of internal phenomena. It is suggested that the most likely internal phenomena are related to internal cracking where there are three possibilities: increase in the number of internal cracks, increase in the length of internal cracks and breaking through of the internal crack nearest to crack surfaces into the cracks.

It should be noted that the change in deformation owing to the loss of tension stiffening is relatively small compared with the initial deformation. This is not to be confused with the situation in more heavily reinforced flexural members where the long-term deformation is dominantly the result of creep in the compression zone, which can lead to large changes in deformation.

The practical consequence of this discussion is that, when calculating the increment in the deflection expected to occur after installation of finishes and partitions, it will be more appropriate to assume the long-term value of tension stiffening to be acting throughout the whole period considered. This differs from current practice where the short-term value for tension stiffening is assumed to be acting at the time of installation of the partitions and finishes. This assumption will lead to a rather large estimate of the initial deflections but a rather smaller value of the deflection occurring after installation of the partitions and finishes. The total deflection will be unaffected (Scott & Beeby, 2005).

Beeby and Scott (2006) also suggested that the loss of tension stiffening with time is largely attributed to an increase in cumulative damage which results from the reduction in tensile strength of concrete with time under load, as is discussed below.

Modulus of Rupture due to Shrinkage Restraint

For two of the design standards, namely the ACI 318 (2002) and the SABS 0100-1 (2000), the modulus of rupture, f_r , is the determining variable for calculating the cracking moment, M_{cr} . The EC2 (2004) requires an accurate prediction of the tensile strength of concrete, f_t , to determine M_{cr} .

To determine the initial deflections, the M_{cr} as determined from the Design standards are adequate, but for time-dependent deflection some short-comings have been identified according to Scanlon and Bischoff (2008) and Vollum (2002). Practical recommendations for a lower cracking moment to account for shrinkage restraint and preloading from construction loads are found to have a significant influence on deflection of lightly reinforced concrete members.

It is well known that tensile stresses can be induced in a concrete member due to shrinkage under drying conditions when the member is restrained. Several sources of shrinkage restraint can be identified in concrete beams and slabs. These include embedded reinforcing bars, stiff supporting elements, adjacent portions of slabs placed at different times and nonlinear gradient of shrinkage strains over the thickness of a member. Development of these tensile stresses is time-dependent, as shown in Figure 2-10 but the nett effect is a reduction in flexural stiffness resulting from the formation of cracks due to the combined effects of stresses caused by shrinkage restraint and applied loading (Scanlon & Bischoff, 2008).

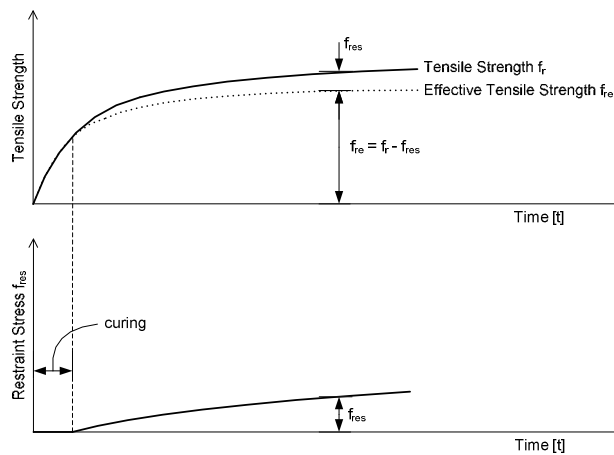


Figure 2-10: Development of restraint stresses in a beam (Scanlon & Bischoff, 2008).

Restraint stresses decrease the cracking moment M_{cr} of the member under applied loads by reducing the effective tensile strength of modulus of rupture of the concrete.

$$f_{re} = f_r - f_{res} \quad (2-29)$$

$$M'_{cr} = f_{re} \frac{I_g}{y_t} = \frac{f_{re}}{f_r} M_{cr} \quad (2-30)$$

where the modulus of rupture of concrete, f_r , is reduced by the restraint stress f_{res} . The value M_{cr} is the unrestrained cracking moment based on f_r and y_t is the distance from the centroidal axis of the uncracked section to the tension face of the section.

Time-dependent stresses that develop in a member restrained with embedded reinforcing bars can be calculated based on the consideration of equilibrium and strain compatibility for an assumed value of free shrinkage strain (Scanlon & Bischoff, 2008). f_{res} is the tensile stress induced at the extreme tensile fibre of concrete due to shrinkage restraint. For uniform shrinkage f_{res} is given by:

$$f_{res} = E_s \varepsilon_{cs} S_u (h - x_u) / I_u + A_s E_s \varepsilon_{cs} / [A_c (1 + \alpha_e (A_s / A_c))] \quad (2-31)$$

where E_s is the modulus of elasticity of steel, ε_{cs} is the free shrinkage strain, S_u is the moment of area of the reinforcement about the centroid of the uncracked section, h is the section depth, x_u is the depth to the neutral axis for the uncracked section and I_u is the moment of inertia of the uncracked section. Then, A_s is the area of tension reinforcement, A_c is the area of concrete and α_e is the modular ratio (Vollum, 2002).

The calculated member stiffness is reduced when a lower cracking moment is used in the expression for the effective moment of inertia. The study done by Bischoff and Scanlon (2008) also pointed out that the shrinkage restraint stress has a more significant effect on flexural stiffness as the reinforcement ratio decreases. It is therefore a more important consideration for slabs than for more heavily reinforced beams.

The restraint stresses decrease the cracking moment considerably at lower reinforcing ratios as proven by Bischoff and Scanlon (2008), as this has little effect on member stiffness for reinforcing ratios greater than approximately 1% when the effective moment of inertia is computed under full service loads. The full service load is at least three times greater than the cracking moment when steel reinforcement ratios are greater than 1%, and the magnitude of cracking moment has little effect on member stiffness at this load level since $I_e \approx I_{cr}$ when $M_a/M_{cr} > 3$ (Bischoff & Scanlon, 2008).

Consequences due to loss of Tension Stiffening and Reduced Cracking Moment

A study conducted by Vollum (2002) investigated how the phenomena of the loss of tension stiffening and a reduced cracking moment influence the prediction of long-term deflections. Vollum concluded that the loss of tension stiffening may be accounted for by using a β value when calculating the effective moment of inertia I_e , for a Section and using M'_{cr} , as in Equation 2-31, to account for a reduced cracking moment due to shrinkage restraint.

Vollum (2002) concluded that tension stiffening is lost more rapidly in slabs which crack extensively on loading than in slabs which barely crack on loading. Shrinkage is not the main cause of loss of tension stiffening in cracked members after loading. Modelling loss of tension stiffening after loading in cracked section using a β factor within the effective moment of inertia I_e , seems adequate for practical purposes. The value of β depends on whether the section is cracked or not. Vollum (2002) also found that slabs that suffer significantly cracking at loading may require $\beta = 0.7$ between one and two days, reducing linearly to 0.6 at seven days and 0.5 at 28 days, for predicting deflections reasonably. While a slab which is uncracked or barely cracked, a $\beta = 1.0$ is sufficient.

Table 2-7 summarizes the variables required for long-term deflection prediction incorporating the effect of loss of tension stiffening and a reduced cracking moment due to shrinkage restraint.

Table 2-7: Distinction between short- and long-term deflections concerning the cracking moment and β factor (Vollum, 2002).

Moment	Short-Term Deflections		Long-Term Deflections	
	Cracking Moment	β factor	Cracking Moment	β factor
$M_a < M_{cr}$ (Section not cracked)	$M_{cr} = M_{cr}$	$\beta = 1.0$	$M_{cr} = M'_{cr}$	$\beta = 1.0$
$M_a \geq M_{cr}$ (Section cracked)	$M_{cr} = M_{cr}$	$\beta = 0.7$ (for 1 – 2 days) $\beta = 0.6$ (for 7 days)	$M_{cr} = M'_{cr}$	$\beta = 0.5$ (for 28 days or longer)

Vollum (2002) also determined that the long-term deflections were governed by cracking during construction. The fact that the β factor in Table 2-7 reduces to less than one when $M_a \geq M_{cr}$ is proof of this phenomenon. Tension stiffening is lost too rapidly in the first few weeks after loading to be attributable to shrinkage, unless the applied moment is near the cracking moment.

The intrinsic parameters include the occurrence of tension stiffening and the reduction in the cracking moment due to shrinkage restraint. The contribution of tension stiffening greatly reduces the deformation of lightly reinforced concrete members, but tension stiffening decreases with time and the development of cumulative crack damage. The effect of shrinkage restraint reduces the cracking moment, which in turn reduces the member stiffness. These effects need to be accounted for using a β factor for tension stiffening and an effective cracking moment for shrinkage restraint as is presented in Table 2-7.

2.2.3 Extrinsic Parameters: Loading History and Construction Methods

This section discusses the extrinsic factors which include how the structure is built and the effects of the loading history applied to the slab on a global level. The loading history (sequence) and timing may be critical in determining the deflection of a suspended slab because it will influence the point at which the slab will crack and is used to calculate the creep factors for the slab. The loading sequence may vary, depending on the construction method (Webster & Brooker, 2006).

Building structures are often subjected to loads during construction before the concrete has attained its specified 28-day strength. Significant loads can arise from shoring and reshoring procedures in multi-story construction in addition to loads from personnel, equipment, and temporary storage of construction materials such as drywall or reinforcing bars. These loads can reach a level approaching and sometimes exceeding the design dead plus live load. Quite often the magnitude of load depends on the shoring/reshoring sequence used for construction. Others have also emphasized the importance of construction loading on long-term serviceability of floor systems (Scanlon & Bischoff, 2008) (Webster & Brooker, 2006).

Figure 2-11 gives a typical representation of loading during and after construction period. Loading during the construction phase is shown as a step function to represent a typical shoring/reshoring sequence, but can also represent construction loads due to personnel, equipment, and materials. Sustained loading after the construction phase consist of the dead load plus the sustained portion of live load (quasi-permanent load). Variable live load is applied intermittently during the life of the structure.

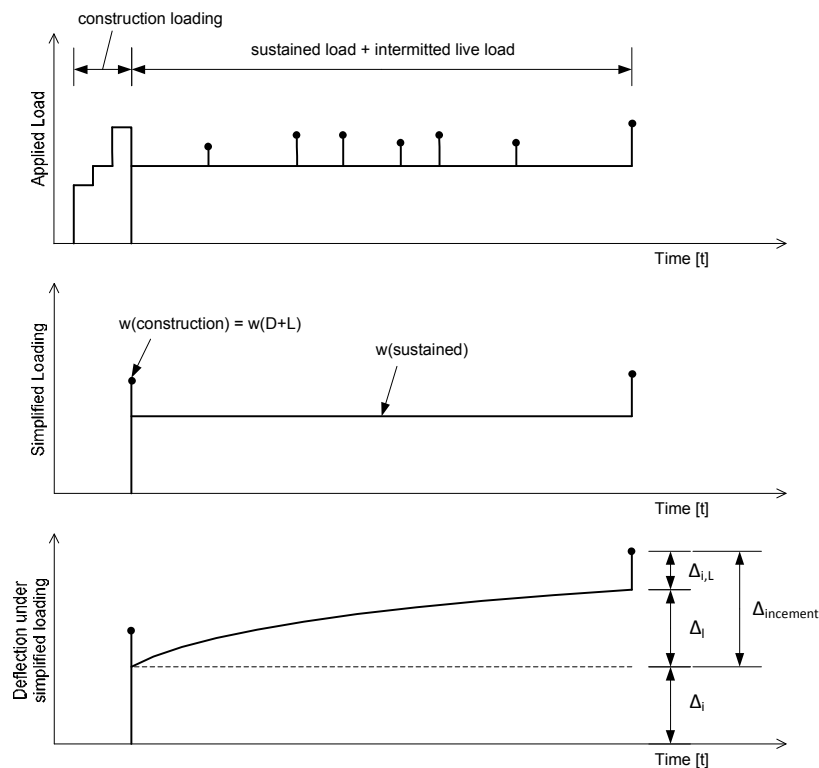


Figure 2-11: Development of a typical loading history and deflection prediction method taking the load history into account (Scanlon & Bischoff, 2008).

In most cases, the deflection occurring after installation of a non-structural element is the most critical condition. This deflection consists of time-dependent deflection from the sustained portion of load and immediate deflection from the remaining live load. Because the time-dependent deflection is typically based on a multiplier of initial deflection from the sustained load (quasi-permanent load), construction loads prior to installation of the non-structural elements can affect the stiffness of the floor system and should be taken into account in the deflection calculations (Scanlon & Bischoff, 2008).

The simplified loading history shown in Figure 2-11 is used as the basis for deflection checks. Maximum estimated construction loads are assumed to be applied just prior to installation of the non-structural element and are taken as the specified dead plus live load unless more detailed information is available. Initial deflection under the sustained load level (quasi-permanent load level) is then calculated using an effective moment of inertia corresponding to the full dead plus live load. Time-dependent deflection is taken as a multiple of this computed value. The same moment of inertia is also used to calculate the remaining load deflection and is much simpler than considering different moments of inertia for dead load and dead plus live load as commonly assumed in the past (Scanlon & Bischoff, 2008).

Although methods are available for calculating construction loads due to shoring and reshoring, the method of construction and shoring sequence are usually unknown at the design stage when deflection checks are being made. Nor will the engineer know the stage at which non-structural elements will be installed as this is usually the contractor's responsibility. The proposed simplified loading history recognizes that these loads can reach and sometimes exceed the specified design loads and, consequently, have a significant effect on the extent of cracking in the member prior to the service loading. Once the construction sequence is known, the corresponding loading history can be used to determine the maximum load expected during construction (Scanlon & Bischoff, 2008).

Commercial pressures often lead to a requirement to strike the formwork as soon as possible and move on to subsequent floors, with the minimum of propping. Tests on flat slabs have demonstrated that as much as 70% of the loads from a newly cast floor (formwork, wet concrete, construction loads) may be carried by the suspended floor below (Webster & Brooker, 2006).

2.2.4 Deflection Derivation from Moment–Curvature Theorem

In this section the empirical equation to calculate the deflection for a slender member is presented. It is shown in Appendix A that the curvature expression for a deflection member is given by Equation 2-32.

$$\frac{1}{r} = \frac{M}{E_c I_x} \quad (2-32)$$

Deflections may be calculated directly from Equation 2-32 by calculations of the curvatures at successive sections along the element and the use of a numerical integration technique such as that proposed by Newmark. Alternatively, it is shown in Appendix A that a simplified approach may be used. The deflection is calculated using Equation 2-33.

$$\Delta = KL^2 \frac{M}{E_c I_e} = KL^2 \frac{1}{r} \quad (2-33)$$

where K is the deflection coefficient dependent on the bending moment diagram, L is the effective span of the member, M the applied moment, E_c is the modulus of elasticity of the member, I_e is the effective moment of inertia, and $1/r$ refers to the curvature (SABS 0100-1, 2000).

The moment of inertia at x along the length of the beam, I_x , is re-evaluated as explained in section 2.3, to reduce to an effective moment of inertia, I_e .

2.2.5 Boundary Conditions and Deflection Coefficients

The factors influencing slender reinforced concrete member deflections are discussed in this section. These factors include the material properties, the intrinsic parameters such as tension stiffening and shrinkage restraint, and the extrinsic parameters including the loading history and the construction

methods. Following the discussion on the factors influencing deflection development, an expression for the deflection prediction is derived. This section discusses one of the variables within the deflection prediction expression, the deflection coefficient, K .

The deflection coefficient, K , takes the shape of the bending moment or curvature diagram into account for the deflection expression. The deflection expression reduces to Equation 2-33 for simple application to a deflected beam problem. The different values of K can be obtained from a table summarizing several cases of beams with different loadings and boundary conditions, being simply supported, continuous or cantilevered. The derivations for the values of K are presented in Kong and Evans (1987) and Branson (1977). Table 2-8 indicates where these tables may be referenced from the different design standards.

Table 2-8: References for deflection coefficients K from design standards.

Design Standards	Reference
BS 8110 (1997)	Table 3.1
SABS 0100-1 (2000)	Figure A.2
Branson (1997)	Chapter 3

The deflections due to shrinkage are also determined using Equation 2-33 with K_{sh} being the deflection coefficient, instead of K . The values of K_{sh} are fully derived by Branson (1977). Only a summary of the final values of K_{sh} is shown below:

Table 2-9: Various Shrinkage Deflection Coefficients for Support Conditions (Branson, 1977).

Support Conditions	Shrinkage Deflection Coefficient, K_{sh}
Cantilever Beam	0.500
Simple Beam	0.125
Two-Span Continuous Beam	0.084
Continuous Beam with three or more Spans	
End Span	0.090
Interior Span	0.065

2.2.6 Time-Dependent Deflections

This section discusses the time-dependent deflection of reinforced concrete members. This involves the interaction of many factors as have been discussed in the previous sections. Uncertainties in material properties and loading make the prediction of deflections a difficult task at the design stage. The following discussion explains the difference between short- and long-term deflections, as well as how the deflection process takes place.

Initial or Short-Term Deflection

The principle factors which affect the initial or short-term deflection of reinforced concrete flexural members under service loads are (Branson, 1977):

- Modulus of Elasticity, E_c
- Load Distribution and Support Conditions (Section on Continuity)
- Variable Cross-Section
- Load Level
- Degree of Cracking along the beam.

The initial load deflection curve of a beam with increasing load is a flat S-shaped curve as shown in Figure 2-12. It has five parts (Varghese, 2005):

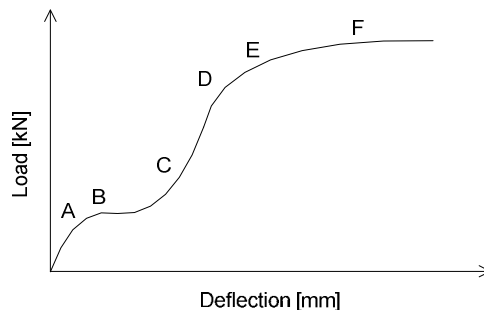


Figure 2-12: Load Deflection Diagram (S-Curve) of a beam (Varghese, 2005).

1. An almost linear portion OA with cracking of the beam starting at A due to tension in concrete.
2. A curvilinear cracked-portion ABC with increasing loads leading to decrease in the value of the moment of inertia I and hence in the rigidity EI .
3. A linear part beyond C extending to D, where EI remains more or less constant (in normal beams this portion corresponds to the service loads where the stress in concrete is of the order of one-third cube strength).
4. A curvilinear part DE where further cracking of concrete occurs.
5. An almost horizontal part beyond E, where a small increase in load produces a large increase in deflection.

Long-Term Deflections

The deflection of a reinforced concrete flexural member increases with time, mainly due to (Pillai & Menon, 2003):

- differential shrinkage (causing differential strains across the cross-section, resulting in curvature); and
- creep under sustained loading.

The factors affecting shrinkage and creep are related to the environment, concrete material and loading history. These have been described in detail in Sections 2.2.1 and 2.2.3. The combined long-term deflection due to shrinkage and creep effects may be as large as two to three times the short-term deflection due to dead and live loads (Pillai & Menon, 2003).

Additional factors which can contribute to increased long-term deflection include formation of new cracks, widening of earlier cracks, and effects of repeated load cycles (Pillai & Menon, 2003). These factors are discussed in Sections 2.2.2 and 2.2.3. The deflection of slabs and beams increases with time for five to nine years after stripping according to Taylor and Heiman (1977), as is shown in Figure 2-13.

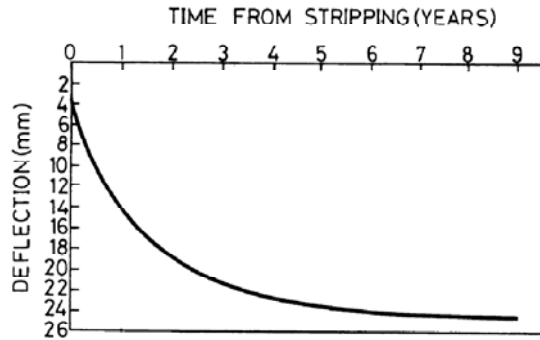


Figure 2-13: Long-Term Deflection of actual structure according to Heiman and Taylor (1977).

The total deflection for a flexural member, slab or beam, may be calculated as follows:

$$(2-34)$$

The long-term deflection, Δ_l uses the equations for the initial deflections, but with the difference in incorporating the long-term properties acquired to account for the increased in cracking and creep due to permanent load. The shrinkage deflection, Δ_{cs} already incorporates the time-dependent effects and is simply added to the long-term deflection. The additional initial deflection due to the temporary imposed load, $\Delta_{i,add}$, is calculated and summed with the rest to obtain the total long-term deflection.

The Deflection Process

The deflection phenomenon for a slab model cast under laboratory conditions was recorded by Taylor (2009) in a piece by piece fashion to discuss the deflection of reinforced concrete. The deflection process as observed by Taylor is described in the following paragraphs.

When the temporary supports are removed from a model slab in a laboratory, initial deflection occurs. At low load levels the slab should undergo elastic deflection. At high load level flexural cracking should occur and some slab cross-sections should therefore be cracked; this portion of the initial deflection is not entirely elastic.

$$\Delta_{initial} = \Delta_{initial,elastic} + \text{increase due to cracking} \quad (2-35)$$

In the long-term, initial deflection under relatively constant load will increase because of shrinkage and creep effects, and increased cracking. Concrete drying shrinkage will cause warping of the slab in zones where there are unequal areas of top and bottom reinforcement. It is usual to omit top reinforcement at mid-panel zones, and so they will warp downwards, thus contributing to long-term deflection. The duration and magnitude of warping is directly proportional to the free drying shrinkage of the concrete. It continues at a decreasing rate with increasing time for several years after casting, and is independent of load.

Concrete creep under an effectively constant sustained load also contributes to the long-term deflection at a decreasing rate with increasing time for several years after casting. Both compressive and tensile creep occurs.

Deflection increases with increasing cracking of the slab cross-sections. Cracking is caused when the tensile stress, induced by flexure, shrinkage and thermal effects acting simultaneously, becomes greater than the tensile strength of the concrete at any time. As concrete drying shrinkage increases with time, then cracking could also be expected to increase with time. When a high level of concrete tensile stress (above the proportional limit) is maintained for some time, more and more cracks will occur. Therefore a slab that is essentially uncracked at the time of stripping will gradually become more cracked, the effective moment of inertia will decrease, and this will contribute to long-term deflection (Taylor, 2009).

$$\Delta_{total} = \Delta_{initial} + \Delta_{shrinkage} + \Delta_{creep} + \text{long-term cracking} \quad (2-36)$$

The equation is simplified when the creep deflection is determined as the initial deflection due to permanent load multiplied by a determined factor to produce the long-term deflection. Any additional imposed load added to the structure is then added as an additional initial deflection. The total deflection reduces to

$$\Delta_{total} = \Delta_{initial,add} + \Delta_{shrinkage} + \Delta_{long-term} + \text{long-term cracking} \quad (2-37)$$

The effect of cracking is included in the effective moment of inertia of the deflection equations and may be removed from the equations. The equations simplify to the equations as was discussed above.

2.3 DEFLECTION PREDICTION ACCORDING TO THE DESIGN STANDARDS

This section presents comprehensively the deflection prediction methods available in the design standards considered in this study. For every design standard, the initial deflection, the shrinkage deflection, the long-term deflection and the methodology proposed for the flat slabs are discussed. The method to predict deflection is always considered as an alternative approach relative to the simplified span/effective depth approach, as discussed in Section 2.4.

The deflection prediction methods discussed in this section usually apply to beam elements. Section 2.5 discusses how these methods are applied to three-dimensional flat slab structures in order to determine a deflection at mid-panel.

2.3.1 Deflection Prediction according to the American Concrete Institute (ACI) 318-02

Reinforced concrete members subjected to flexure shall be designed to have adequate stiffness to limit deflections or any deformations that adversely affect strength or serviceability of a structure. (Clause 9.5.1, ACI 318, 2002).

Where deflections are to be computed, deflections that occur immediately on application of load shall be computed by usual methods for short-term deflection, considering effects of cracking and reinforcement on member stiffness. For the calculation of initial deflection of uncracked prismatic

members, the usual methods or short-term deflections may be used with a constant value of $E_c I_g$ along the length of the member. However, if the member is cracked at one or more sections, or if its depth varies along the span, a more exact calculation becomes necessary.

Short-Term Deflection

Unless stiffness values are obtained by a more comprehensive analysis, the initial deflection shall be computed with the modulus of elasticity E_c for concrete (clause 8.5.1, ACI 318, 2002) and with the effective moment of inertia, I_e , calculated as follows. I_e may not be greater than the gross moment of inertia, I_g (Section 2.2.1).

$$I_e = \left(\frac{M_{cr}}{M_a}\right)^3 I_g + \left[1 - \left(\frac{M_{cr}}{M_a}\right)^3\right] I_{cr} \quad (2-38)$$

where $M_{cr} = \frac{f_r I_g}{y_t} \quad (2-39)$

as the cracking moment and the modulus of fracture, f_r , as

$$f_r = 0.623 \sqrt{f'_c} \quad (2-40)$$

for normal weight concrete. The modulus of rupture is a function of the cylinder compressive strength of concrete, f'_c .

The initial deflection is then calculated using Equation 2-33. Creep and shrinkage effects are not applicable for short-term deflection calculations (ACI 318, 2002).

Shrinkage Deflection

The ACI 318 (2002) does not explicitly provide the expression for the shrinkage deflection. The design standard uses an expression combining the effects of shrinkage and creep. To allow a more specified comparison between the predicted shrinkage deflections from the various design standards, the shrinkage and creep influences are separated.

Branson (1977) suggested an empirical method for computing shrinkage curvature. The empirical derivation relates the proposition that the shrinkage curvature or slope of the strain diagram is a direct function of the free shrinkage and steel content, and an inverse function of the depth of the Section (Figure 2-14). The equation for shrinkage curvature, $1/r_{cs}$, is shown in Section 2.2.2., and is expressed as follows:

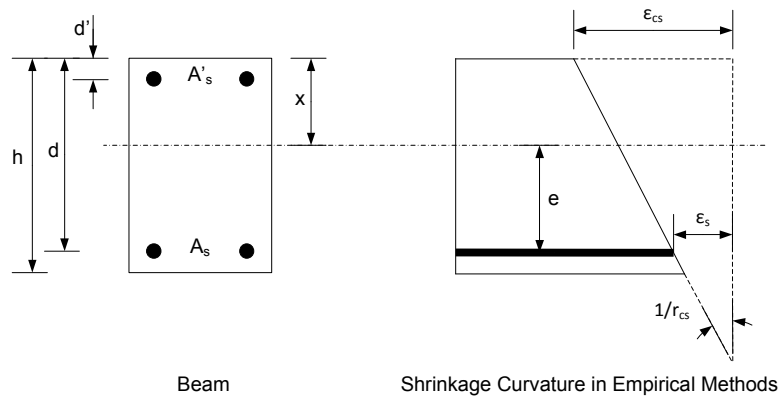


Figure 2-14: Assumed shrinkage curvature for empirical methods (Branson, 1977).

$$\frac{1}{r_{cs}} = 0.7 \frac{\epsilon_{cs}}{h} (\rho - \rho')^{1/3} \left[\frac{\rho - \rho'}{\rho} \right]^{1/2} \tag{2-41}$$

for $\rho - \rho' \leq 3.0\%$

The variables are defined as ϵ_{cs} for the free shrinkage strain, h for the depth of the section, $\rho = 100A_s/bd$ and $\rho' = 100A'_s/bd$. The area tension reinforcement is noted as A_s , b is the width of the section, d the effective depth and A'_s as the compression reinforcement for the section. The free

shrinkage strain, ϵ_{cs} is determined from recorded experimental results. Branson (1977) published tables for various curing conditions.

The shrinkage deflection is calculated as follows:

$$\Delta_{cs} = K_{sh} L^2 \frac{1}{r_{cs}} \quad (2-42)$$

where K_{sh} is the shrinkage deflection coefficient, L is the effective length of the span, and $1/r_{cs}$ is the shrinkage curvature from Equation 2-41.

Long-Term Deflection

The deflection computed in accordance with this section is the additional long-term deflection due to the dead load and the portion of the live load that will be sustained (permanent load) for a sufficient period to cause significant time-dependent deflections (ACI 318, 2002).

The long-term deflection for a flexural member shall be determined considering the effects of creep. The long-term deflection is a function of the initial deflection as suggested by Branson (1977). The long-term deflection, Δ_l , is given in Equation 2-43.

$$\Delta_l = k_r \cdot \phi \cdot \Delta_i \quad (2-43)$$

Where k_r is the reduction factor, ϕ is the creep coefficient and Δ_i is the initial deflection as a result of the moment due to the permanent load. The creep coefficient, ϕ is determined from recorded experimental results. Branson (1977) published tables for various curing conditions.

Branson (1977) recommends equation 2-44 for the reduction factor considering only the effects of creep.

$$k_r = 0.85 / (1 + CA'_s / A_s) \quad (2-44)$$

where $C = 50\rho$ and $\rho = A_s/bd$. The area tension reinforcement is noted as A_s , b is the width of the section, d the effective depth and A'_s as the compression reinforcement for the section. Simplifying this equation produces Equation 2-44.

$$k_r = 0.85 / (1 + 50 / \rho') \quad (2-45)$$

The ACI 318 (2002) uses an equation to account for both the effects of creep and shrinkage in Clause 9.5.2.5. The equation takes the same form as Equation 2-43, with a few changes due to the fact that two phenomena are considered. The factor, λ , is multiplied with the initial deflection due to the sustained load to obtain the long-term deflection. Even though the equation is not presented in the study the combined effect of both the shrinkage and creep equations will produce the same effect.

The initial deflection, Δ_i , required in Equation 2-43 is the short-term deflection calculated due to the permanent load. The similar equations to calculating the short-term deflection should be used, with the exception that the moment due to the permanent loads, M_p , should be used in Equations 2-38 and 2-33 (Robberts & Marshall, 2008).

The total deflection, Δ_t , is simply calculated by adding the long-term deflection, Δ_l , the shrinkage deflections, Δ_{cs} , and the additional initial deflection, $\Delta_{i,add}$, due to the remaining imposed load. The additional deflection is the difference between the short-term deflection calculated with the full service load, M_a and the permanent load, M_p .

$$\Delta_t = \Delta_l + \Delta_{cs} + \Delta_{i,add} \quad (2-46)$$

Refer to Section 2.5 to apply the above equations to predict deflections according to the ACI 318 (2002) for flat slab structures.

2.3.2 Deflection Prediction according to the British Standards (BS) 8110: Part 2: 1997

The British Standard's (BS) 8110: Part 2: 1997 deflection method is based on the curvature area method and is described in Clause 3.7. In this procedure, a reduction in the applied moment causing deflection is made, as in reality the concrete below the neutral axis can carry limited tension between the cracks. Its effect, called tension stiffening, can be considered as the reduction of moment causing deflection to $(M-\Delta M)$, where ΔM is the moment carried out by the tension in concrete (Varghese, 2005).

The BS 8110 method does not assume I_e , as in ACI 318 (2002) and SABS 0100-1 (2000). Instead, the method calculates $E_c I_{cr}$ for short-term and long-term loadings separately by using the appropriate $E_{c,i}$ and $E_{c,l}$ values, respectively (Varghese, 2005). The procedure is shown in the following paragraphs.

Short-Term Deflection

As explained in Section 2.2.1 the concept of a partially cracked section has been introduced. The BS 8110 (1997) uses a different approach to simulate a partially cracked section mathematically. For convenience during calculations, the maximum concrete tension, f_t at the centre of gravity of the steel, is 1.0 MPa for short-term loading and 0.55 MPa for long-term loading, which is independent of the applied moment as assumed in BS 8110. ΔM is the moment of these tensile forces about the neutral axis as shown in Figure 2-15 (Varghese, 2005).

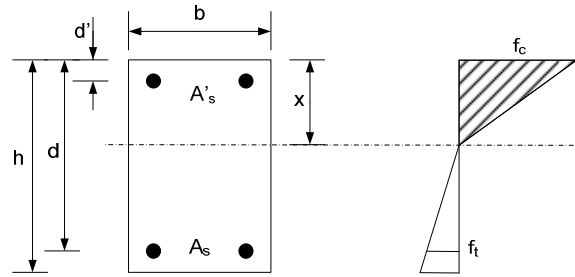


Figure 2-15: Effect of tension in concrete on Deflection on Beams (BS 8110, 1997).

Assuming f_t is the tensile concrete stress at the centre of gravity of the tensile reinforcing steel, we proceed as follows:

$$\text{Tension at the extreme tension fibre} = f_t \frac{h-x}{d-x} \quad (2-47)$$

Taking the moment of this triangular distribution of tension about the neutral axis of the section, the expression changes to:

$$\Delta M = \frac{b(h-x)^3}{3(d-x)} f_t \quad (2-48)$$

The moment causing curvature is $(M - \Delta M)$, therefore the initial curvature simplifies to

$$\frac{1}{r_i} = \frac{M - \Delta M}{EI} \quad (2-49)$$

If the applied moment M is larger than ΔM , Equation 2-49 will yield a positive curvature. It may then be assumed that the concrete below the neutral axis is cracked and $f_t = 1.0$ MPa for short-term deflections. Assuming the section is cracked, it is required that all other curvatures' variables be obtained from the cracked sectional properties, including x_{cr} and I_{cr} . When the applied moment M is

less than ΔM , Equation 2-49 will yield a negative curvature. This is obviously unrealistic, thus it may be assumed the applied moment is small enough not to crack the section. If no cracking occurs, then the section follows the properties of an uncracked Section and no tension stiffening occurs. In other words, ΔM plays no role and reduces to zero and the curvature variables should be obtained from the uncracked sectional properties. Table 2-10 summarizes the process:

Table 2-10: Summary of Initial Curvature Criteria for BS 8110 (1997).

Applied Moment	$M > \Delta M$	$M \leq \Delta M$
Section	Cracked	Uncracked
Initial Curvature	$\frac{1}{r_i} = \frac{M - \Delta M}{E_c I_{cr}}$	$\frac{1}{r_i} = \frac{M}{E_c I_u}$

For a simply supported beam, the short-term deflection is calculated using Equation 2-33. Creep and shrinkage effects are not applicable for short-term deflection calculations (Kong & Evans, 1987).

Shrinkage Deflection

A plain concrete member undergoing a uniform shrinkage would shorten without warping. However, in a reinforced concrete beam, the reinforcement resists the shrinkage and produces a curvature. Consider the beam section in Figure 2-16.

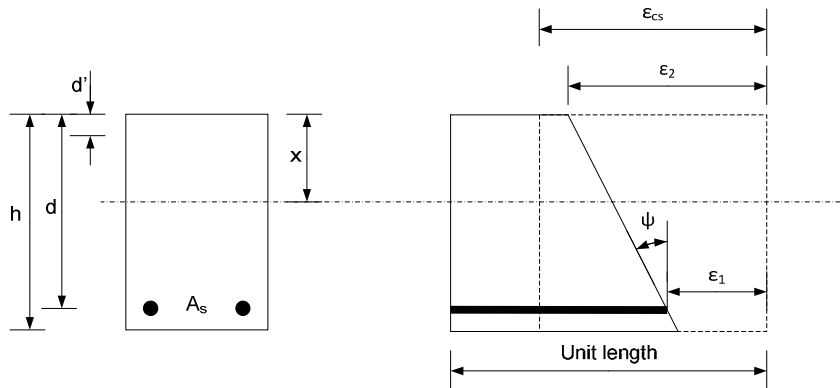


Figure 2-16: Deflection due to Shrinkage (BS 8110, 1997)(Kong & Evans, 1987).

A unit length of the beam is shown in the Figure 2-16. ϵ_{cs} represents the concrete shrinkage and is the uniform shortening which would occur over the unit length, has the beam been unreinforced; ϵ_1 is the actual shortening over the unit length, at the level of the tension reinforcement; ϵ_2 is the actual shortening at the top. It is thus seen that the shrinkage curvature $1/r_{cs}$ of the beam at the section considered is equal to the angle ψ . Therefore, the curvature may be derived from Figure 2-16 to be

$$\frac{1}{r_{cs}} = \frac{\epsilon_2 - \epsilon_1}{d} \quad (2-50)$$

Equation 2-50 reduces to Equation 2-51 when considering Figure 2-16. The shrinkage curvature is to be calculated separately in BS 8110 (1997) by the resulting Equation 2-51.

$$\frac{1}{r_{cs}} = \frac{\alpha_e S_{cr} \epsilon_{cs}}{I_{cr}} \quad (2-51)$$

Where α_e represents the modular ratio, S_{cr} represents the first moment of area of the reinforcement about the centroid of the cracked beam section; ϵ_{cs} represents the concrete shrinkage and I_{cr} , the moment of inertia of the cracked beam section (Kong & Evans, 1987).

Values of concrete shrinkage ϵ_{cs} are given in BS 8110 (1997), Clause 7.4.

Long-Term Deflection

In assessing the total long-term deflection, the procedure of BS 8110 (1997) Clauses 3.6 and 3.7 may conveniently be summarized as follows (Kong & Evans, 1987):

- Calculate the instantaneous curvature $1/r_{it}$ under the total load and the instantaneous curvature $1/r_{ip}$ due to the permanent load. The instantaneous curvature due to non-permanent load $1/r_{in} = (1/r_{it} - 1/r_{ip})$

$$\frac{1}{r_{in}} = \frac{1}{r_{it}} - \frac{1}{r_{ip}} = \frac{M_a - M_p}{E_c I_{cr}} \quad (2-52)$$

- Calculate the long-term curvature $1/r_{ip}$ due to the permanent load.

$$\frac{1}{r_{ip}} = \frac{M_p - \Delta M}{E_{eff} I_{cr}} \quad (2-53)$$

- Add the long-term curvature due to permanent load $1/r_{ip}$ to the instantaneous curvature due to non-permanent load $1/r_{in}$, to obtain the long-term curvature $1/r_l$.

$$\frac{1}{r_l} = \frac{1}{r_{ip}} + \frac{1}{r_{in}} \quad (2-54)$$

- Calculate the shrinkage curvature $1/r_{cs}$.

$$\frac{1}{r_{cs}} = \frac{\alpha_e S_{cr} \epsilon_{cs}}{I_{cr}} \quad (2-55)$$

- The long-term deflection, Δ_l and shrinkage deflection Δ_{cs} , can be obtained using the curvature-area theorems or Equations 2-33 and 2-42, respectively. Use the deflection coefficient K , for the long-term curvature $1/r_l$ and the shrinkage deflection coefficient K_{sh} , for the shrinkage curvature $1/r_{cs}$. (Even though BS 8110 (1997) does not calculate the long-term deflection, Δ_l and shrinkage deflection Δ_{cs} separately, it is done here to simplify the comparison between the design standards. Usually a total curvature $1/r$ is considered and the deflection calculated from the curvature using the deflection coefficient K and span length L .)
- Find the total deflection, Δ_t by adding the long-term deflection, Δ_l and the shrinkage deflection, Δ_{cs} . (Note that the additional initial deflection is included within the $1/r_{in}$ curvature)

$$\Delta_t = \Delta_l + \Delta_{cs} \quad (2-56)$$

Refer to Section 2.5 to apply the above equations to predict deflections according to the BS 8110 (1997) for flat slab structures.

2.3.3 Deflection Prediction according to the Eurocode 2: Part 1-1

According to Eurocode 2: Part 1-1 (EC2, 2004), the limit state of deformation may be checked by either:

- By limiting the span/depth ratio, according to Clause 7.4.2 or
- By comparing a calculated deflection, according to Clause 7.5.3, with a limiting value.

It is also noted that the actual deformations may differ from the estimated values, particularly if the values of applied moments are close to the cracking moment. The differences will depend on the dispersion of the material properties, on the environment conditions, on the load history, on the restraint at the supports, ground conditions, ect (Webster & Brooker, 2006).

Where a calculation is deemed necessary, the deformation shall be calculated under the serviceable load condition. The calculation method adopted shall represent the true behaviour of the structure under relevant actions to an accuracy appropriate to the objectives of the calculation.

Two methods for calculating deflection are presented below, and discussed in EC2 (2004). The rigorous method for calculating deflections is the most appropriate method for determining a realistic estimate of deflection. However, it is only suitable for use with computer software. The rigorous method uses a long-term modulus of elasticity together with a critical loading stage (loading stage at which cracking first occurs). The curvature for the beam or slab is determined at several points along the length of the beam or slab and repeated for all loading stages. If the deflection affects cladding and/or partitions, then the calculations are repeated for the frequent loading combination and the loading stage at the time of installation of the partitions and/or cladding. The two final deflections include (Webster & Brooker, 2006):

- Overall deflection due to the quasi-permanent combination.
- Deflection affecting the partitions or cladding which will be the frequent combination deflection less the deflection at the time of installation.

A more simplified method for calculating deflection is also presented in EC2 (2004). This method is the less tedious approach and is suggested for the swifter deflection calculation procedure. The rigorous method is similar to the simplified method but it is possible to carry out these calculations by hand, and roughly verify deflection results from computer software, or used where a computer is not available. The major simplification is that the effects of early age loading are not considered explicitly; rather an allowance is made for the effect when calculating the cracking moment. Simplified creep factors are used and deflection from the curvature of the slab is approximated using a factor (Webster & Brooker, 2006).

Short-Term Deflection

Members which are not expected to be loaded above the level which would cause the tensile strength of the concrete to be exceeded anywhere within the member should be considered to be uncracked. Members which are expected to crack, but may not be fully cracked, will behave in a manner intermediate between the uncracked and fully cracked conditions and, for members subjected mainly to flexure, an adequate prediction of behaviour is given by the following expression (EC2, 2004):

$$\alpha = \zeta\alpha_{II} + (1 - \zeta)\alpha_I \quad (2-57)$$

where α is the deformation parameter considered which may be, for example, a strain, a curvature or a rotation. α_I , α_{II} are the values of the parameter calculated for the uncracked and fully cracked conditions respectively and ζ is a distribution coefficient (allowing for tension stiffening) given by the following expression:

$$\zeta = 1 - \beta \left(\frac{M_{cr}}{M_a} \right)^2 \quad (2-58)$$

where $\zeta = 0$ for an uncracked section and β is a coefficient taking account of the influence of the duration of the loading or repeated loading on the average strain. For a single short-term loading, $\beta = 1.0$ and for sustained loads or many cycles of repeated loading, $\beta = 0.5$. M_a is the moment due to the serviceable load applied to the member and M_{cr} is the cracking moment calculated by Equation 2-62 to determine the point of first cracking (EC2, 2004).

If α in Equation 2-57 is assumed to represent the curvature, $1/r$, at a section while ignoring concrete in tension, and is rewritten using the curvature expression from Equation 2-32, the following expression is produced:

$$\frac{M_a}{E_c I_e} = \zeta \left(\frac{M_a}{E_c I_{cr}} \right) + (1 - \zeta) \left(\frac{M_a}{E_c I_u} \right) \quad (2-59)$$

If $\beta = 1.0$ for short-term loading, then Equation 2-58 reduces to

$$\zeta = 1 - \left(\frac{M_{cr}}{M_a} \right)^2 \quad (2-60)$$

Using Equation 2-59 and 2-60 the effective moment of inertia for short-term deflection prediction may be derived.

$$\begin{aligned} \frac{M_a}{E_c I_e} &= \left(1 - \left(\frac{M_{cr}}{M_a} \right)^2 \right) \left(\frac{M_a}{E_c I_{cr}} \right) + \left(1 - \left(1 - \left(\frac{M_{cr}}{M_a} \right)^2 \right) \right) \left(\frac{M_a}{E_c I_u} \right) \\ \frac{1}{I_e} &= \frac{1}{I_{cr}} - \left(\frac{1}{I_{cr}} - \frac{1}{I_u} \right) \left(\frac{M_{cr}}{M_a} \right)^2 \\ \Rightarrow I_e &= \frac{I_{cr}}{1 - \left(\frac{I_{cr}}{I_u} \right) \left(\frac{M_{cr}}{M_a} \right)^2} \leq I_u \end{aligned} \quad (2-61)$$

The cracking moment, M_{cr} , is calculated with the Equation 2-62 and is based on the uncracked properties of the section under inspection. M_a is calculated due to the quasi-permanent actions at the critical section (i.e. mid-span or at the support for cantilevers). Therefore M_{cr} should also be inspected at the critical section (Webster & Brooker, 2006).

$$M_{cr} = \frac{f_t I_u}{h - x_u} \quad (2-62)$$

f_t is the highest stress reached under concentric tensile loading (direct tensile strength) according to Clause 3.1.2 from EC2 (2004). I_u and x_u depend on the properties of a cracked section (Section 2.2.1)

and h is the height of the section. An equation for f_t in terms of the cylinder compressive stress, f'_c , is provided in Table 3.1 in EC2 (2004):

$$f_t = 0.3f'_c{}^{(2/3)} \quad (2-63)$$

for \leq Concrete 50/60

$$f_t = 2.12\ln(1 + (f'_c + 8)/10) \quad (2-64)$$

for \leq Concrete 50/60

If only the flexural tensile strength of the concrete, f_{tf} , is provided, then the following approximation may be made. According to Clause 3.1.8 from EC2 (2004), the flexural concrete tensile strength of slender members depend on the concrete tensile strength and the depth of the cross-section in mm. The following relationship is suggested:

$$f_{tfl} = \max\{(1.6 - h/1000)f_t; f_t\}$$

On further inspection the main variable is h , height of the Section, and is the determining factor. If $h < 600$ mm then,

$$f_t = \frac{f_{tfl}}{(1.6 - h/1000)} \quad (2-65)$$

If $h > 600$ mm, then $f_t = f_{tf}$. These expressions may be used to convert the flexural tensile strength of concrete to the concrete tensile strength to be used to determine the cracking moment, M_{cr} in Equation 2-62.

Then, the short-term deflection may be calculated using Equation 2-33.

Shrinkage Deflection

The shrinkage curvature may be assessed using Equation 2-66.

$$\frac{1}{r_{cs}} = \epsilon_{cs} \alpha_e \frac{S}{I} \quad (2-66)$$

where $1/r_{cs}$ is the curvature due to shrinkage, ϵ_{cs} is the free shrinkage strain and S is the first moment area of the reinforcement about the centroid of the section. I is the moment of inertia of the section and α_e is the effective modular ratio based on the effective modulus of elasticity of the concrete, E_{eff} . S and I should be calculated for the uncracked condition and the fully cracked conditions. The shrinkage curvature may be assessed by using Equation 2-57. The final equation for shrinkage curvature expands into

$$\frac{1}{r_{cs}} = \zeta \epsilon_{cs} \alpha_e \frac{S_u}{I_u} + (1 - \zeta) \epsilon_{cs} \alpha_e \frac{S_{cr}}{I_{cr}} \quad (2-67)$$

where S_u and S_{cr} can be expressed as follows:

$$S_u = A_s(d - x_u) - A'_s(x_u - d')$$

$$S_{cr} = A_s(d - x_{cr}) - A'_s(x_{cr} - d')$$

The distribution coefficient, ζ , may be determined using Equation 2-60. Table 2-11 summarizes the equations for the uncracked and fully cracked conditions.

Table 2-11: Distribution Coefficient ζ , for the uncracked and cracked Section according to clause 7.4.3 in EC2 (2004).

Section is Uncracked	Section is Cracked
$M \leq M_{cr}$	$M > M_{cr}$
$\zeta = 0$	$\zeta = 1 - 0.5(M_{cr}/M_a)^2$

The shrinkage deflection may be calculated using Equation 2-42 with the shrinkage curvature from Equation 2-67.

Long-Term Deflection

The main variable concerning the long-term deflection according to EC2 (2004) is the β value within the effective moment inertia derivation. Another modification includes using the effective modulus of elasticity, E_{eff} . This is required to account for the effects of creep, thus no reference is made to calculate a specific creep deflection.

If $\beta = 0.5$ due to sustained loads, then Equation 2-58 reduces to

$$\zeta = 1 - 0.5 \left(\frac{M_{cr}}{M_a} \right)^2 \quad (2-68)$$

Then, following the same approach as explained during the short-term deflection prediction, the effective moment of inertia used for long-term deflection prediction, is derived as:

$$I_e = \frac{I_{cr}}{1 - 0.5 \left(1 - \frac{I_{cr}}{I_u} \right) \left(\frac{M_{cr}}{M_a} \right)^2} \leq I_u \quad (2-69)$$

Then similar to Equation 2-33, the long-term deflection may be calculated:

$$\Delta_l = KL^2 \frac{M_a}{E_{eff} I_e} \quad (2-70)$$

where M_a is the maximum moment due to the quasi-permanent load at midspan and L is the effective span of the member. The effective modulus of elasticity of concrete is E_{eff} (refer to Section 2.2.2), the effective moment of inertia is I_e and K is the deflection coefficient that depends on the shape of the bending moment diagram.

The total deflection, Δ_t , is simply calculated by adding the long-term deflection, Δ_l , and the shrinkage deflections, Δ_{cs} .

Refer to Section 2.5 to apply the above Equations to predict deflections according to the EC2 (2004) for flat slab structures.

2.3.4 Deflection Prediction according to the South African Bureau of Standards (SABS) 0100-1

Annexure A from the South African Bureau of Standards (SABS) 0100-1 (2000) discusses two methods to predict deflections. The first method, seen in Clause A.2.3, discusses the prediction of deflections from curvatures. The approach based on the assumptions of the element curvature is similar to the curvature theory from the BS 8110 (1997) as discussed in Section 2.3.2 in this study. Many similar assumptions are made and it may be assumed that the SABS 0100 duplicated this procedure and included it in Annexure A. No further reference will be made to this method of deflection prediction.

The second method is discussed in Clause A.2.4 of Annexure A and is known as the alternative method, as stated in SABS 0100-1. The alternative method is similar to the deflection prediction method from the ACI 318, as discussed in Section 2.3.1, but with a few exceptions. Due to these exceptions, the alternative method will be considered in the comparison study for the design standards. This method is presented in the following paragraphs.

Short-Term Deflection

In the absence of more reliable information, it is recommended that the immediate deflection, Δ_i , at the midspan of a member due to applied characteristic load be calculated using Equation 2-33.

The moment of inertia I_e should incorporate the degree of cracking in the element and can be approximated with Equation 2-38, which also accounts for tension stiffening of the concrete.

The value of the cracking moment, M_{cr} is calculated with equation 2-71.

$$M_{cr} = \frac{f_r I_g}{y_t} \quad (2-71)$$

where f_r is the modulus of rupture, such that:

$$f_r = 0.65\sqrt{f_c} \quad \text{for unrestrained beams and slabs; and} \quad (2-72)$$

$$f_r = 0.30\sqrt{f_c} \quad \text{for restraint beams and slabs where pre-loading} \quad (2-73)$$

cracking is likely to occur.

The rest of the variables I_g , the moment of inertia of the concrete section (ignoring reinforcement), y_t which is the distance from the centroidal axis for the uncracked concrete section (ignoring reinforcement) to the extreme fibre in tension and f_c , which is the cube concrete strength of concrete.

Shrinkage Deflection

The shrinkage deflection may be calculated as follows as presented in Clause A.2.5 in SABS 0100-1 (2000):

$$\Delta_{cs} = K_{sh} k_{cs} \frac{\epsilon_{sh} L^2}{h} \quad (2-74)$$

where K_{sh} is defined for different beam types in Table 2-12, ϵ_{cs} is the free shrinkage strain of concrete and L is the effective span of the member.

Table 2-12: Shrinkage Deflection Coefficient K_{sh} according to the SABS 0100-1 (2000).

Beam Type	Shrinkage Deflection Coefficient, K_{sh}
Cantilever Beam	0.500
Simply Supported Beam	0.125
Continuous Beam	
End Span	0.086
Interior Span	0.063

The value for k_{cs} is defined separately for uncracked and a fully cracked members.

$$k_{cs} = 0.7 \sqrt{\rho \left(1 - \frac{\rho'}{\rho}\right)} \quad \text{for uncracked members} \quad (2-75)$$

limited to $0.0 \leq k_{cs} \leq 1.0$;

$$k_{cs} = 1 - \frac{\rho'}{\rho} [1 - 0.11(3 - \rho)^2] \quad \text{for fully cracked members} \quad (2-76)$$

limited to $0.3 \leq k_{cs} \leq 1.0$

$$\text{with } \rho = \frac{100A_s}{bd} \leq 3 \quad \text{and } \rho' = \frac{100A'_s}{bd} \quad \text{limited to } \rho'/\rho \leq 1.0$$

The percentage tension and compression reinforcement is defined as ρ and ρ' , respectively. A_s is the area tension reinforcement of the section, b is the width of the section d is the effective depth of the section and A'_s is the area compression reinforcement of the section.

Long-Term Deflection

The long-term creep deflection, Δ_l , shall be calculated by multiplying the initial deflection, calculated by using the moment applied due to sustained load, by a factor λ . The resulting equation is as follows (SABS 0100-1, 2000):

$$\Delta_l = \lambda \Delta_i \quad (2-77)$$

Δ_l is the long-term deflection based on the creep coefficient and Δ_i is the initial deflection due to the permanent loading. The initial deflection, Δ_i , required in Equation 2-77 is the short-term deflection calculated due to the permanent load. Similar equations to calculate the short-term deflection should be used, with the exception that the moment due to the permanent loads, M_p , should be used in Equations 2-33 and 2-38 (Robberts & Marshall, 2008).

The factor λ from Equation 2-77 is defined in the Equation 2-78.

$$\lambda = 1 + x_i \phi \quad \text{where } x_i = \frac{x_{cr}}{d} \quad (2-78)$$

where x_i is the ratio of neutral axis depth to effective depth of cracked element due to the modulus of elasticity at instant of loading and ϕ is the creep factor considering age of concrete loading, humidity, surface-to-volume ratio, ect.

Where compression reinforcement is present, ϕ shall be substituted by ϕ' where

$$\phi' = \phi \left(1 - \frac{\rho}{2}\right) \quad (2-79)$$

and ρ is the ratio of the area of compression reinforcement to the area of tension reinforcement, $\rho = A'_s/A_s$.

The total deflection, Δ_t , is simply calculated by adding the long-term deflection, Δ_l , the shrinkage deflections, Δ_{cs} , and the additional initial deflection, $\Delta_{i,add}$. The additional initial deflection is calculated as the difference between the short-term deflection calculated due to the total serviceable moments, M_a and the permanent moments, M_p .

Refer to Section 2.5 to apply the above equations to predict deflections according to the SABS 0100-1 (2000) for flat slab structures.

2.4 SPAN/EFFECTIVE DEPTH RATIO ACCORDING TO DESIGN STANDARDS

The span/effective depth ratio is the first method considered to evaluate whether a slender horizontal member meets the requirements of the serviceability limit state. The results produced by the span/effective depth ratios are evaluated with the deflection prediction methods in order to establish a serviceability trend from the various design standards. Within this study, the span/effective depth ratio is referred to as the span/depth (L/d) ratio for simplification.

The methods of span/depth calculation produce the allowable span/depth ratio, $(L/d)_{ALLOWABLE}$. The actual span/depth ratio, $(L/d)_{ACTUAL}$ need to be determined from the dimensions of the slender member and compared to the allowable span/depth ratio. If the actual span/depth ratio is less or equal to the allowable ratio, the member is deemed serviceable.

2.4.1 Span/Depth Ratio according to the American Concrete Institute (ACI) 318-02

The American Concrete Institute (ACI) 318 (2002) presents several Tables addressing the span/depth ratios limits to suggest members of sufficient serviceability. The span/depth ratios are divided into two criteria. The first table, Table 9.5 (a) (ACI 318, 2002) is directed for members spanning in one direction. The second table, Table 9.5 (c) (ACI 318, 2002) is directed for members spanning in two directions.

The ACI 318 (2002) is specifically different concerning the span/depth values in comparison to other design standards due to the fact the span/depth ratios are not related to the effective depth of the section considered, but to the total height of the section. Despite this difference the span/height results are still compared with the span/depth results from the other design standards.

One-Way Construction

The minimum thickness stipulated in Table 9.5 (a) (ACI 318, 2002) shall apply for one-way construction not supporting or attached to partitions or other construction likely to be damaged by large deflections, unless computation of deflections indicates a lesser thickness can be used without adverse effects.

For normal weight concrete the following values in Table 9.5 (a) apply. Table 9.5 is reproduced in Table 2-13.

FLAT SLAB DESIGN FOR THE SERVICEABILITY LIMIT STATE

Table 2-13: Minimum thickness of nonprestressed beams or one-way slabs as in Table 9.5 (a) in the ACI 318 (2002).

Minimum thickness, h				
	Simply Supported	One End Continuous	Both Ends Continuous	Cantilever
Member	Members not supporting or attached to partitions or other construction likely to be damaged by large deflections.			
Solid One-way Slabs	L/20	L/24	L/28	L/10
Beams or Ribbed One-Way Slabs	L/16	L/18.5	L/21	L/8

The variable L is the span length of the beam under consideration.

Two-Way Construction

In the ACI 318 (2002) Clause 9.5.3, presents the minimum thickness for flat slabs or two-way constructed slabs without interior beams in Table 9.5(c). The table is reproduced in Table 2-14.

Table 2-14: Minimum thickness of Slabs without Interior Beams according to Table 9.5 (c) in ACI 318 (2002).

Reinforcement Yield Strength f_y [MPa]	Without Drop Panels			With Drop Panels		
	Exterior Panels		Interior Panels	Exterior Panels		Interior Panels
	Without Edge beams	With Edge Beams		Without Edge beams	With Edge Beams	
300	$L_n/33$	$L_n/36$	$L_n/36$	$L_n/36$	$L_n/40$	$L_n/40$
420	$L_n/30$	$L_n/33$	$L_n/33$	$L_n/33$	$L_n/36$	$L_n/36$
520	$L_n/28$	$L_n/31$	$L_n/31$	$L_n/31$	$L_n/34$	$L_n/34$

The variable L_n is the clear span in the long direction of two-way construction, measured face-to-face from the supports in slabs without beams and face-to-face of the beams or other supports in other cases (ACI 318, 2002).

For the values of reinforcement yield strength between the values presented in Table 2-14, the minimum thickness shall be determined by linear interpolation.

2.4.2 Span/Depth Ratio according to the British Standards (BS) 8110: Part 2: 1997

The British Standards (BS) 8110 (1997) states that the final deflection, including the effects of creep and shrinkage, should not exceed either of the following limits:

- Span/250;
- Span/500 or 20 mm, whichever is the lesser, after the construction of the partitions or the application of finishes (BS 8110, 1997) (Kong & Evans, 1987).

These deflection limits are given as being reasonable values for use in practical design. The first limit of span/250 is considered to be that beyond which the deflection will be noticed by the user of the structure. The second limit is to prevent damage to partitions and finishes.

In design, it is usual to comply with the above deflection limits by a straight-forward procedure of limiting the ratio of the span to the effective depth. The practical procedure recommended by BS 8110: Clause 3.4.6 may conveniently be summarized as follows (BS 8110, 1997)(Kong & Evans, 1987):

Step 1: Basic span/depth ratio

Select the basic span/depth ratios in Table 2-15. For flanged sections with $b_w/b > 0.3$, obtain the span/depth ratio by linear interpolation between the values given in Table 2-15 for rectangular sections and for flanged sections with $b_w/b = 0.3$ (For flanged section, b is the beam flange width and b_w is the web width) (BS 8110, 1997).

Table 2-15: Basic span/effective depth ratios (BS 8110: Clause 3.4.6.3, 1997).

Support Condition	Rectangular Sections	Flanged Section $b_w/b \leq 0.3$
Cantilever	7	5.6
Simply Supported	20	16.0
Continuous	26	20.8

Step 2: Long Spans

For spans exceeding 10 m, there are three cases to consider, depending on whether it is necessary to limit the increase in deflection (to span/500 or 20 mm as stated above) after the construction of the partitions or finishes:

- If it is not necessary to limit such an increase in deflection, then the basic span/depth ratio obtained from Table 2-15 remains valid.
- If it is necessary to limit such an increase, and the structural member is not a cantilever, then the basic span/depth ratio obtained from Table 2-15 should be multiplied by a modification factor equal to $10/\text{span}$.
- If it is necessary to limit the increase in deflection, and the structural member is a cantilever, then the design must be justified by deflection calculation (BS 8110, 1997).

Step 3: Modification Factor for Tension Reinforcement

Deflection is influenced by the amount of tension reinforcement and its stress. The span/depth ratio should therefore be modified according to the area reinforcement provided and its service stress at the centre of the span (or the support in case of a cantilever). Values of span/depth ratio obtained from Table 2-15 should be multiplied by the appropriate factor obtained from Table 3.11 in BS 8110 (1997). Table 2-16 shows the equivalent equation applicable for the modification factor for tension reinforcement.

Table 2-16: Modification factor for Tension Reinforcement (BS 8110: Clause 3.4.6.5, 1997).

Notes from Table 3.11 in BS 8110 (1997)	Applicable Equation
<p>NOTE 1:</p> <p>The values in Table 3.11 from BS 8110 are derived from the Equation, where M is the design ultimate moment at the centre of the span or, for a cantilever, at the support.</p>	$\text{Modification factor} = 0.55 + \frac{(477 - f_s)}{120(0.9 + \frac{M}{bd^2})} \leq 2.0$
<p>NOTE 2:</p> <p>The design service stress in the tension reinforcement in a member may be estimated from the Equation.</p>	$f_s = \frac{5f_y A_{s,req}}{8A_{s,prov}} \times \frac{1}{\beta_b}$
<p>NOTE 3:</p> <p>For a continuous beam, if the percentage of redistribution is not known but the design ultimate moment at mid-span is obviously the same as or greater than the elastic ultimate moment.</p>	$f_s = \frac{5}{8} f_y$

The variables include f_s as the design service stress, M the applied moment due to the ultimate limit state loads, b the width of the section, d the effective depth of the section, f_y the yield stress of the reinforcing steel, $A_{s,req}$ is the area tension reinforcement required for the section to resist moment due to ultimate loads, $A_{s,prov}$ is the area tension reinforcement provided for the section to resist moment due to ultimate loads and β_b is the ratio of the moment after relative to the moment before redistribution.

Step 4: Modification Factor for Compression Reinforcement

If the beam is doubly reinforced, the span/depth ratio may be further multiplied by a modification factor, obtained from Table 3.12 in BS 8110 (1997), to allow for the effect of the compression reinforced. Table 2-17 provide the equation for these modification factors.

Table 2-17: Modification factor for Compression Reinforcement (BS 8110: Clause 3.4.6.6, 1997).

Notes from Table 3.12 in BS 8110 (1997)	Applicable Equation
<p>NOTE 1: The values in Table 3.12 from BS 8110 are derived from the following Equation.</p>	<p>Modification factor for compression reinforcement = $1 + \frac{100A'_{s,prov}}{bd} / \left(3 + \frac{100A'_{s,prov}}{bd} \right) \leq 1.5$</p>
<p>NOTE 2: The area of compression reinforcement $A'_{s,prov}$ used in this Table may include all bars in the compression zone, even those not effectively tied with stirrups (links).</p>	

The variables include b the width of the section, d the effective depth of the section and $A'_{s,prov}$ is the area compressive reinforcement provided for the section to resist moment due to ultimate loads.

Step 5: Deflection due to Creep and Shrinkage

Permissible span/depth ratios obtained from Table 2-15 to 2-17 take account of normal creep and shrinkage deflections. If it is expected that creep and shrinkage of the concrete may be particularly high (e.g. if the free shrinkage strain is expected to be greater than 0.00075 or the creep coefficient greater than 3) or if other abnormally adverse conditions are expected, the permissible span/depth ratio should be suitably reduced. A reduction of more than 15 % is unlikely to be required (BS 8110, 1997).

Step 6: Deflection for Slab Structures

According to Clause 3.5.7 in BS 8110 (1997) it is appropriate to evaluate the serviceability of a deflecting member using the steps as discussed above. For two-way spanning slabs, only the reinforcement at the centre of the span in the width of slab under consideration should be considered to influence deflection. The span/depth ratio for a two-way spanning slab should be based on the shorter span and its amount of reinforcement in that direction.

For the evaluation of the span/depth ratio for a flat slab the following is presented in Clause 3.7.8 in BS 8110 (1997). For a slab with drops of gross width in both directions at least equal to one-third of the respective spans, the span/depth steps from above are applicable. If the flat slab has no drops, the resulting span/depth ratio from the steps above should be multiplied by an additional 0.9 factor. This check should be carried out for the more critical direction, thus the longer span.

2.4.3 Span/Depth Ratio according to the Eurocode 2: Part 1-1

Generally, it is not necessary to calculate the deflections explicitly as simple rules, for example limits to span/depth ratio may be formulated, which will be adequate for avoiding deflection problems in normal circumstances. The procedure may be broken down into a step-by-step process. The approach for the span/depth ratio of the EC2 (2004) is presented in Clause 7.4.2 and is discussed below.

Step 1: Choose the Appropriate Equation

The limiting span/depth ratio may be estimated using Equations 2-80 and 2-81 and multiplying this by correction factors to allow for the type of reinforcement used and other variables. No allowance has been made for any pre-camber in the derivation of the expressions.

$$\frac{l}{d} = K \left[11 + 1.5\sqrt{f'_c} \cdot \frac{\rho_0}{\rho} + 3.2\sqrt{f'_c} \cdot \left(\frac{\rho_0}{\rho} - 1 \right)^{\frac{3}{2}} \right] \quad \text{if } \rho \leq \rho_0 \quad (2-80)$$

$$\frac{l}{d} = K \left[11 + 1.5\sqrt{f'_c} \cdot \frac{\rho_0}{\rho - \rho'} + \frac{1}{12}\sqrt{f'_c} \cdot \sqrt{\frac{\rho'}{\rho_0}} \right] \quad \text{if } \rho > \rho_0 \quad (2-81)$$

Where L/d is the limit span/depth, K is the factor to take into account the different structural systems. ρ_0 is the reference reinforcement ratio $= 10^{-3} \sqrt{f'_c}$, ρ is the required tension reinforcement ratio at mid-span to resist the moment due to the design loads (at the support for cantilevers), while ρ' is the required compression reinforcement ratio at mid-span to resist the moment due to design loads (at the supports for cantilevers) and f'_c is the cylinder compressive strength of concrete in MPa units.

Equations 2-80 and 2-81 have been derived on the assumption that the steel stress under the appropriate design load at serviceability limit state (SLS) at a cracked Section at the mid-span of a beam or slab, or at the support of a cantilever, is 310 MPa, corresponding to roughly the service stress of reinforcement steel with $f_y = 500$ MPa.

Where other stress levels are used, the values obtained using expressions 2-80 and 2-81 should be multiplied by $310/\sigma_s$. It will normally be conservative to assume that:

$$310/\sigma_s = 500/(f_y A_{s,req}/A_{s,prov}) \quad (2-82)$$

where σ_s is the tensile steel stress at mid-span (at the support for cantilevers) under the design load at SLS. The area of steel provided at the Section is $A_{s,prov}$ and the area of steel required at this Section at ultimate limit state is $A_{s,req}$.

Step 2: Modification Factor for Flanged Beams

For flanged sections where the ratio for the flange breadth to the web breadth exceed 3, the values of span/depth ratio as given by Equations 2-80 and 2-81 should be multiplied by 0.8 (EC2, 2004).

Step 3: Modification Factor for Beams and Slabs

For beams and slabs, other than flat slabs, with spans exceeding 7.0 m, which support partitions liable to be damaged but excessive deflections, the values of span/depth ratio as given in Equations 2-80 and 2-81 should be multiplied by $7/L_{eff}$, where L_{eff} is in metres. The effective span L_{eff} for a slab is discussed in Clause 5.3.2.2 in EC2 (2004).

Step 4: Modification Factor for Flat Slabs

For flat slabs where the greater span exceeds 8.5 m, and which support partitions liable to be damaged by excessive deflection, the values of span/depth ratio as given in Equations 2-80 and 2-81 should be multiplied by $8.5/L_{eff}$, where L_{eff} is in metres. The effective span L_{eff} for a slab is discussed in Clause 5.3.2.2 in EC2 (2004).

Step 5: Value of K

The basic ratios of span/depth for reinforced concrete members without axial compression are provided in Table 7.4N in EC2 (2004). The Table is reproduced in Table 2-18.

Table 2-18: Basic ratios of span/effective depth for reinforced concrete members without axial compression as shown in Table 7.4N in EC2 (2004).

Structural System	K	Concrete highly stressed	Concrete lightly stressed
		$\rho = 1.5\%$	$\rho = 0.5\%$
Simply supported beam, one- or two-way spanning simply supported slab	1.0	14	20
End span of continuous beam or one-way continuous slab or two-way spanning slab continuous over one long side	1.3	18	26
Interior span of beam or one-way or two-way spanning slab	1.5	20	30
Slab supported on columns without beams (flat slab) (based on longer span)	1.2	17	24
Cantilever	0.4	6	8

A few notes have been included with the data from Table 2-18. These note state the following:

- The values given have been chosen to be generally conservative and calculation may frequently show that thinner members are possible.
- For two-way spanning slabs, the check should be carried out on the basis of the shorter span. For flat slabs the longer span should be taken.
- The limits given for flat slabs correspond to a less severe limitation than a mid-span deflection of span/250 relative to the columns.

2.4.4 Span/Depth Ratio according to the South African Bureau of Standards (SABS) 0100-1

The basic span/effective depth ratios for rectangular beams are given in Table 10 in the SABS 0100-1 (2000). These are based on limiting the deflection to span/250 and this should normally prevent damage to finishes and partitions for beams of span up to 10 m. For cantilevers, add or subtract, as appropriate, the support rotation times the cantilever span.

The following paragraphs present the steps to calculate the allowable span/depth as presented by the SABS 0100-1 (2000).

Step 1: Basic span/ depth ratios for Rectangular Beams

Table 10 in the SABS 0100-1 (2000), as reproduced in Table 2-19, may be used for spans exceeding 10 m but only when it is not necessary to limit the increase in deflection after the construction of partitions and finishes. Otherwise, in order to prevent damage to finishes and partitions, the values given in Table 10 should be multiplied by 10/span, except for cantilevers, where the design should be justified by calculation.

Table 2-19: Basic span/depth ratios for beams as in SABS 0100-1 (2000).

Support Condition	Rectangular Section
Simply supported beam	16
Simply supported with nominally restrained ends	20
One end continuous	24
Both ends continuous	28
Cantilevers	7

Step 2: Modification of span/depth ratio due to Tension Reinforcement

Since deflection is influenced by the amount of tension reinforcement and its stresses, it is necessary to modify the span/depth ratios according to the ultimate design moment and the service stress at the centre of the span (or at the support in the case of a cantilever). Therefore, values of span/depth ratio obtained from Table 10 should be multiplied by the appropriate factor obtained from Table 11 in SABS 0100-1 (2000).

The values in Table 11 are based on the equation presented in Table 2-16, Note 1.

For a section with a given reinforcement strength, the strain at the end of the elastic range is a fixed value. As the moment increases, the area of tension reinforcement must be increased and the neutral axis depth increases. With the strain in the reinforcement fixed, this leads to greater curvatures, and so greater deflections. Therefore the modification factor decreases as the moment increases. It is also interesting to note that the strength of the beam increases more than the stiffness for an increase in tension reinforcement (SABS 0100-1, 2000).

The design service stress in the tension reinforcement in a beam may be estimated with Equation 2-83.

$$f_s = 0.87 f_y \cdot \frac{\gamma_1 + \gamma_2}{\gamma_3 + \gamma_4} \cdot \frac{A_{s,req}}{A_{s,prov}} \cdot \frac{1}{\beta_b} \quad (2-83)$$

where f_s is the estimated service stress in tension reinforcement and f_y is the characteristic strength of reinforcement. The factor γ_1 , is the self-weight load factor for serviceability limit state, γ_2 is the imposed load factor for serviceability limit state, γ_3 is the self-weight factor for the ultimate limit state and γ_4 is the imposed load factor for ultimate limit state. $A_{s,req}$ is the area of tension reinforcement required at midspan to resist moment due to ultimate loads (at the support in the case of a cantilever). $A_{s,prov}$ is the area of tension reinforcement provided at midspan (at the support in the case of a cantilever). Finally, β_b is the ratio of resistance moment at midspan obtained from redistributed maximum moments diagram to that obtained from maximum moments diagram before redistribution.

If the percentage of redistribution is not known but the design ultimate moment of midspan is clearly the same or exceed the elastic ultimate moment, the stress f_s may be calculated from the above equation where $\beta_b = 1$.

The magnitude of f_s depends on the following (SABS 0100-1, 2000):

- If more reinforcement is provided than required, the stress in the steel will be reduced.

- If moment redistribution has been applied, the steel service stress will be greater. Higher service stresses in the tension reinforcement leads to greater reinforcement strains, greater curvatures, and hence, greater deflections.

Step 3: Modification Factor of span/depth ratio due to Compression Reinforcement

The compression reinforcement also influences deflection (SABS 0100, 2000):

- The depth of the neutral axis is reduced, reducing curvatures and deflections.
- Creep and shrinkage is significantly reduced and compression reinforcement therefore has a substantial effect on the long-term deformations.
- It is also interesting to note that for an increase in compressive reinforcement the increase in stiffness is greater than the increase in strength.

The span/depth ratio therefore increases for an increase in compressive reinforcement. The value of the span/depth ratio modified with a factor due to tensile reinforcement may be multiplied by a further modification factor due to the compressive reinforcement. The modification factors due to compressive reinforcement are shown in Table 12 in SABS 0100-1 (2000) may be calculated from the equation presented in Table 2-17, Note 1.

The area of compression reinforcement at midspan A_{vs} used in the equation in Table 2-17 may comprise all bars in the compression zone, including those not effectively tied with links (SABS 0100-1, 2000).

Step 4: Deflection due to Creep and Shrinkage

Permissible span/depth ratios obtained from Steps 1 to 3 take account of normal creep and shrinkage deflection. If it is expected that creep or shrinkage of the concrete might be particularly high (concrete very poor quality and workmanship, high long-term loadings) the permissible span/depth ratio should be reduced. A reduction of more than 15 % is unlikely to be required (SABS 0100-1, 2000).

Step 5: Span/Depth Ratio for Flanged Beams

For a flanged beam, the span/depth ratio may be determined as in Step 1 but, when the web width is less than 0.3 times the effective flange width, multiply the final ratio obtained by 0.8. For values of web width to effective flange width that exceed 0.3, this factor may be increased linearly from 0.8 to 1.0 as the ratio of web width to effective flange width increases to unity.

In the case of inverted flanged beams with the flange in tension, the tension reinforcement within the width of the web must be taken into consideration.

The compressive reinforcement should be that which is within the effective width of the flange (SABS 0100-1, 2000).

Step 6: Span/Depth Ratio for Slabs

According to Clause 4.4.6 in the SABS 0100-1 (2000) the span/depth ratio for a slab may be calculated as stipulated in the steps above. The reinforcement at the middle of the span in the width of the slab under consideration should be considered to influence deflection. In the case of a two-way spanning slab, the ratio should be based on the shorter span and its amount of reinforcement in the direction.

For flat slabs, Clause 4.6.3 in the SABS 0100-1 (2000), provide span/depth ratio specifications. For slabs with column drops of a total width on both directions equal to at least one-third of the respective spans, follow the span/depth ratio calculations as stipulated in the steps above. The calculations should be applied to the longer span for flat slabs. In other cases, for flat slabs with no column drops, the span/depth ratio should be multiplied by an additional 0.9 factor.

2.5 METHOD FOR PREDICTING FLAT SLAB DEFLECTIONS: EQUIVALENT FRAME METHOD

The deflection prediction methods as presented in Section 2.4, include procedures to calculate the deflection for beams. The flat slab system may be approached as beams spanning in two directions. The method for predicting slab deflections is essentially the same for flat plates, flat slabs, and two-way slabs, coffer slabs, and combination slabs, with the various stiffness, equivalent stiffness, and

distribution factors according to Branson (1977). The following section discusses how these deflection prediction methods from Section 2.4 are used to predict the mid-panel deflection for three-dimensional slab structure.

Equivalent Frame Method

This section discusses how the mid-panel deflection is predicted for a single slab panel. The individual deflections in each direction are determined from the deflection prediction methods as discussed in Section 2.4.

Following the moment analysis and design by either the equivalent frame or direct design methods, the midpanel deflection is computed as the sum of the deflection at midspan of the column strip or column line in one direction, and the deflection at midspan of the middle strip or middle line between columns in the other direction. For rectangular panels, or other panels that have different characteristics in the two directions, an average for the two deflections thus determined is used. The column strip in both directions is defined as the width on each side of the column centreline equals to one-fourth the smaller of the two panel dimensions. The middle strip is the strip bounded by two column strips (Branson, 1977).

The present empirical method for calculating deflection of a slab is shown in Figure 2-17.

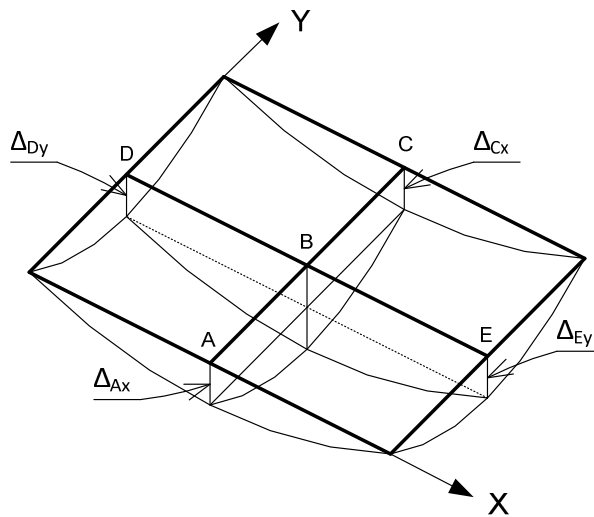


Figure 2-17: Deflection of slabs: Δ_{Bx} and Δ_{By} are deflections of middle strips in X and Y directions, respectively (Varghese, 2005).

Maximum deflection of slab is the mean mid-span deflection of column strip in the long direction added to the mean mid-span deflection of middle strip in the short direction (Varghese, 2005).

Referring to Figure 2-17, take deflections, Δ in both directions along the strips. The average deflections are obtained as follows:

$$\Delta_{1B} = \frac{1}{2}(\Delta_{Ax} + \Delta_{Cx}) + \Delta_{By} \quad (2-84)$$

$$\Delta_{2B} = \frac{1}{2}(\Delta_{Dy} + \Delta_{Ey}) + \Delta_{Bx} \quad (2-85)$$

$$\Delta = \frac{1}{2}(\Delta_{1B} + \Delta_{2B}) \quad (2-86)$$

The deflection of column strips contributes more to the total deflection (as much as 75%), as explained by Varghese (2005).

Effect of Continuity

The equivalent frame method only accounted for the mid-panel deflection of a single panel within a flat slab framework of panels. The ACI 318 (2002) and the SABS 0100-1 (2000) requires the designer to account for the effect of the continuity of the column and middle strips as defined during the explanation of the equivalent frame methods. In the absence of more comprehensive analysis, the following approximate method is usually satisfactory.

For column or middle strips sections in slabs, having a variable flexural rigidity due to changes in cross-section, and/or reinforcement pattern, and/or effects of cracking such as I_e , the following method for determining the average flexural rigidity, $E_c I_{ea}$, is to be used as discussed by Branson (1977). For a continuous span a simple average seems appropriate as presented in Equation 2-87.

$$E_c I_{ea} = \frac{1}{2} E_c [I_{em} + \frac{1}{2}(I_{e1} + I_{e2})] \quad (2-87)$$

The ACI 318 (2002) and the SABS 0100-1 (2000) design standards, favour this approach and mentions the effect of continuity within the deflection procedure without much elaboration on the exact approach. The variables include I_{ea} , the average effective moment of inertia of the beam or slab strip, I_{em} , the effective moment of inertia at the midspan section, and I_{e1} and I_{e2} , are the effective moment of inertia at each support of the beam.

2.6 CONCLUDING SUMMARY

The aim of this chapter was to discuss how a slender member is evaluated in order to comply with the serviceability limit state. Specifically, the chapter is focused to evaluate the serviceability for a flat slab structure. It was first important to discuss the influences on the flat slab deflection development and how these influences are to be determined. The influences include the material properties, the intrinsic parameters, the extrinsic parameters, the derivation of the deflection prediction expression, the derivation of the deflection coefficient K and the different types of deflection that develop at different instances.

The material properties include the determination of the uncracked and cracked sectional properties of a flexural member. It was determined that the uncracked sectional properties for the different design standards do differ, namely the different gross and uncracked sectional properties for the uncracked state of the section. The gross sectional properties do not take the effect of the reinforcement into account during the uncracked state of the section while the uncracked sectional properties do include the effect. The cracked sectional properties for the various design standards do not differ due since the expressions are mostly similar.

Other material properties that influence flat slab deflections include the effects of creep and shrinkage. The effect of creep is accounted for using an effective modulus of elasticity, E_{eff} , to account for a decrease in concrete stiffness with the increase in time. A comparison between the creep models from the various design standards suggest that the creep model for the BS 8110 (1997) present the best creep prediction for use during the design stage of a structure, during which limited data is available of the exact conditions contributing to creep development.

The methods presented for the prediction of the shrinkage curvature from the various design standards also differ. It was shown that the shrinkage curvature between the cracked and uncracked states differ, thus the shrinkage curvature prediction should account for the amount of cracking in a deflection member.

The influence of the material properties on the deflection of flat slabs also included the effect of the concrete tensile strength and the Poisson's Ratio. The determination of the concrete tensile strength is important in order to estimate the point of first cracking (or cracking moment, M_{cr}) for a flexural member under loading. The various design standards present different methods to predict the cracking moment. It was also shown that an adequate Poisson's Ratio of 0.2 is suitable for the deflection prediction for flat slabs.

The various intrinsic and extrinsic parameters influencing flat slab deflections were also discussed. The intrinsic parameters include the effect of tension stiffening and shrinkage restraint. The tension stiffening contributes significantly to stiffness of a lightly reinforced member, such as a flat slab structure, thus reducing the deflection. Therefore, it is critical that this should be accounted for during deflection prediction. The effect of shrinkage restraint reduces the point of first cracking of a member, thus decreasing the cracking moment. When a slab shows significant restraint against shrinkage the cracking moment should be reduced to allow for an increased deflection.

The extrinsic parameters include the loading history and the construction methods applied to the flat slab structure. It is difficult to accurately predict the exact loading applied to the slab, but it is important to acknowledge the load peaks and recognise the additional crack development (loss in stiffness) instigated by the occurrence.

The derivation of the deflection prediction expression is obtained from the moment-curvature approach. The complex integral is reduced to a simple expression for simple application. One variable that include the shape of the bending moment shape for the deflecting member include the deflection coefficient K . Many sources in literature present the different values of K for different loading and support conditions.

This chapter also discussed the different components part of the final total deflection for a deflecting member. These components include the development of the short-term, the long-term and the shrinkage deflections (time-dependent deflections).

The chapter continued the discussion of the serviceability requirements, by firstly discussing the different methods presented by the various design standards to predict the deflections in beams. These deflection prediction methods were extended to apply to flat slab structures by considering the equivalent frame method and the effect of continuous members. Usually the span/depth ratio is calculated prior the predicting a mid-panel deflection for panel within a flat slab framework. The chapter also discussed the different methods presented by the various design standards to calculate the allowable span/depth ratios. The procedures to evaluate the serviceability of a flat slab structure have been established in this chapter. The next chapter quantifies their limitations when predicting time-dependent deflections.

3 DEFLECTION PREDICTION FOR LIGHTLY REINFORCED CONCRETE SLABS

3.1 INTRODUCTION

This chapter compares the different methods used to calculate the predicted deflection and the span/depth ratios (Section 3.2). It is observed that significant differences occur and it is further discussed in Section 3.3 how these differences may be quantified. The topic of crack development and the occurrence of tension stiffening have been important phenomena in slender members. The use of equations to simulate this occurrence is quite important and this chapter explains how different authors approached this problem. In this way it is possible to identify how the design standards incorporated the concepts as presented in literature. The concepts from Branson (1977) and Bischoff (2005) are thoroughly explained and the limitations of their models are also incorporated into the discussion.

Several comparisons are made to evaluate the effectiveness of the mathematical models. The comparisons include the influence of the tension reinforcement (ρ), the stiffening ratio (I_g/I_{cr}), the M_a/M_{cr} ratio applied to the flexural member and the use of either I_u or I_g within the mathematical model. These influences (limitations) are discussed in Sections 3.4 to 3.6. The chapter concludes by considering the limits of the different models and presenting an Alternative Approach (Section 3.7) to predict deflections more effectively.

3.2 COMPARISON OF THE EMPIRICAL METHODS FOR SERVICEABILITY EVALUATION

The aim of this section is to present the variations of the curvature (deflection) behaviour for lightly reinforced slabs as predicted by the various deflection prediction methods in Section 2.3. Section 3.2.1 presents the predicted deflection behaviour according to the methods from Section 2.3 for simply-supported one-way slabs. In an experimental study conducted by Gilbert (2007), the deflection behaviour of ten one-way simply supported slabs were recorded. The predicted behaviour is compared to the experimental behaviour to evaluate which of the deflection prediction methods produces the better approximation. The span/depth ratio methods are also compared for one of the

Gilbert (2007) slab specimens. The percentage tension reinforcement for the section is varied to observe span/depth variation as a function of the percentage tension reinforcement.

3.2.1 Deflection Prediction Comparison for the Design standard Methods

It is well-known that cracking reduces flexural stiffness in concrete members and this effect is accounted for by using an effective moment of inertia I_e to model the gradual reduction in stiffness as load increases and cracking progress along the member. The main variable within the deflection expression is the stiffness (rigidity) that relates the amount of curvature undergone by the member due to the material properties and amount of loading applied. In this section the comparison is aimed at observing which of the stiffness expressions from the various design standards produce the deflection that best compares to the experimental deflection.

The comparison was done for three different one-way slab specimens from the Gilbert (2007) experimental results. The comparison is done in terms of the curvatures, similar to deflections, to observe the deflection behaviour as the moment increases from zero to above the cracking moment, M_{cr} . The moments are presented in terms of ratios, namely the level of cracking ratio, M_a/M_{cr} , where the applied moment is expressed with reference to the cracking moment. The curvature is a function of the applied moment, modulus of elasticity and effective moment of inertia.

The study by Gilbert (2007) recorded the experimental data for the specimens at an applied moment of $1.1M_{cr}$ to $1.3M_{cr}$. Table 3-1 show the sectional properties of the three slabs presented in this comparison and Figures 3-1 to 3-3 show the resulting curves for the comparison. All three slab specimens have a percentage tension reinforcement less than 1.0%. Most flat slab structures fall within this percentage tension reinforcement range (Gilbert, 2007), thus the behaviour presented below is representative to what would be expected for a typical flat slab system. The three slab specimens, part of this comparison, have different percentages tension reinforcement (ρ).

DEFLECTION PREDICTION FOR LIGHTLY REINFORCED CONCRETE SLABS

Table 3-1: Sectional properties of the Gilbert (2007) slabs.

Slab	h [mm]	L [mm]	d [mm]	ρ [%]	f'_c [MPa]	f_c [MPa]	E_c [MPa]	f_t [MPa]
1	106.2	2000	83.2	0.480	38.0	47.5	27.47	4.42
2	106.6	2000	85.9	0.485	38.0	47.5	27.47	4.42
3	100.0	2000	82	0.203	38.4	48.0	27.39	3.60

The first graph shows the behaviour of the simply-supported slab at midspan over a large range of applied moments, while the second shows an enlarged section of the same graph. The enlargement aids to observe the comparison between the predicted behaviour and the experimental behaviour, because the experimental behaviour is only recorded over the M_a/M_{cr} range of 1.1 to 1.3. The extended curvature behaviour of the experiment slabs is presented as a dashed line. Appendix B presents the calculation done to produce the graphs in Figures 3-1 to 3-3.

In each graph where the deflection (curvature) behaviour of the specimen is presented, six different curves are shown. The uncracked curvatures include the curves produced using the gross moment of inertia, I_g as presented by the SABS 0100-1 (2000), and the uncracked moment of inertia, I_w , as presented by the EC2 (2004). The ACI 318 (2002) presents a similar equation for the gross moment of inertia, I_g , thus the uncracked curvature produced from the SABS 0100-1 (2000) is representative of the uncracked curvature from the ACI 318 (2002) approach. The BS 8110 (1997) and the EC2 (2004) present similar approaches for the uncracked curvature as calculated using the uncracked moment of inertia, thus the uncracked curvature from the EC2 (2004) is representative of the BS 8110 (1997) uncracked curvature. The curvatures presenting the predicted curvature behaviour from the various design standards include the ACI 318 (2002), the EC2 (2004), the SABS 0100-1 (2000) and the BS 8110 (1997). The last of the six curvatures present the cracked curvature for a fully cracked section. From the comparison in Section 2.2.1 it was observed that the cracked section properties from the various design standards are similar. The cracked curvature presented within the resulting graphs present the cracked curvature as calculated from the EC2 (2004) approach, but due to the similarity of the cracked sectional properties from the various design standards, the EC2 (2004) curvature is representative for all the other design standards.

DEFLECTION PREDICTION FOR LIGHTLY REINFORCED CONCRETE SLABS

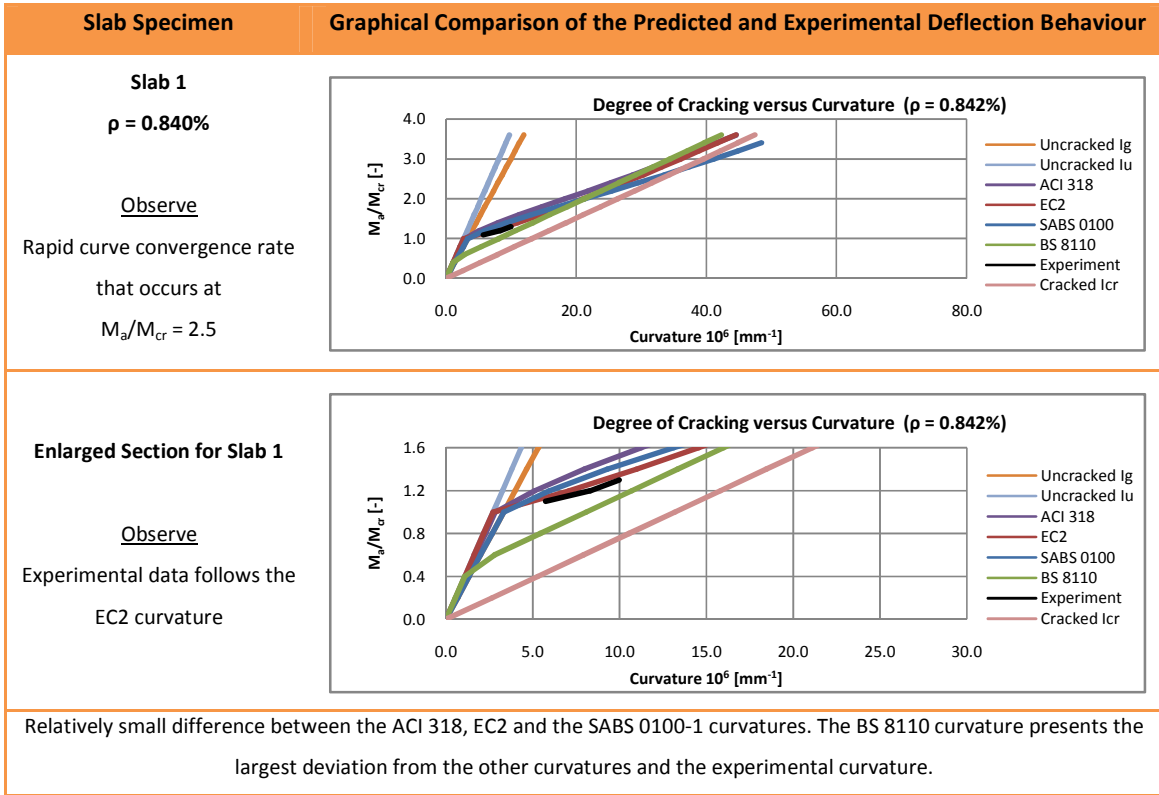


Figure 3-1: Graphical comparison of the initial curvatures for the design standards with $\rho = 0.842\%$.

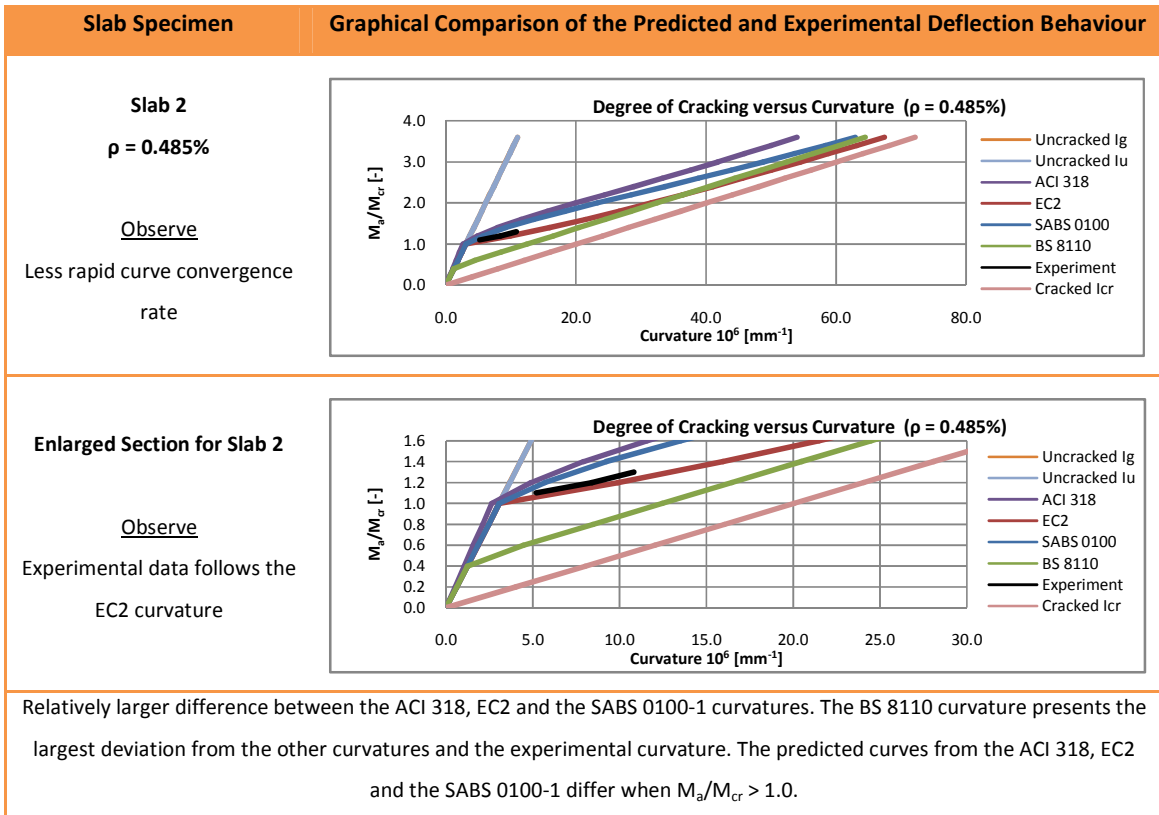


Figure 3-2: Graphical comparison of the initial curvatures for the design standards with $\rho = 0.485\%$.

DEFLECTION PREDICTION FOR LIGHTLY REINFORCED CONCRETE SLABS

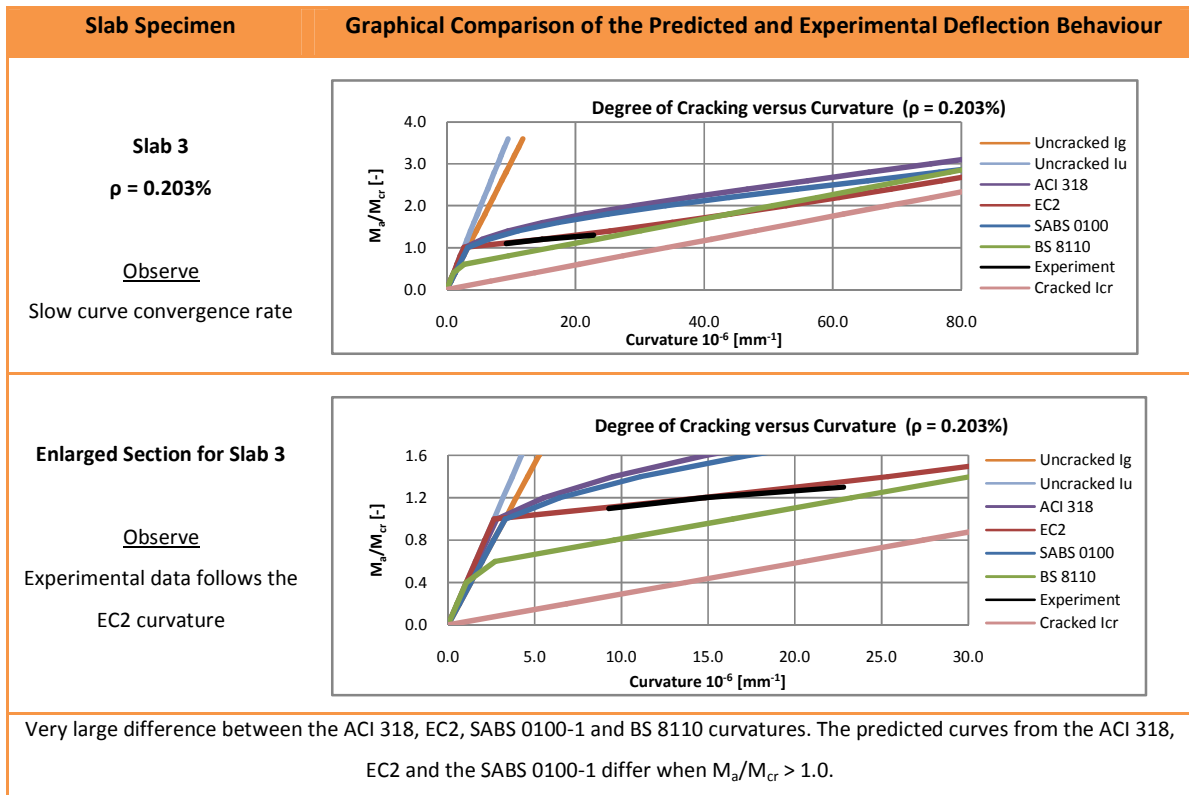


Figure 3-3: Graphical comparison of the initial curvatures for the design standards with $\rho = 0.203\%$.

The bilinear behaviour for the moment against curvature of the reinforced concrete is presented clearly in the graphs in Figures 3-1 to 3-3. The uncracked linear behaviour is presented by the linear curve when an applied moment is applied which is less than the cracking moment. As the applied moment exceeds the cracking moment the curves show the elasto-plastic non-linear behaviour of a partially cracked section.

As the percentage tension reinforcement for the section increases, so does the convergence rate of the curvatures produced by the design standards. In other words, the more tension reinforcement present in a section, the less cracking occurs and the smaller the curvature for the same applied moment. It is evident that the experimental curves tend toward the EC2 curve for all three slab specimens.

It was observed that the predicted curvatures from the different design standards differ for every slab specimen. The BS 8110 curvature presented predicted the point of first cracking at a M_a/M_{cr} ratio less than 1.0 as is seen from the graphs where the BS 8110 curvature deviates from the

uncracked curvatures before the curvatures from the other design standards. The EC2, the ACI 318 and the SABS 0100-1 predict the point of first cracking, i.e. the point where the slab specimen undergoes a change in stiffness due to cracking, occurs at $M_a/M_{cr} = 1.0$. The predicted curvature from the SABS 0100-1 and the ACI are fairly similar close to the point of first cracking, but shows significant difference from the predicted curvature produced from the EC2 approach. This occurrence is due to the different approaches used to predict the reduced member stiffness due to crack development. More detail on this occurrence is discussed in Section 3.3.

The predicted curvature behaviour as presented by the BS 8110 does not show any correlation to the curves from the other design standards when the M_a/M_{cr} ratio is just below and above 1.0. This curve also deviates strongly from the experimental curves. The behaviour is a result of the poor assumptions that the concrete in tension carries a fixed concrete tensile stress. More detail on this occurrence is discussed in Section 3.3.

From the above results, it may be observed that the short-term deflection is heavily dependent on the precise state of cracking at the moment when the load is applied, which is highly unpredictable. It is for this reason that the predicted curvatures differ between the various methods from the design standards. For all three slab specimens, the EC2 (2004) approach best follows the predicted experimental curvatures.

3.2.2 Span/Depth Ratio Comparison for the Design standard Methods

The previous section presented comparative results produced by the deflection prediction methods as presented by the various design standards (Section 2.3). The preferred design method to check the serviceability of a flexural member is the span/depth ratio. A comparison was done to determine whether the methods from the different design standards show any trends that are as noticeable. This section compares the results from the different span/depth ratio methods of calculations as presented by the various design standards in Section 2.4.

The span/depth rules in the EC2 (2004), BS 8110 (1997) and SABS 0100-1 (2000) design standards aim to limit long-term deflections to span/250 mm and deflections after installation of partitions to the least of span/500 or 20 mm with the exception of flat slabs for which EC2 (2004) states

DEFLECTION PREDICTION FOR LIGHTLY REINFORCED CONCRETE SLABS

deflections will be greater. EC2 justifies its span/depth rules for flat slabs on the basis of experience but give no indication of expected deflections of slabs designed using EC2 span/depth rules, which according to Vollum and Hossain (2002), gives significantly thinner sections than BS 8110. The restrictions presented in the ACI 318 (2002) are essentially determined based largely on experience as explained by Branson (1977).

The sets of span/depth equations are applied to two simply-supported one-way slab specimens with the following properties. Table 3-2 presents the properties for the one-way slabs. The amount of percentage tension reinforcement, ρ was varied between $0.20\% \leq \rho \leq 2.40\%$.

Table 3-2: Sectional properties two sections for the purpose of the span/depth comparison.

Slab	h [mm]	L [mm]	d [mm]	b [mm]	f _c [MPa]	f _c [MPa]	E _c [MPa]	f _t [MPa]	f _y [MPa]
1	100.0	2000.0	82.0	850.0	38.4	48.0	27.39	3.60	500.0
2	160.0	2000.0	142.0	850.0	38.4	48.0	27.39	3.60	500.0

The detailed calculations are presented in Appendix B. Figures 3-4 and 3-5 present the comparative span/depth ratios.

The percentage difference between the maximum and minimum value was calculated in order to quantify the trend between the different span/depth approaches by the different design standards.

The maximum allowable span/depth value was taken as the maximum of the values calculated from the SABS 0100-1 (2000), EC2 (2004) and BS 8110 (1997). The values resulting from the ACI 318 (2002) were not included because the ACI 318 considered a span/height ratio, rather than a span/depth ratio. The minimum span/depth ratio was selected in a similar way.

An expression for the percentage difference between the maximum and minimum value is specified below:

$$\%diff = 100 \times (AllowableMAX - AllowableMIN) / AllowableMAX \quad (3-1)$$

DEFLECTION PREDICTION FOR LIGHTLY REINFORCED CONCRETE SLABS

It should be noted that in Figures 3-4 and 3-5 there are no difference between the actual span/depth ratio limit according to the SABS 0100-1 (2000), EC2 (2004) and the BS 8110 (1997). The effective depth of the section is considered to calculate the actual span/depth ratio which stays constant through each comparison. For the ACI 318 (2002) the actual span/height ratio limit, considers the height of the section, thus presenting a slightly higher ratio than the span/depth ratio.

Figure 3-4 supports the statement by Vollum and Hoissan (2002), that the EC2 (2004) produces thinner sections for lightly reinforced members. It is also evident that the differences between the span/depth ratios are far more significant at low levels of tension reinforcement. The difference between the design standards is up to 48.3% for a percentage tension reinforcement of 0.2%. The ratios for the EC2 (2004) and BS 8110 (1997) are almost identical at a percentage tension reinforcement of 1.0%. For slab sections with a percentage tension reinforcement of less than 1.0%, the EC2 (2004) presented the less conservative span/depth ratios, while for slab section with a percentage tension reinforcement larger than 1.0%, the BS 8110 (1997) presented the less conservative span/depth ratio. It is also noted that the lesser ratios are presented by the SABS 0100-1 (2000) over the whole range of percentage tension reinforcement contents, which suggest that the SABS 0100-1 is the most conservative approach for the span/depth ratio.

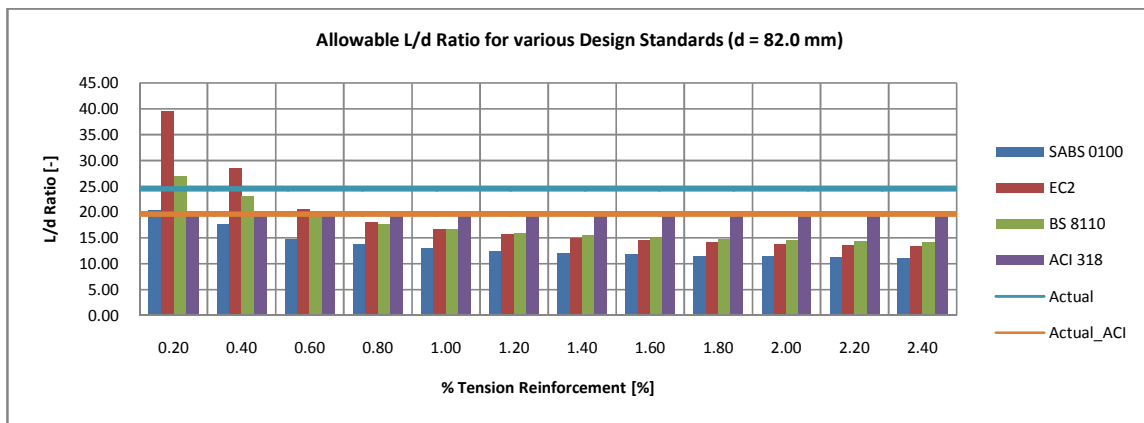


Figure 3-4: Allowable span/depth ratios for the various design standards for Slab 1.

The second slab, Slab 2 has the same properties as Slab 1 with the one exception of an increased section height, resulting in an increased effective depth of the section. The calculated span/depth ratios for Slab 2 are presented in Figure 3-5. The calculations for the span/depth ratios are presented in Appendix B.

DEFLECTION PREDICTION FOR LIGHTLY REINFORCED CONCRETE SLABS

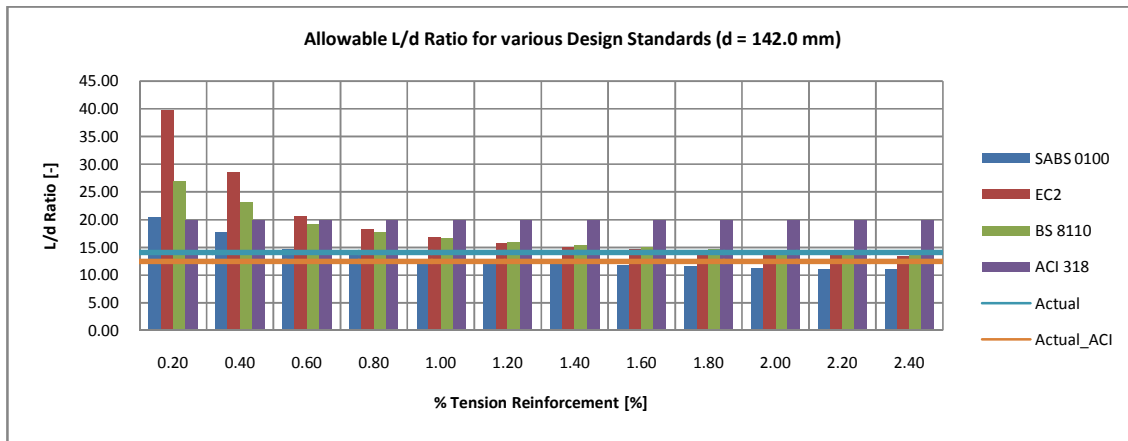


Figure 3-5: Allowable span/depth ratios for the various design standards for Slab 2.

The increased depth allows a much similar trend relative to the thinner slab (Figure 3-5). The major difference is that the actual span/depth and actual span/height of Slab 2 differ less relative to what was observed from the results for Slab 1.

In both the data from Slab 1 and Slab 2, the percentage differences between the maximum and minimum allowable span/depth ratios from the different methods reach a constant range of percentages of 22.0% to 21.5%. These percentages suggest that at a percentage tension reinforcement larger than 1.0%, the expected maximum difference between the methods as presented in the design standards, range between 22.0% and 21.5%. This difference is reasonably small and indicates that any of the span/depth methods may be used to calculate the span/depth ratio for a slender member with a percentage tension reinforcement larger than 1.0%.

Vollum and Hoissan (2002) concluded that the main benefits of using the EC2 (2004) approach, where the concrete strength is one of the parameters, rather than BS 8110 (1997) or SABS 0100-1 (2000) rules are:

- Slab thicknesses are almost independent of the load applied to the member
- The benefit of increasing concrete strength is included, and
- The effect of cracking during construction is incorporated.

It is further shown, by Vollum and Hoissan (2002), that it is more efficient to reduce slab thickness by increasing concrete strength than reinforcement area and that the EC2 (2004) span/depth rules overestimate the benefit of adding extra reinforcement.

3.3 RELEVANCE OF CRACK DEVELOPMENT AND TENSION STIFFENING

This section aims to discuss the way in which the deflection prediction methods predict the gradual change of the member in flexure from an uncracked to a cracked state. The first approximation is presented by Branson's approach (Branson, 1977) while another approach was presented by Bischoff (2005). The different approaches are compared with the data as presented by Gilbert (2007), to illustrate the differences in deflection prediction from the various prediction methods.

Deflections of concrete members are closely linked to the extent of cracking and the degree to which the cracking capacity is exceeded. The point at which cracking occurs is determined by the moments induced in the slab and the tensile strength of the concrete, which increases with age. Often the critical condition occurs when the slab formwork is removed and the slab loads are applied. At this point the slab undergoes flexural bending and cracking starts. Once the slab has cracked its stiffness is permanently reduced (Webster & Brooker, 2006).

Approximating Crack Development Mathematically

The phenomenon of crack development is presented in the Figures 3-6 and 3-7. The concrete is uncracked (I_g , the gross moment of inertia, or more accurately I_u , the uncracked moment of inertia, is effective) in regions of small moment and more or less fully cracked (I_{cr} , the cracked moment of inertia, is effective) in regions of large moment, with the cracks extending to close to the neutral axis in the latter case. Between the small and large moments, the depth and width of cracks vary in some manner with the moment diagram. In addition, the concrete between the cracks still carries some tension (tension stiffening). As a result, the actual effective moment of inertia, I_e at a given cross-section will be between the uncracked and the fully cracked value, and the same is true of an average effective moment of inertia, I_{ae} for the entire span (Branson, 1977).

DEFLECTION PREDICTION FOR LIGHTLY REINFORCED CONCRETE SLABS

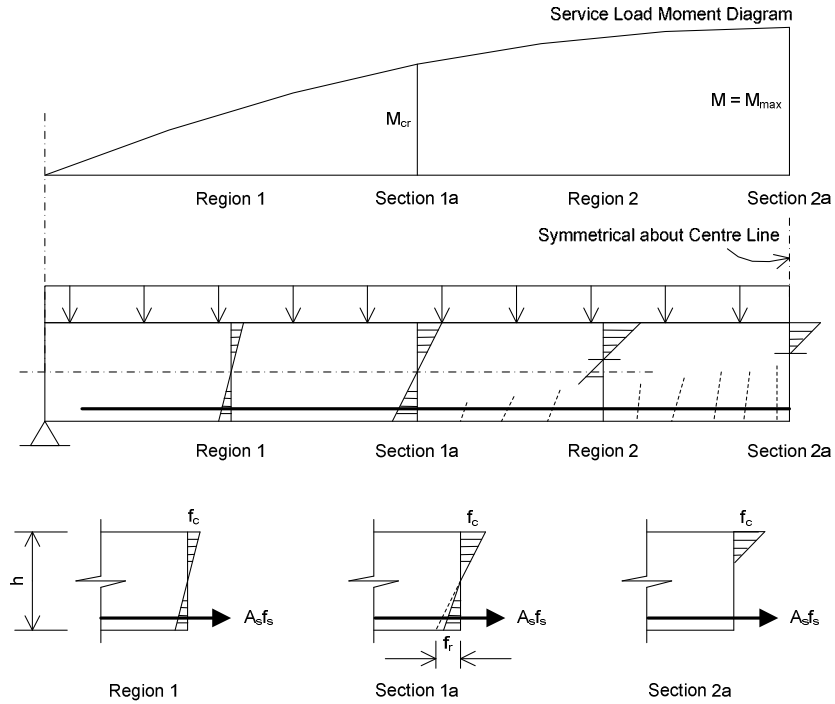


Figure 3-6: Various regions of stress and cracking in a reinforced concrete beam carrying service loads (Branson, 1977).

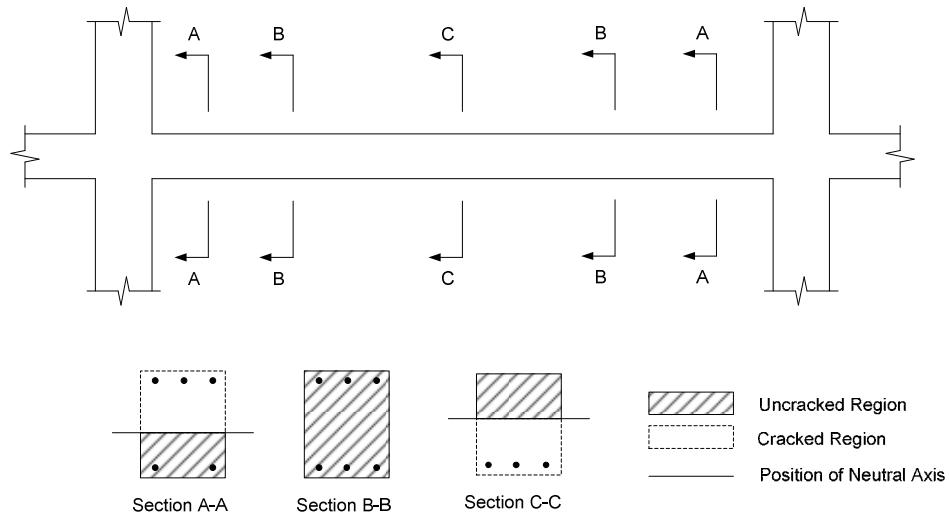


Figure 3-7: Limiting Effective Sections for a Continuous Beam (Branson, 1977)

A logical form of an expression for the effective moment of inertia, I_e at an individual cracked section that satisfies the limiting conditions is suggested by Branson (1977). The equations result that $I_e = I_g$ when the moment at the individual section $M = M_{cr}$, while I_e approaches I_{cr} when M is very large

compared to M_{cr} (Branson, 1977). When $M < M_{cr}$, the applied moment is less than the cracking moment, suggesting the section is still uncracked, therefore the condition where $I_e = I_g$ is extended to $M \leq M_{cr}$. When $M > M_{cr}$:

$$I_e = I_g - (I_g - I_{cr})[1 - (M_{cr}/M)^m] \quad (3-2)$$

where m is an unknown power and M_{cr}/M takes the level of cracking into consideration.

From the design standards, namely the SABS 0100-1 (2000) and ACI 318 (2002), m is taken as 3. Some authors in literature may take m as 4, according to Branson (1977). The solutions for equation 3-2 for $m = 3$ and $m = 4$ differs by a maximum of 3% for members with a percentage tension reinforcement larger than 1.0%. It may be demonstrated by hand calculations that the results from these two Equations are not particularly sensitive to the exact powers of 3 and 4. Equation 3-2 may be rewritten with $m = 3$ to produce the following expression for $M \geq M_{cr}$:

$$I_e = (M_{cr}/M_a)^3 I_g + [1 - (M_{cr}/M_a)^3] I_{cr} \quad (3-3)$$

Where M_a is the maximum moment at the loading stage for which the deflection is being computed. When M in Equation 3-2 or M_a in Equation 3-3 is less than M_{cr} , $I_e = I_g$. I_e in both equations provides a transition between the well-defined upper and lower bounds of I_g and I_{cr} , presented as a function of the level of cracking which can be expressed in the form of M/M_{cr} or M_a/M_{cr} .

DEFLECTION PREDICTION FOR LIGHTLY REINFORCED CONCRETE SLABS

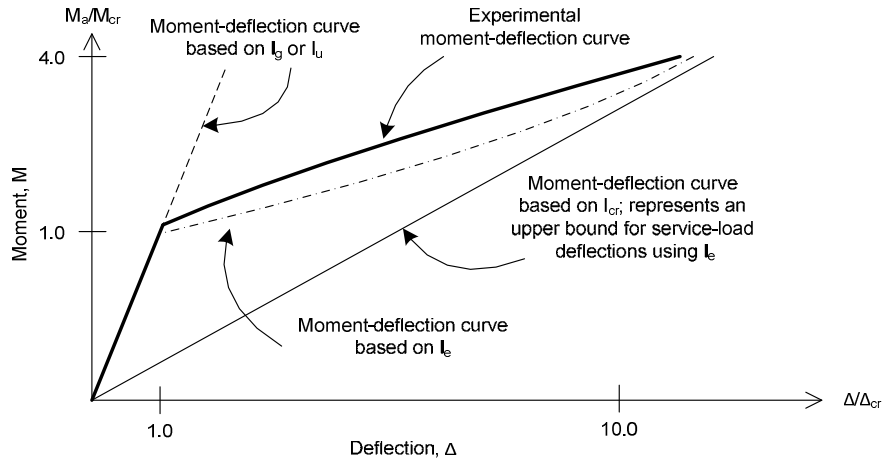


Figure 3-8: Experimental moment-deflection curve for beam with 0.93 % reinforcement compared with theoretical moment-deflection curves (Branson, 1977).

A typical experimental moment versus deflection curve is reproduced from the data provided by Branson (1977) for a simply supported reinforced concrete flexural member as shown in Figure 3-8. The bilinear behaviour of the experimental and the predicted (Equation 3-3) moment-deflection curves are also shown in Figure 3-5.

It is noted that the slope of the moment versus deflection curve in Figure 3-8 changes sharply after cracking, and this is reflected in a sharp decrease in I_e following cracking, as can also be seen in Figure 3-9. In Figure 3-9, the I_g/I_{cr} ratio increases the slope as the decrease in I_e becomes more pronounced, and approaches an abrupt drop in I_e for loads just above $M_a/M_{cr} = 1.0$. This latter condition would result in a brittle failure type load or moment-deflection curve, which would be the case for an unreinforced beam or $I_g/I_{cr} = \text{infinity}$. However, for most reinforced beams there is a significant rise in the load or moment-deflection relation above the point of first cracking because of the gradual development of hairline cracks vertically, the distribution of cracks along the span, and the effect of tensile concrete between cracks (Branson, 1977).

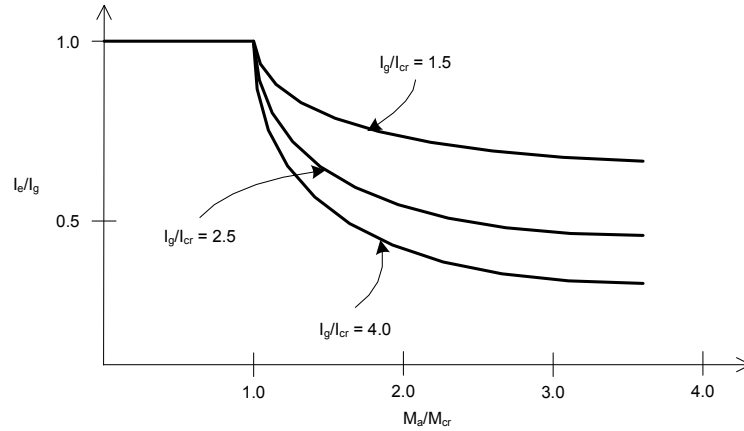


Figure 3-9: Generalized effective moment of inertia versus bending moment relation in the cracking range – I_e/I_g versus M_a/M_{cr} curves for different values of I_g/I_{cr} as computed by Equation 3-2 (Branson, 1977).

In the usual working range ($M_a/M_{cr} =$ up to 3 to 4), Equation 3-3 shows good agreement with experimental results according to Branson (1977). The result is improved if I_u is used instead of I_g , which would raise the point of first cracking, had it been used in Equation 3-3.

In an evaluation by Bischoff (2005) on Branson's Equation for I_e , it was found that the accuracy of Equation 3-3 is affected by the ratio of I_g/I_{cr} of the section. Others have also recognised the influence of reinforcing ratio on Branson's approach (Branson, 1977). Bischoff also found the tension stiffening effect in Equation 3-1 is highly dependent on both the power of m and the ratio of I_g/I_{cr} for lightly reinforced members (less than 1.0%), and is usually overestimated for the member response for $I_g/I_{cr} > 3$ when $m = 3$. The ratio I_g/I_{cr} in turn, depends on the reinforcing ratio ρ as well as the modular ratio α_e . Reasonable values of I_e are only obtained for steel reinforced concrete members when $\rho = 1.0\%$ since this corresponds to a ratio of $I_g/I_{cr} \approx 3$. Lightly reinforced members with a high I_g/I_{cr} cause the value of I_e to be grossly overestimated (Bischoff, 2005).

Branson's Equation Revisited: the Tension Stiffening Factor

Bischoff (2005) evaluated the approach and presented a new derivation to estimate the moment of inertia of a partially cracked Section. This section discusses Bischoff's (2005) approach.

It is discussed that Branson's approach was calibrated to accurately predict member deformation within a specified applied moment and stiffening ratio, I_g/I_{cr} , limit. For more lightly reinforced

DEFLECTION PREDICTION FOR LIGHTLY REINFORCED CONCRETE SLABS

members, the applied moment and stiffening ratio, I_g/I_{cr} , are beyond the limits as specified by Bischoff (2005). Bischoff proposed a new derivation for an effective moment of inertia equation, by applying the basic concepts of tension stiffening. The effect of tension stiffening within lightly reinforced members result in the member having an increased stiffness, due to the significant tensile strength of the concrete between the cracks, as was discussed in Section 2.2.2.

According to Bischoff's (2005) study Branson's approximation for an effective moment of inertia I_e tends toward I_g as the ratio I_g/I_{cr} increases. Tension stiffening is modelled reasonably well for $I_g/I_{cr} = 2$ which is not surprising since Branson calibrated his work using beams with $I_g/I_{cr} = 2.2$. However, as the ratio I_g/I_{cr} is increased to 4, tension stiffening starts to become excessive at load levels less than about twice the cracking moment. Tension stiffening is grossly overestimated at higher values of I_g/I_{cr} . This leads to a much stiffer response and smaller deflection than expected, which is why the expression does not work well for lightly reinforced concrete members (Bischoff, 2005).

Branson's equation gives a weighted average of the gross and cracked moments of inertia at any given load levels. This is analogous to having an uncracked and cracked spring placed in parallel as shown in Figure 3-10, where the equivalent spring stiffness $k_e = k_g + k_{cr}$ approaches the uncracked stiffness k_g of the stiffer spring, as the difference between the two spring stiffness values increases. This occurs when the ratio k_g/k_{cr} becomes larger as the cracked stiffness k_{cr} decreases for smaller values of I_{cr} . Consequently, the member response is incorrectly "pulled" towards a weighted value of the uncracked response $E_c I_g (M_a/M_{cr})^3$ as the reinforcing ratio and elastic modulus of the reinforcing bar decreases. This results in an unrealistically high amount of tension stiffening and smaller deflections than expected, the moment I_{cr} drops below one-third of I_g , according to Bischoff (2007).

DEFLECTION PREDICTION FOR LIGHTLY REINFORCED CONCRETE SLABS

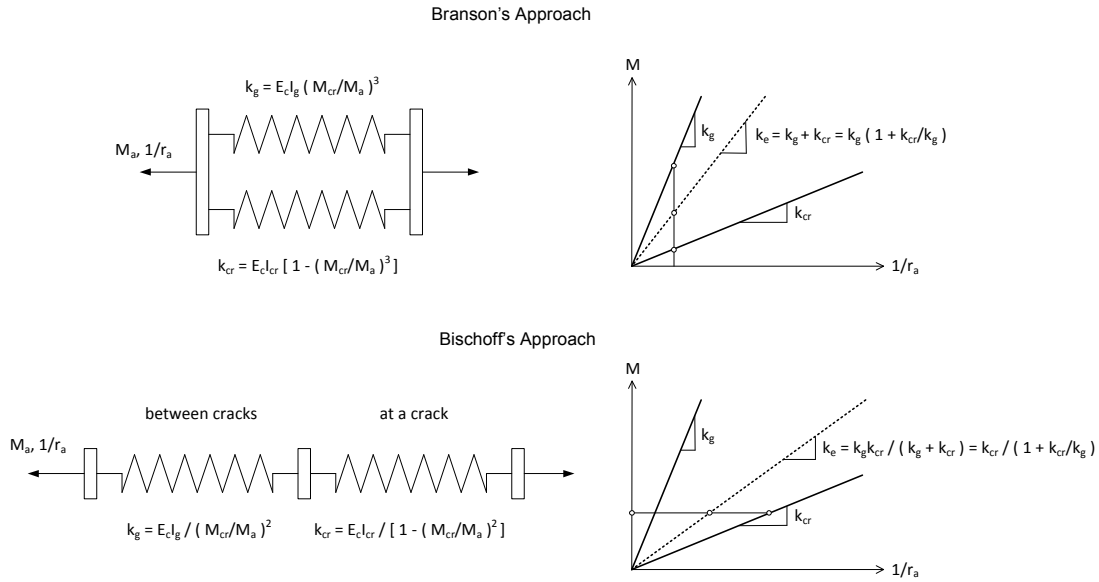


Figure 3-10: Equivalent spring model for Branson's and Bischoff's expressions (Bischoff, 2007).

According to Bischoff (2007) the tension stiffening is modelled properly by putting the uncracked and cracked springs in series, as seen in Figure 3-10, to represent the variation in stiffness of the uncracked and cracked parts of the beam along the member length. Using this approach, the member stiffness is then “pulled” more realistically towards the response with the lower stiffness. The equivalent or effective spring stiffness is now determined by taking a weighted average of the inverse stiffness values ($1/EI$), leading to a subtle change in Branson's original Equation 3-3 as given in Equation 3-4.

$$\frac{1}{I_e} = \left(\frac{M_{cr}}{M_a}\right)^m \frac{1}{I_g} + \left[1 - \left(\frac{M_{cr}}{M_a}\right)^m\right] \frac{1}{I_{cr}} \geq \frac{1}{I_g} \quad (3-4)$$

Calibration of this Equation with Equation 3-3 for a beam with $I_g/I_{cr} = 2.2$ (Branson calibrated his original equation using beams with this ratio) gives a power of $m = 2$ (Bischoff, 2005). Rearranging Equation 3-4 with $m = 2$ reduces to a new expression known as Bischoff's approach (Bischoff, 2005), where η is known as the tension stiffening factor with $\eta = M_{cr}/M_a$.

$$I_e = \frac{I_{cr}}{1 - \left(1 - \frac{I_{cr}}{I_u}\right) \eta \frac{M_{cr}}{M_a}} \leq I_g \quad (3-5)$$

DEFLECTION PREDICTION FOR LIGHTLY REINFORCED CONCRETE SLABS

Setting η equal to one gives a bilinear response with constant tension stiffening that represents an upper bound on member stiffness, as shown in Figure 3-11, while a η value of zero gives a lower bound response with no tension stiffening that essentially gives the I_{cr} response. To approximate a partially cracked Section η is taken as M_{cr}/M_a .

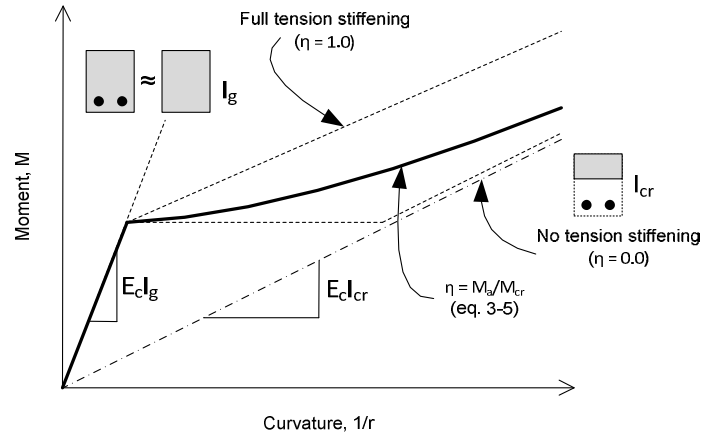


Figure 3-11: Theoretical moment curvature response at the critical section using Equation 3-5 with different tension stiffening values (Bischoff, 2008).

Equation 3-5 is also the same as the curvature-based equation used in EC2 (2004) for deflection calculations. Equation 3-5 is thus proposed as a suitable replacement for Branson’s equation because it represents a physical model that correctly accounts for tension stiffening in reinforced concrete beams and slabs.

A graphical comparison between Bischoff and Branson’s approach is shown in Figure 3-12 (Bischoff, 2007). Results are compared at the full service load. According to Bischoff (2007) the service load moments ($M_a = M_r / \alpha_{load}$) are approximately equal to 60% of the nominal moment capacity (M_n) provided that the beam is under-reinforced, where M_r is the factored moment resistance calculated using material resistance factors, and α_{load} is an average load factor equal to 1.375 for an assumed dead to live load ratio of 1:1. All calculations are carried out for concrete with a cylinder compressive strength f'_c of 35 MPa and steel with a yield strength f_y of 400 MPa. The vertical axis shows the ratio of the service load deflection, Δ_a to the deflection at first cracking, Δ_{cr} while the horizontal axis shows the increasing steel reinforcing ratio. The results in Figure 3-12 show that both Branson’s and Bischoff’s approach, give comparable results for reinforcing ratios between 1.0% and 2.0%. However, differences between the two approaches become evident once steel reinforcing ratios

drop below 1.0%, with Branson's approach under-predicting deflection by up to half of the calculated value using Bischoff's approach for a beam with a reinforcing ratio of 0.3% (Bischoff, 2007).

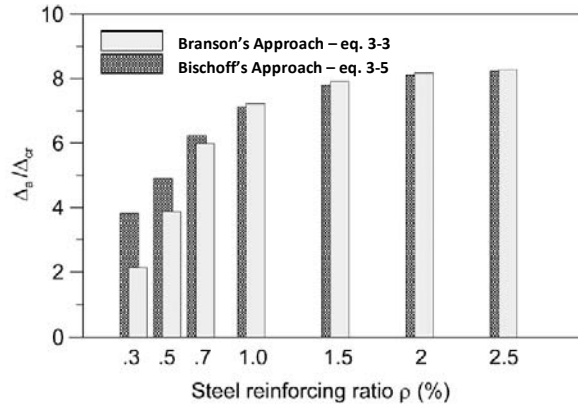


Figure 3-12: Deflection comparison using Branson's and Bischoff's expressions for I_e (Bischoff, 2007).

Comparison between Branson and Bischoff's Approach

The different expressions available to numerically model a partially cracked member have been discussed. Bischoff (2005) and Branson (1977) presented two different approaches. Clear differences are observed between the resulting deflections from these approaches (Figure 3-12). This section compares the resulting deflections as calculated from the different design standards, as presented in a study by Gilbert (2007).

From the discussions from Section 2.3, it may be established that the SABS 0100-1 (2000) and ACI 318 (2002) follow Branson's approach, while the EC2 (2004) follow a similar approach to Bischoff's approach. The BS 8110 (1997) uses an approach involving the calculation of the curvature at particular cross sections and then integrating over the span to obtain the deflection. The BS 8110 (1997) approach assumes the section of a flexural member is either uncracked or cracked and presents no specific modelling approach for predicting gradual cracking.

In an experimental study by Gilbert (2007), eleven one-way simply supported slabs were tested to obtain short-term deflections over a moment range of $1.1M_{cr}$ to $1.3M_{cr}$. The equations used to calculate the curvatures from the effective moment of inertia expressions for the different design

DEFLECTION PREDICTION FOR LIGHTLY REINFORCED CONCRETE SLABS

standards, are presented in Table 3-3. The exercise was repeated here for the SABS 0100-1 (2000) approach and included in the comparison.

Table 3-3: Summary of the different model of I_e for the various design standards.

Design standard	Effective Moment of Inertia, I_e	Curvature, $1/r_i$
ACI 318 (2002)	$I_e = \left(\frac{M_{cr}}{M_a}\right)^3 I_g + \left[1 - \left(\frac{M_{cr}}{M_a}\right)^3\right] I_{cr} \leq I_g$	$\frac{1}{r_i} = \frac{M_a}{E_c I_e}$
BS 8110 (1997)	$\Delta M = \frac{b(h-x)^3}{3(d-x)} f_t$	$M_a > \Delta M:$
		$\frac{1}{r_i} = \frac{M_a - \Delta M}{E_c I_{cr}}$
EC2 (2004)	$I_e = \frac{I_{cr}}{1 - \left(1 - \frac{I_{cr}}{I_u}\right) \left(\frac{M_{cr}}{M_a}\right)^2} \leq I_u$	$M_a \leq \Delta M:$
		$\frac{1}{r_i} = \frac{M_a}{E_c I_u}$
SABS 0100-1 (2000)	$I_e = \left(\frac{M_{cr}}{M_a}\right)^3 I_g + \left[1 - \left(\frac{M_{cr}}{M_a}\right)^3\right] I_{cr} \leq I_g$	$\frac{1}{r_i} = \frac{M_a}{E_c I_e}$

The results from the equations are presented in the article by Gilbert (2007). Table 3-4 summarizes the results from Gilbert's recorded data. The results for the SABS 0100-1 (2000) are presented in Appendix C. The data is presented as a ratio of the predicted deflection over experimental deflection on the vertical axis versus the percentage tension reinforcement, ρ , on the horizontal axis. The percentage tension reinforcement varies from $0.18\% \leq \rho \leq 0.84\%$. Table 3-4 shows the data tendencies for every moment series from every deflection calculation approach. The more the deflection ratios tend towards 1.0, the closer the model resembles the experimental results. The data tendencies (deflection ratios) are designated as the average (Avg.), the maximum (Max.) and the minimum (Min.). The average presents the average of the data points plotted for each of the curve, while the maximum and the minimum data points represents the highest and lowest data point for each curve, respectively.

DEFLECTION PREDICTION FOR LIGHTLY REINFORCED CONCRETE SLABS

The results from the ACI 318 (2002) and the SABS 0100-1 (2000) model (Branson's model) show a uniform response for all three levels of applied moment. The deflection ratios show a trend of equating to less than 1.0, indicating that the Branson's approach underestimates deflection for low levels of reinforcement. The BS 8110 (1997) shows the most radical model with the deflection ratios showing the largest varying trend, thus supporting the hypothesis that the BS 8110's model presents the most unreliable results. It is noted from results for the BS 8110 (1997) model, that as the moment increases from a $1.1M_{cr}$ to $1.3M_{cr}$, the deflection is first overestimated and then underestimated. The results from the EC2 (2004) model, (Bischoff's model) show the best resemblance to the experimental data owing to the deflection ratios nearest to the value 1.0.

DEFLECTION PREDICTION FOR LIGHTLY REINFORCED CONCRETE SLABS

Table 3-4: Summary of the results as recorded from Gilbert (2007).

Moment	Deflection Ratios			Graphical Representation of Data for each Model
	Avg.	Max.	Min.	
1.1M _{cr}	0.59	0.78	0.42	<p style="text-align: center;">Deflection Ratio VS %A_s for ACI 318</p>
1.2M _{cr}	0.55	0.81	0.35	
1.3M _{cr}	0.54	0.70	0.31	
1.1M _{cr}	1.02	1.35	0.80	<p style="text-align: center;">Deflection Ratio VS %A_s for Eurocode 2</p>
1.2M _{cr}	1.10	1.39	0.88	
1.3M _{cr}	1.09	1.36	0.91	
1.1M _{cr}	2.03	2.44	1.24	<p style="text-align: center;">Deflection Ratio VS %A_s for BS 8110</p>
1.2M _{cr}	1.64	2.04	1.08	
1.3M _{cr}	0.39	0.76	0.01	
1.1M _{cr}	0.56	0.89	0.32	<p style="text-align: center;">Deflection Ratio VS %A_s for SABS 0100-1</p>
1.2M _{cr}	0.46	0.74	0.22	
1.3M _{cr}	0.44	0.74	0.18	

3.4 INFLUENCE OF PERCENTAGE REINFORCEMENT AND STIFFENING RATIO ON DEFLECTION PREDICTION

This section evaluates the effect of the percentage reinforcement (ρ) and the stiffening ratio (I_g/I_{cr}) on the effectiveness of the approaches to predict the actual deflection behaviour.

In order to observe the effect of the percentage tension reinforcement on the predicted deflection behaviour, the different deflection prediction methods as presented in Section 2.3, were used to calculate the deflection behaviour of a slab specimen with a varied reinforcing percentage. A simply supported one-way slab specimen was used in this comparison and the slab properties are presented in Table 3-9. The percentage tension reinforcement for the section was varied between $0.18\% \leq \rho \leq 2.10\%$. The set of equations applied to obtain the predicted behaviour only apply to the equations provided for short-term deflection calculations.

Table 3-5: Slab properties for a simply-supported one-way slab.

Slab Properties							
b [mm]	h [mm]	L [mm]	d [mm]	f'_c [MPa]	f_c [MPa]	E_c [MPa]	f_t [MPa]
850.0	100.0	2000	79.0	48.8	60.5	30.5	4.04

Appendix D presents the detailed calculations, while Table 3-5 presents the summarized results. In Table 3-6, M_a/M_{cr} depicts the degree of cracking of the section on the vertical axis, while the curvature is presented on the horizontal axis. While $M_a/M_{cr} \leq 1.0$ the section undergoes linear behaviour, but when $M_a/M_{cr} > 1.0$ the section undergoes non-linear behaviour representing a partially cracked section.

Six different graphs are presented for the comparison in Figure 3-13. In every graph seven different curves are presented. The uncracked curves present the curvatures that would be obtained using the gross moment of inertia, I_g (SABS 0100-1, 2000) and the uncracked moment of inertia, I_u (EC2, 2004). These curves present the behaviour for an uncracked member. The cracked curve is produced from the EC2 (2004) approach. This curve is similar for the cracked curves calculated from the other design standards (Section 2.2.1). Also, a predicted curve for each of the design standards is presented.

DEFLECTION PREDICTION FOR LIGHTLY REINFORCED CONCRETE SLABS

Degree of Cracking relative to Various Percentages of Tension Reinforcement for a specific Section

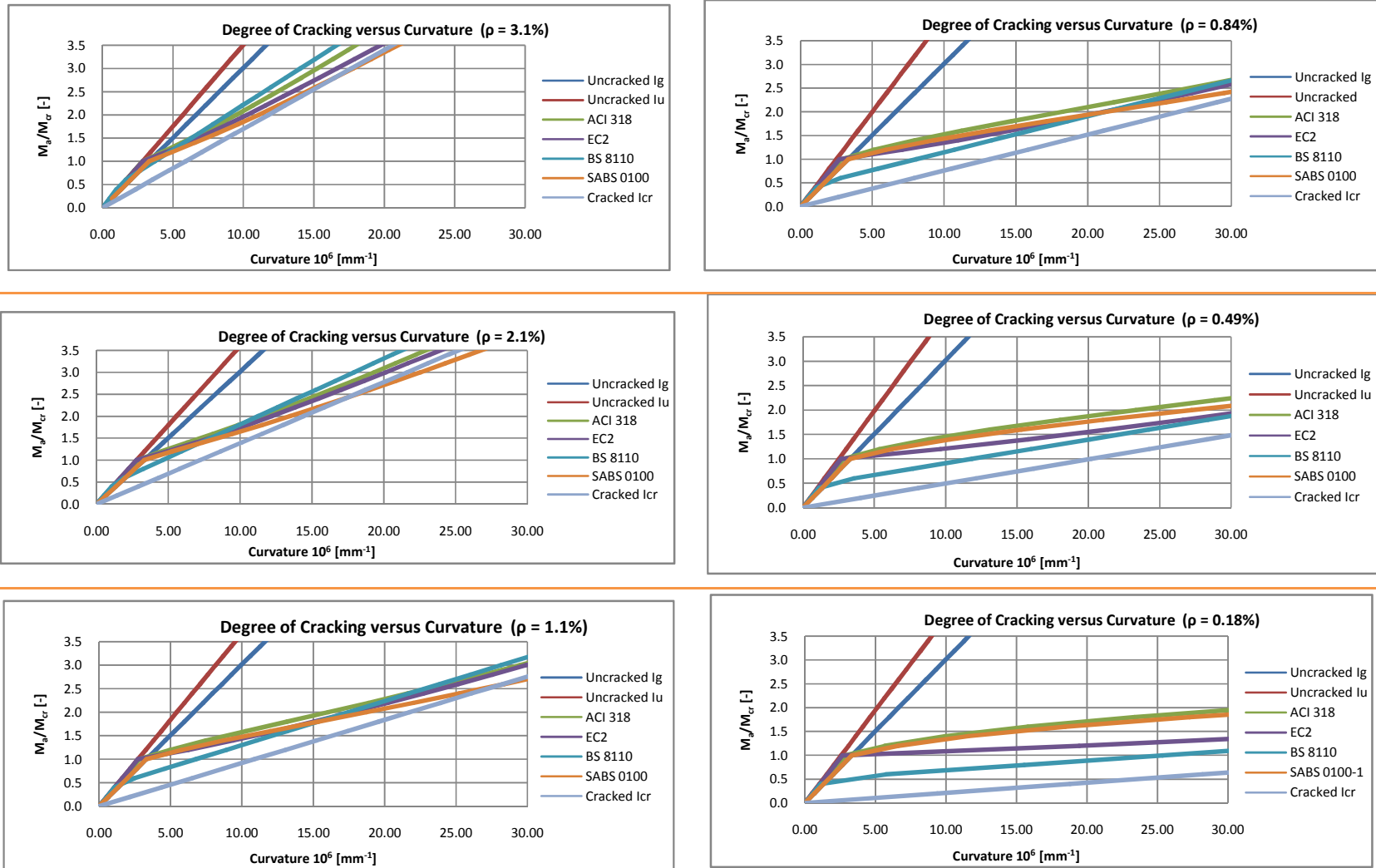


Figure 3-13: Degree of cracking relative to various percentages of tension reinforcement for a specific section.

DEFLECTION PREDICTION FOR LIGHTLY REINFORCED CONCRETE SLABS

For sections containing large percentages of tension reinforcement the same level of bending moment produce a smaller curvature than for the section with a small percentage of tension reinforcement. It is also evident from Figure 3-13 that the curves tend more to the uncracked curvatures as the percentage tension reinforcement increases. Then, as would be expected, the curves show a diverging trend as the percentage tension reinforcement decreases.

According to Bischoff (2007) and Gilbert (1999), the empirically derived relationship for the ACI 318 (2002) and SABS 0100-1 (2000), also known as Branson's equation (Equation 3-3), was calibrated for steel-reinforced concrete beams with a reinforcing ratio between 1.0% and 2.0%. This corresponds to beams with an uncracked to cracked stiffness (I_g/I_{cr}) ratio between 2 and 3. Branson's approach underestimates short-term deflection for lightly-reinforced members with a service load near or below the cracking moment (Bischoff, 2007). When the service moment is near the cracking moment and I_g/I_{cr} becomes very large, Branson's equation does not accurately predict the amount of cumulative cracking and tension stiffening within a member, and thus under predicts the deflections.

Figure 3-14 is also a product from the series of calculations performed to obtain Figure 3-13. Figure 3-14 shows the exponential trend of the I_g/I_{cr} ratio with decreasing percentage reinforcing steel. A similar result is obtained by Bischoff's study (Bischoff, 2007). The curves below may be divided into two parts. The exponential behaviour, first part, of the curve is observed over a reinforcing percentage of 0.18% to 1.70%. The more linear behaviour, second part, is observed over a reinforcing percentage of 1.70% to 3.10%

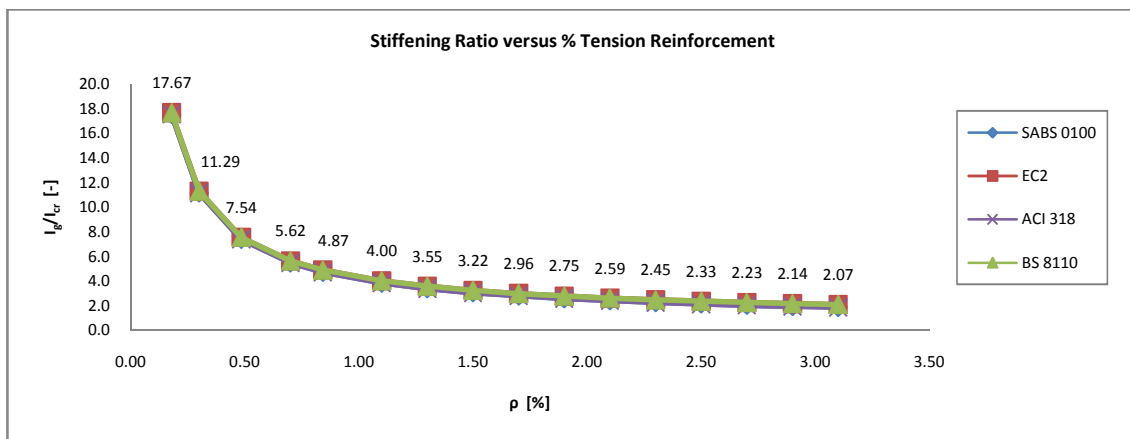


Figure 3-14: Stiffness Ratio versus percentage tension reinforcement based on the Section described in Table 3-5.

DEFLECTION PREDICTION FOR LIGHTLY REINFORCED CONCRETE SLABS

According to Bischoff (2007), the Branson's approach adequately predict the actual deflection behaviour at a stiffening ratio of less than 3.0 which corresponds to the second part of the curve in Figure 3-14. Bischoff's approach effectively predicts a good approximation of the actual deflection behaviour over the entire range of stiffening ratios (Bischoff, 2007).

Gilbert (2007) did a more comprehensive study on exactly how tension stiffening affects member stiffness in lightly reinforced concrete members. For the BS 8110 (1997) approach, Gilbert concluded that by limiting the concrete tensile stress at the level of the tensile reinforcement to just 1.0 MPa, the BS 8110 (1997) approach overestimates the deflection of the test slabs both below and immediately above the cracking moment. This is not unreasonable and accounts for the loss of stiffness that occurs in practice due to restrain shrinkage according to Gilbert (2007). Nevertheless, the BS 8110 (1997) approach provides a relatively poor model of the post cracking stiffness and incorrectly suggests that the average tensile strength carried by the cracked concrete actually increases as the moment increases and the neutral axis rises. Thus, it may be observed from the graphs in Figure 3-13 that the slope of the BS 8110 approach at first cracking is steeper than the other curves.

The approach by the EC2 (2004) is known as Bischoff's approach (Bischoff, 2005). In order to examine the behaviour of this equation at low levels of tension reinforcement some data from Figure 3-3 is reproduced below. The data is obtained similarly to the data presented in Figure 3-13 with the addition of experimental data recorded by Gilbert (2007) to present the actual one-way slab curvature response. Gilbert (2007) only published three experimental data points within the range $1.1M_{cr}$ to $1.3M_{cr}$.

Two graphs are presented in Table 3-11. The first graph shows the deflection-curvature results for a Section defined in Section 3.2.1 with a percentage tension reinforcement of 0.203%. The second graph is an enlargement of the first graph.

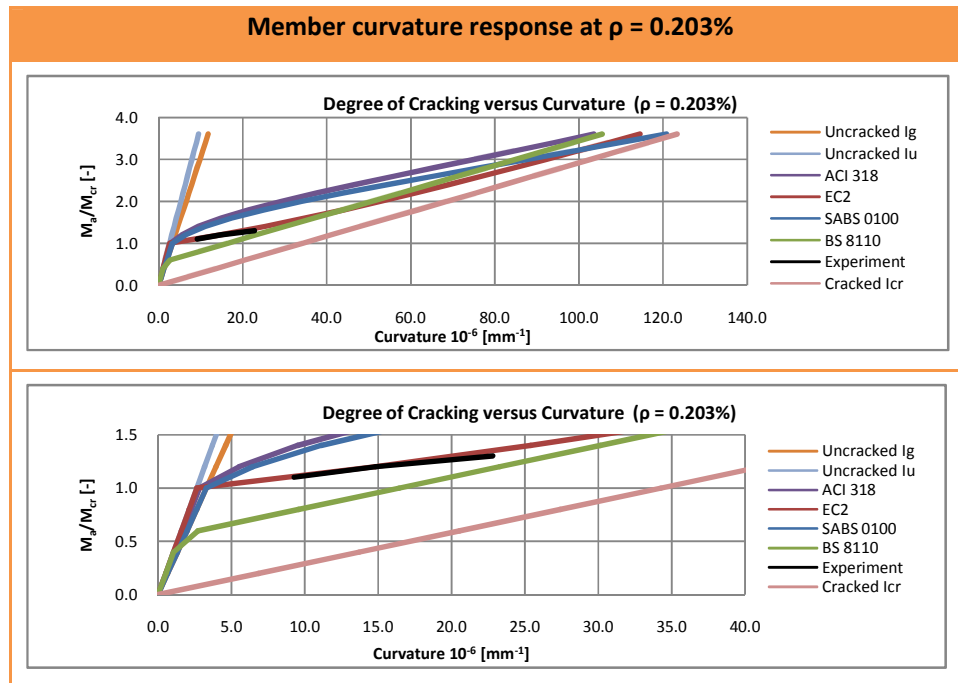


Figure 3-15: Member curvature response at a percentage tension reinforcement of 0.203%.

Attending to the second plot in Figure 3-15 it is evident that the experimental data follows the curve presented by Bischoff’s Equation or the EC2 (2004) approach. This results show that the EC2 (2004) models the experimental curvature behaviour of lightly reinforced members, more accurately than the BS 8110 (1997), ACI 318 (2002) and SABS 0100-1 (2000) approaches.

3.5 INFLUENCE OF APPLIED MOMENT TO CRACKING MOMENT RATIO ON DEFLECTION PREDICTION

Section 2.3 presented the different empirical approaches by Bischoff (2005) and Branson (1977), to quantify the partially cracked behaviour of a deflecting flexural member. An aspect influencing the effectiveness of these approaches was discussed in Section 3.3, the percentage tension reinforcement (ρ) and the stiffening ratio (I_g/I_{cr}). Another aspect of influence is the level of cracking, M_a/M_{cr} ratio. This section discusses the influence of the M_a/M_{cr} ratio of the effectiveness of the different deflection prediction methods.

The member responses from the discussion in Section 3.3 were dependent on the level of applied moment, M_a , relative to the cracking moment, M_{cr} , thus the level of service load applied. The

DEFLECTION PREDICTION FOR LIGHTLY REINFORCED CONCRETE SLABS

amount of reinforcement in a member influences the level of service load the member can withstand. It was also evident that the bilinear curves in Figure 3-13 diverge when the applied moment is just above the cracking moment and converges at a later stage as the applied moment increases. The rate at which these curves converge is dependent on the amount of tension reinforcement, where large amounts of reinforcement produce a swift convergence rate over a small range of curvature, while low amounts of reinforcement produce a slow convergence rate over a larger range of curvatures.

This diverging trend may be quantified to identify the M_d/M_{cr} range where the largest difference between the deflection prediction methods occurs. For the purpose of this comparison this range was named the *Critical M_d/M_{cr} Range*. In order to obtain a comparative trend, the percentage differences between the effective moment of inertia, I_e , relative to the gross moment of inertia, I_g , was calculated. The values for I_e were varied over a range of percentage tension reinforcement of $0.1\% \leq \rho \leq 4.1\%$. The section dimensions and properties used for the evaluation are defined in Table 3-6.

Table 3-6: One-way slab sectional dimensions and properties.

Slab Properties							
b [mm]	h [mm]	L [mm]	d [mm]	f'_c [MPa]	f_c [MPa]	E_c [MPa]	f_t [MPa]
850.0	100.0	2000	79.0	48.8	60.5	30.5	4.04

The percentage difference (%diff) of the effective moment of inertia, I_e , relative to the gross moment of inertia, I_g was calculated. The small differences between the uncracked moment of inertia, I_u and gross moment of inertia, I_g resulted that the percentage difference of the I_e relative to the I_u was also calculated. The equation used to calculate the %diff of the I_e for each design standards is presented in Equation 3-6.

$$\%diff = 100 \times [(I_g - I_e)/I_g] \quad (3-6)$$

Equation 3-6 is also used to calculate the %diff relative to I_u , by substituting I_g with I_u .

The results for the %diff of the I_e relative to the different moment of inertia are compared in Figure 3-16. The curves are presented as the %diff of I_e versus the increasing M_d/M_{cr} ratio. Note that at a

DEFLECTION PREDICTION FOR LIGHTLY REINFORCED CONCRETE SLABS

M_a/M_{cr} less than one, the %diff of the I_e are constant and represents the linear behaviour of the member. At a M_a/M_{cr} equal to or larger than one, the equivalent (cracked) section governs the member behaviour, as seen from the SABS 0100-1 (2000), ACI 318 (2002) and EC2 (2004) curves. The curves produced from the SABS 0100-1 (2000) and the ACI 318 (2002) are similar since both assumes Branson's (1977) expression for the calculation of I_e . The BS 8110 (1997) curve represents a different behaviour due to the assumptions within the approach. The section is either uncracked (at a low %diff of the I_e) or fully cracked (at a high %diff of the I_e). The BS 8110 approach does not model the gradual change from an uncracked to a partially cracked section, as is demonstrated by the other approaches.

In Figure 3-16 the left graph shows the %diff of the I_e relative to I_g and the right, the %diff of the I_e relative to I_u . The calculations for the data are presented in Appendix E.

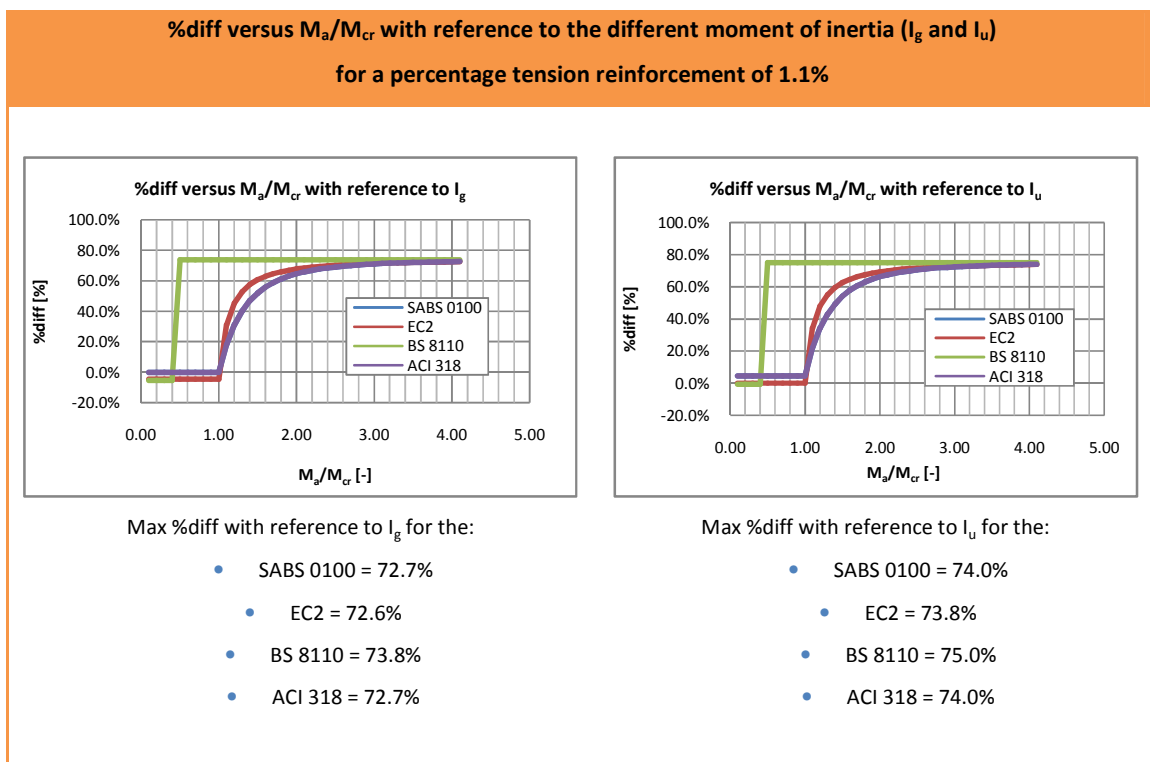


Figure 3-16: %diff versus M_a/M_{cr} for a section at a percentage tension reinforcement of 1.1%.

The values of every %diff of the I_e of the different design standards, differ slightly but not to such a large extent to cause any concern. Thus, at low levels of reinforcement it is irrelevant to which %diff of the I_e (relative to I_g or I_u) is preferred for the evaluation. The moment of inertia (I_g or I_u) will

DEFLECTION PREDICTION FOR LIGHTLY REINFORCED CONCRETE SLABS

produce roughly similar results. The curve shapes in Figure 3-16 support this assumption showing almost exactly similar behaviour for both graphs.

The graphs in Figure 3-16 are reproduced in Table 3-7 for a percentage tension reinforcement range of $0.18\% \leq \rho \leq 1.50\%$. The maximum %diff of the I_e for each percentage reinforcement data sets, are also presented in Table 3-7.

The maxima for the %diff of the I_e decrease as the percentage tension reinforcement increases. At a low percentage tension reinforcement, the %diff of the I_e range from about 93.0%, and at a high percentage tension reinforcement, the %diff of the I_e decrease to about 65.5%. This is sensible, since the more reinforcement in a section, the higher the point of first cracking (cracking moment).

The BS 8110 (1997) model shows the largest jump from a low %diff to a high %diff of the I_e . This supports the observation that the BS 8110 model does not account for the gradual change from an uncracked to a partially cracked section. The ACI 318 (2002) and SABS 0100-1 (2000), representing Branson's equation and the EC2 (2004), representing Bischoff's equation, show the gradual change from the uncracked to cracked section as can be seen from the curve for the low %diff to the high %diff of the I_e . The SABS 0100-1 (2000), similar to ACI 318 (2002), curves differ from the EC 2(2004) curves, thus presenting the difference between the Branson's (1977) and Bischoff's (2005) approach, respectively. This difference decreases as the percentage tension reinforcement increases.

DEFLECTION PREDICTION FOR LIGHTLY REINFORCED CONCRETE SLABS

Table 3-7: %diff of I_e versus M_a/M_{cr} with reference to I_g for a range of percentage tension reinforcement.

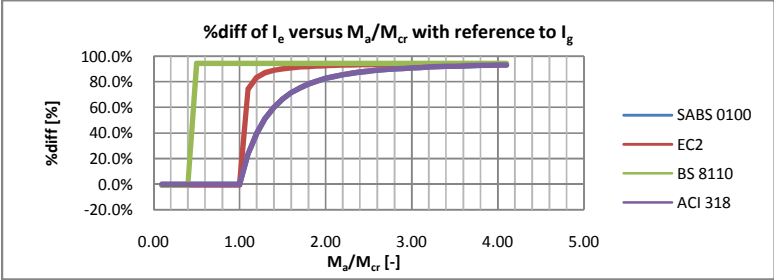
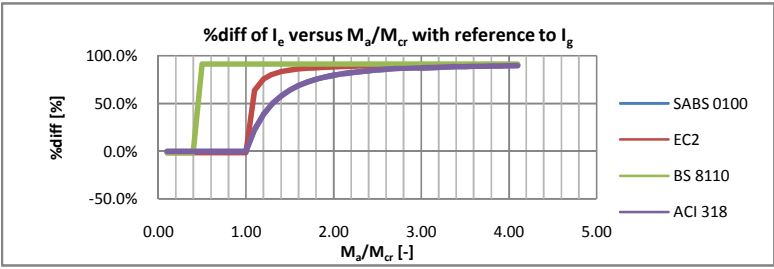
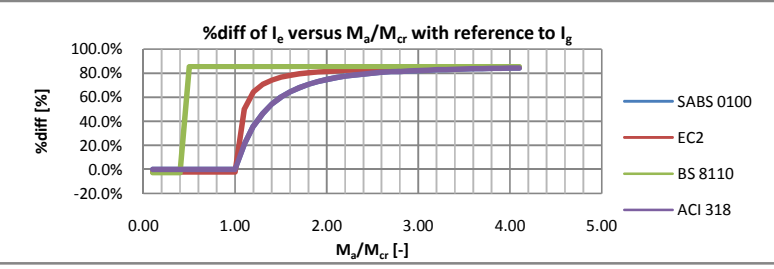
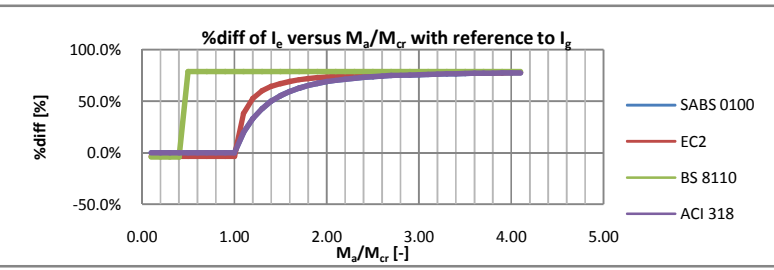
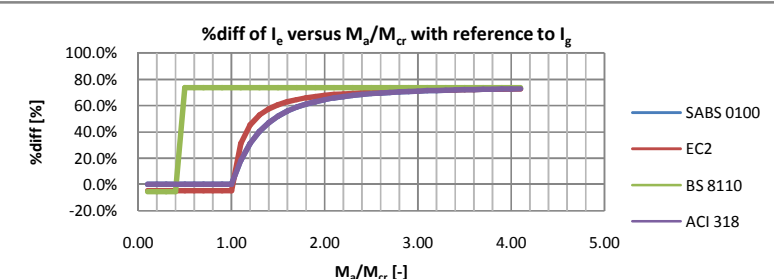
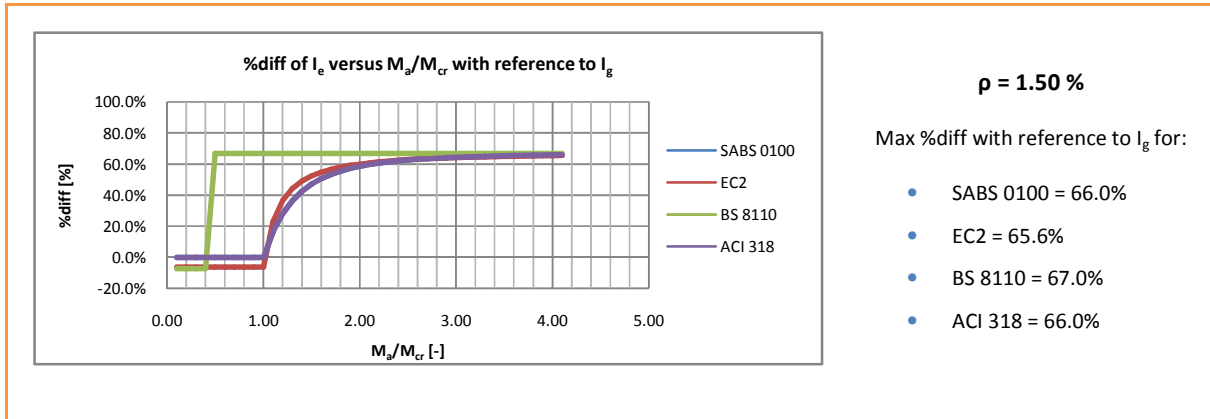
%diff of I_e versus M_a/M_{cr} with reference to I_g	Finding
	<p style="text-align: center;">$\rho = 0.18 \%$</p> <p>Max %diff with reference to I_g for:</p> <ul style="list-style-type: none"> • SABS 0100 = 92.9% • EC2 = 94.0% • BS 8110 = 94.3% • ACI 318 = 92.4%
	<p style="text-align: center;">$\rho = 0.30 \%$</p> <p>Max %diff with reference to I_g for:</p> <ul style="list-style-type: none"> • SABS 0100 = 89.7% • EC2 = 90.5% • BS 8110 = 91.0% • ACI 318 = 89.7%
	<p style="text-align: center;">$\rho = 0.52 \%$</p> <p>Max %diff with reference to I_g for:</p> <ul style="list-style-type: none"> • SABS 0100 = 84.4% • EC2 = 84.8% • BS 8110 = 85.6% • ACI 318 = 84.4%
	<p style="text-align: center;">$\rho = 0.84 \%$</p> <p>Max %diff with reference to I_g for:</p> <ul style="list-style-type: none"> • SABS 0100 = 77.6% • EC2 = 77.7% • BS 8110 = 78.7% • ACI 318 = 77.6%
	<p style="text-align: center;">$\rho = 1.10 \%$</p> <p>Max %diff with reference to I_g for:</p> <ul style="list-style-type: none"> • SABS 0100 = 72.7% • EC2 = 72.6% • BS 8110 = 73.8% • ACI 318 = 72.7%

Table 3-7: (continued).



In order to quantify the difference between the %diff of the I_e for the data sets, the covariance is calculated. The first data set is the %diff of I_e calculated relative to I_u , while the second data set is the %diff of I_e calculated relative to I_g . The covariance is defined as the measure of the linear relationship between random variables, according to Montgomery and Runger (2003). The covariance returns the average of the products of the deviations for each data point pair. The equation used to calculate the covariance between random variables X and Y, is presented in Equation 3-7 (Montgomery & Runger, 2003).

(3-7)

where μ_x and μ_y denotes the sum of the values in each series in the data set and X and Y denote the series numbers.

The covariance is calculated for two scenarios. Cov_A refers to the covariance where the %diff of the I_e include the data from all the design standards, while cov_s refers to the covariance where the %diff of the I_e only include the data for the SABS 0100-1 (2000) and for the EC2 (2004). It was chosen to include the cov_s , because the results from the BS 8110 (1997) overestimates the effect of cracking (overestimate the covariance) and the ACI 318 (2002) produces the exact similar result as the SABS 0100-1 (2000). The resulting plots are shown in Table 3-8.

DEFLECTION PREDICTION FOR LIGHTLY REINFORCED CONCRETE SLABS

Table 3-8: Covariance versus M_a/M_{cr} for a range of percentage tension reinforcements of $0.18\% \leq \rho \leq 1.50\%$.

Graphical Representation	Finding	Graphical Representation	Finding
<p style="text-align: center;">Covariance versus M_a/M_{cr}</p> <p>The graph shows covariance [%] on the y-axis (0.00% to 20.00%) and M_a/M_{cr} on the x-axis (0.00 to 5.00). Two curves are shown: covA (blue) and covS (red). covA peaks at approximately 16.6% around $M_a/M_{cr} = 1.0$. covS peaks at approximately 6.4% around $M_a/M_{cr} = 1.2$.</p>	<p>$\rho = 0.18\%$</p> <p>Max $cov_A = 16.6\%$</p> <p>Max $cov_S = 6.4\%$</p>	<p style="text-align: center;">Covariance versus M_a/M_{cr}</p> <p>The graph shows covariance [%] on the y-axis (0.00% to 15.00%) and M_a/M_{cr} on the x-axis (0.00 to 5.00). Two curves are shown: covA (blue) and covS (red). covA peaks at approximately 11.6% around $M_a/M_{cr} = 1.0$. covS peaks at approximately 0.9% around $M_a/M_{cr} = 1.2$.</p>	<p>$\rho = 0.84\%$</p> <p>Max $cov_A = 11.6\%$</p> <p>Max $cov_S = 0.9\%$</p>
<p style="text-align: center;">Covariance versus M_a/M_{cr}</p> <p>The graph shows covariance [%] on the y-axis (0.00% to 20.00%) and M_a/M_{cr} on the x-axis (0.00 to 5.00). Two curves are shown: covA (blue) and covS (red). covA peaks at approximately 15.5% around $M_a/M_{cr} = 1.0$. covS peaks at approximately 4.2% around $M_a/M_{cr} = 1.2$.</p>	<p>$\rho = 0.30\%$</p> <p>Max $cov_A = 15.5\%$</p> <p>Max $cov_S = 4.2\%$</p>	<p style="text-align: center;">Covariance versus M_a/M_{cr}</p> <p>The graph shows covariance [%] on the y-axis (0.00% to 15.00%) and M_a/M_{cr} on the x-axis (0.00 to 5.00). Two curves are shown: covA (blue) and covS (red). covA peaks at approximately 10.2% around $M_a/M_{cr} = 1.0$. covS peaks at approximately 0.5% around $M_a/M_{cr} = 1.2$.</p>	<p>$\rho = 1.10\%$</p> <p>Max $cov_A = 10.2\%$</p> <p>Max $cov_S = 0.5\%$</p>
<p style="text-align: center;">Covariance versus M_a/M_{cr}</p> <p>The graph shows covariance [%] on the y-axis (0.00% to 20.00%) and M_a/M_{cr} on the x-axis (0.00 to 5.00). Two curves are shown: covA (blue) and covS (red). covA peaks at approximately 13.7% around $M_a/M_{cr} = 1.0$. covS peaks at approximately 2.1% around $M_a/M_{cr} = 1.2$.</p>	<p>$\rho = 0.52\%$</p> <p>Max $cov_A = 13.7\%$</p> <p>Max $cov_S = 2.1\%$</p>	<p style="text-align: center;">Covariance versus M_a/M_{cr}</p> <p>The graph shows covariance [%] on the y-axis (0.00% to 10.00%) and M_a/M_{cr} on the x-axis (0.00 to 5.00). Two curves are shown: covA (blue) and covS (red). covA peaks at approximately 8.5% around $M_a/M_{cr} = 1.0$. covS peaks at approximately 0.2% around $M_a/M_{cr} = 1.2$.</p>	<p>$\rho = 1.50\%$</p> <p>Max $cov_A = 8.5\%$</p> <p>Max $cov_S = 0.2\%$</p>

DEFLECTION PREDICTION FOR LIGHTLY REINFORCED CONCRETE SLABS

The values of cov_A and cov_S in Table 3-8 show a decreasing tendency as the percentage tension reinforcement increases. At the minimum percentage covariance, corresponding to the applied moment less than the cracking moment (uncracked section) or the applied moment larger than twice the cracking moment (almost fully cracked section), the difference between the different models is almost zero. The covariance increases to larger values when the different approaches try to simulate partially cracked section at M_a/M_{cr} larger than 1.0. The bending moment range over which the covariance change is the most prominent is known as the *Critical M_a/M_{cr} Range*. This range occurs from 1.0 M_a/M_{cr} to 2.5 M_a/M_{cr} . This range decreases as the percentage tension reinforcement increases. Figure 3-17 shows the covariance peaks from Table 3-8.

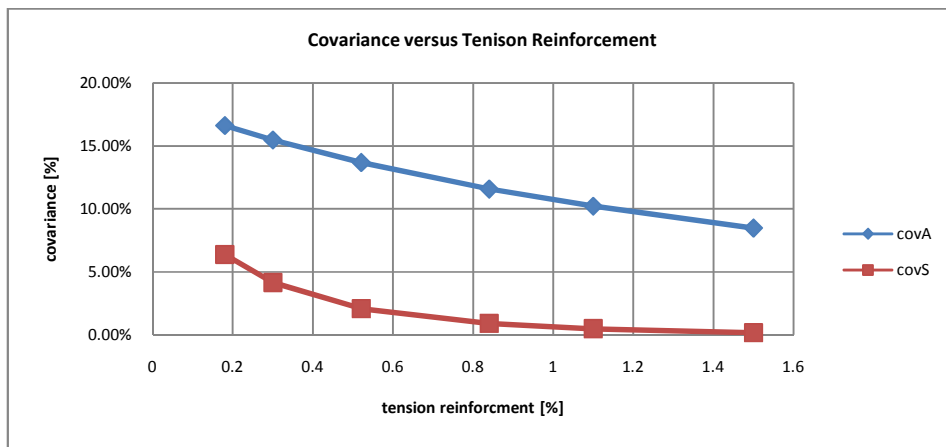


Figure 3-17: Covariance peaks from Table 3.8.

The critical M_a/M_{cr} range has been identified from Table 3-8 and the trends in Table 3-8 show that this range decreases as the percentage tension reinforcement increases. The results in Figure 3-17 show that the covariance peaks decrease with an increase in percentage tension reinforcement. The peaks for cov_A are far larger than the peaks for cov_S . Figure 3-17 supports the use of either Branson's or Bischoff's approach to predict deflections for lightly reinforced members as is evident with a $cov_S = 6.36\%$ for $\rho = 0.18\%$. The BS 8110 (1997) approach varies greatly with the predicted behaviour of the partially cracked section relative to the other approaches as is seen at $\rho = 0.30\%$ in Figure 3-17, the $cov_A = 15.48\%$ and $cov_S = 4.15\%$. Therefore, the BS 8110 approach is not recommended within the specific critical M_a/M_{cr} range at percentage tension reinforcement less than 1.0. However, the use of either the SABS 0100-1 (2000), the ACI 318 (2002) or the EC2 (2004) is recommended when the applied load lies within the critical M_a/M_{cr} range.

3.6 INFLUENCE OF THE GROSS AND UNCRACKED MOMENT OF INERTIA ON DEFLECTION PREDICTION

This section discusses the third influence on deflection prediction, which include the difference between the gross (I_g) and uncracked moments of inertia (I_u). Some difference result from the use of the gross (I_g) or uncracked (I_u) moment of inertia, to approximate the uncracked properties of a flexural member. According to Branson (1977), I_u might be more accurately used instead of I_g especially for heavily reinforced members and lightweight concrete members (low E_c and high modular ratio α_e). The principle effect of using I_u , rather than I_g , is in the calculation of an increased value of M_{cr} (Section 2.2.1). Thus if the modulus of rupture, f_r is evaluated correctly, the accuracy in predicting the point of first cracking would be improved using I_u . The effect of using I_u versus I_g at points well beyond the point of first cracking is small (approaching zero).

It has been established that the cracking moment of inertia, I_{cr} , is the same for the different approaches, as was discussed in Section 2.2.1. For a specific section, the ratio I_{cr}/I_u and I_{cr}/I_g may be compared relative to an increasing percentage of the tension reinforcement. The details on the calculations are presented in Annexure E. Figure 3-18 shows the results of the comparison.

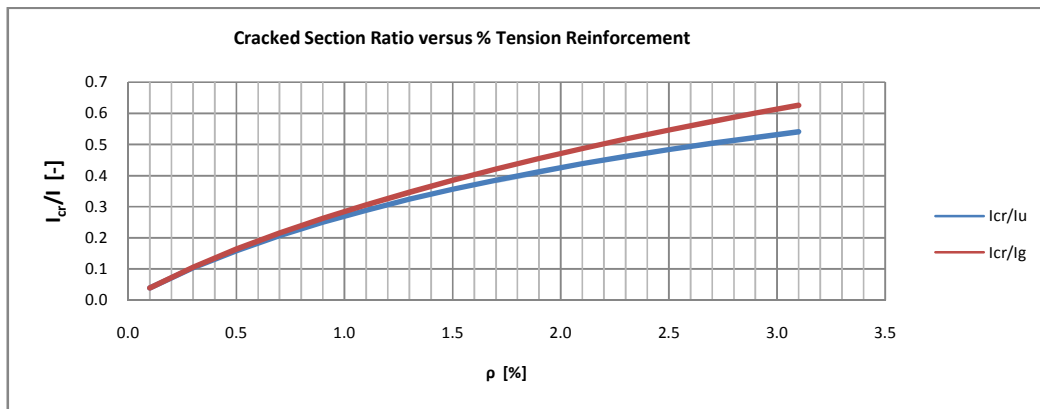


Figure 3-18: Comparison of I_{cr}/I_u and I_{cr}/I_g for a section as the percentage tension reinforcement increase.

Figure 3-18 shows that significant difference occurs as the percentage tension reinforcement grows larger than 1.0%. It is thus evident that using either I_u and I_g for sections for lightly reinforced members is possible, but it is critical to using I_u for section with a percentage reinforcement ratio of 1.0% or higher.

3.7 EFFECT OF PATTERN LOADING ON THE FLAT SLABS

This section discusses the effect of pattern loading on slab structures to obtain an accurate predicted deflection.

In the equivalent frame method the effect of pattern loading is included in the frame moment analysis, and implicitly when using the direct design moment coefficients. The effect of both checkerboard and strip pattern loading on moments and deflections was studied by Branson (1977). For example, the deflection of an interior panel under checkerboard loading was found to vary less than 14% from that with all panels loaded with the serviceable loading. Also, solutions obtained for checker board loading consisting of a uniform load on the interior and corner panels indicated that pattern loading seldom resulted in critical deflections, and where it did, the deflections were only marginally greater than those for all panels loaded. The dead load to live load ratio is in the order of 0.5 to 0.6 and since dead load (which contributes to both short-term and long-term deflection) usually acts on all panels, this is further reason for not laboriously considering various patterns of live load when calculating approximate slab deflections (Branson, 1977).

The effect of line loads such as wall loads acting along panel edges, or occasionally across the panels themselves, can be included directly in the equivalent frame method when determining moments in the column or middle strips (Branson, 1977).

3.8 ALTERNATIVE APPROACH TO DEFLECTION CALCULATIONS

The discussions in Sections 2.2.2 and 2.2.3 suggest certain factors that need to be accounted for to predict the short- and long-term deflections for a lightly reinforced member, such as a flat slab structure. During the discussions of the different deflection prediction methods, as presented in Section 2.3, it was found that not all the factors discussed in Sections 2.2.2 and 2.2.3 are accounted for. It is for these reasons that an Alternative Approach here to be included in the final comparisons for the deflection prediction methods in Chapter 5.

From the discussions in Sections 3.2 and 3.3, the EC2 (2004) or Bischoff's (2005) expression was identified to approximate the actual deflection behaviour more effectively than the other methods. It is for this reason that this approach is used in the Alternative Approach presented here to predict the short-term deflections. A modification from the β coefficient in the EC2 (2004) approach is discussed in Section 2.2.2 and included for the short-term deflection prediction (Table 3-9). The β coefficient accounts for the loss in tension stiffening of the member in flexure over time.

The prediction of the shrinkage deflection presented by the EC2 (2004) is similar for the Alternative Approach introduced here. The discussions in Section 2.2.1 suggest that the shrinkage for both the uncracked and cracked sections should be taken into account. The shrinkage deflection method presented by the EC2 (2004) approach, does allow this.

The long-term deflection for the proposed Alternative Approach is different from the method presented from the EC2 (2004) approach. From the discussions in Section 2.2.2, an effective cracking moment (M'_{cr}) should be used for the long-term deflection prediction, to account for the reduction of the concrete tensile strength over time. Also, only the sustained load should be used to determine the long-term deflection. Any additional live load peaks should be accounted for by using the change in moment due to the live load peak with the short-term deflection prediction expression to calculate an additional short-term (initial) deflection.

Short-Term Deflection

It has been shown that the EC2 (2004) approach is the more effective method in predicting deflections for lightly reinforced members; therefore the following procedure is suggested for the short-term deflection in the proposed Alternative Approach. Bischoff's (2005) expression is presented in Equation 3-8. It is thus proposed that the following form of the effective moment of inertia, I_e be used.

$$I_e = \frac{I_{cr}}{1 - \beta \left(1 - \frac{I_{cr}}{I_u}\right) \left(\frac{M_{cr}}{M_a}\right)^2} \leq I_u \quad (3-8)$$

where I_{cr} is the cracked moment of inertia, I_u is the uncracked moment of inertia, M_{cr} is the cracking moment, M_a is the applied moment for the loading condition under consideration and β is a

DEFLECTION PREDICTION FOR LIGHTLY REINFORCED CONCRETE SLABS

coefficient taking account of the influence of the loss in tension stiffening. The cracking moment should be calculated as presented in Section 2.3.3 Equation 2-62, with similar assumptions regarding the calculation of the tensile strength of concrete, f_t . (Equations 2-61 to 2-65).

The short-term deflections are dependent on whether the section was cracked at the time of loading and this in turn, is dependent on the loading history applied to the member. The value of β is dependent on the level of cracking and period of loading as is discussed in Section 2.2.2. Table 3-9 summarizes the proposed equations and variables relevant for the uncracked and cracked condition for the Alternative Approach.

Table 3-9: Alternative Equations for the short-term deflection (Section 2.2.2).

Short-Term Deflections		
Variables for Equation 3-6	Section not Cracked	Section Cracked
	$M_a < M_{cr}$	$M_a \geq M_{cr}$
β	1.0	0.7 for 1-2 days 0.6 for 7 days or longer
M_{cr}	M_{cr} from Equation 3-9	M_{cr} from Equation 3-9

It is then suggested that the effective moment of inertia I_e be calculated from Equation 3-8 and by applying the conditions shown in Table 3-9. The short-term deflection may be determined using Equation 2-33, taking care that the E_c in Equation 2-33 is the modulus of elasticity at the day of the first loading.

Shrinkage Deflection

The shrinkage deflection is a time-dependent phenomenon based on the long-term properties for the section. As was discussed in Section 2.2.1, the shrinkage is independent on the loading history, but dependent on the amount of cracking in the section. It is therefore suggested that the EC2 (2004) method be used to predicting shrinkage deflection in the Alternative Approach, since the EC2 is the only design standard using an expression which includes the effect of cracking, be used to determine the shrinkage curvature (Section 2.2.1). The equation for shrinkage curvature, $1/r_{cs}$, is Equation 2-67, as is presented in Section 2.3.3.

DEFLECTION PREDICTION FOR LIGHTLY REINFORCED CONCRETE SLABS

The distribution coefficient, ζ , in Equation 2-67 is dependent on the cracking moment, M_{cr} and β . Table 3-10 shows the expressions relevant for ζ to be used in the Alternative Approach, depending on whether the section is uncracked or cracked.

Table 3-10: Alternative Equations for the shrinkage deflection (EC2, 2004)(Section 2.2.2).

Shrinkage Deflection		
Variables for Equation 3-9	Section not Cracked	Section Cracked
	$M_a < M_{cr}$	$M_a \geq M_{cr}$
ζ	0.0	$1 - \beta(M'_{cr}/M_a)^2$ where $\beta = 0.5$

The equation and relevance of the effective cracking moment, M'_{cr} is discussed in Section 2.2.2. The use of M'_{cr} instead of M_{cr} , is to include the effect of shrinkage restraint induced by the shrinkage phenomenon. The expressions for M'_{cr} are given below:

$$f_{te} = f_t - f_{res} \quad (3-9)$$

where $f_{res} = E_s \epsilon_{cs} S_u (h - x_u) / I_u + A_s E_s \epsilon_{cs} / [A_c (1 + \alpha_e (A_s / A_c))]$ (3-10)

In the above expressions, f_{te} is the effective tensile strength of concrete, f_t is the tensile strength of concrete and f_{res} is the strength of concrete induced by shrinkage restraint. The equation for f_{res} is shown in Equation 3-10. The variables for Equation 3-10 include the modulus of elasticity of steel E_s , the free shrinkage strain ϵ_{cs} , S_u is the first moment area of the reinforcement about the centroid of the section for the uncracked section, h is the total height of the section, x_u is the distance of the neutral axis to the top of the section for the uncracked section and I_u is the moment of inertia for the uncracked section. A_s is the area tension reinforcement, A_c is the gross area of concrete and α_e is the modular ratio based on the effective modulus of elasticity of the concrete, E_{eff} (Section 2.2.1).

The expression for M'_{cr} is determined from Equation 3-11 with the cracking moment assumed to be Equation 2-62.

$$M'_{cr} = f_{te} \frac{I_u}{(h - x_u)} = \frac{f_{te}}{f_t} M_{cr} \quad (3-11)$$

When substituting Equation 3-10 into Equation 3-11:

$$M'_{cr} = \frac{f_t - f_{res}}{f_t} M_{cr} = \left(1 - \frac{f_{res}}{f_t}\right) M_{cr} \quad (3-12)$$

Then, to calculate the shrinkage deflection from the shrinkage curvature (Equation 2-67) use Equation 2-42.

Long-Term Deflection

The long-term deflection requires estimates of time-dependent effects such as the reduction of tension stiffening and the effect of shrinkage restraint. Taking the discussion from Section 2.2.2 and 2.2.3 into consideration, the following procedure is suggested to find the long-term deflections using the Alternative Approach. Table 3-11 summarizes the necessary expressions.

Table 3-11: Alternative equations for the long-term deflection (Sections 2.2.2 and 2.2.3).

Long-Term Deflections		
Variables for Equation 3-6	Section not Cracked	Section Cracked
	$M_a < M_{cr}$	$M_a \geq M_{cr}$
B	1.0	0.5 (for 28 days or longer)
M_{cr}	$M_{cr} = M'_{cr}$ (as from Equation 3-12)	$M_{cr} = M'_{cr}$ (as from Equation 3-12)
M_a	$M_a = M_p$	$M_a = M_p$

The long-term deflection in the Alternative Approach is then calculated using Equation 2-70 in Section 2.3.3.

Total Deflection

The total deflection includes the shrinkage deflection, Δ_{cs} , long-term deflection, Δ_l and the additional short-term (initial) deflection, $\Delta_{i,add}$ due to any additional short-term live load. The equation for the additional initial deflection is as follows:

$$\Delta_{i,add} = KL^2 \frac{M_a - M_p}{E_c I_e} \quad (3-13)$$

where K is the deflection coefficient as was presented in Section 2.2.5, L is the distance between the column centres of the span under consideration, M_p is the moment due to permanent load on the member, M_a is the total load acting on the member and E_c is the modulus of elasticity of concrete at instance of loading and I_e is the effective moment of inertia as calculated for the short-term deflection.

The total deflection is calculated by the sum of the long-term Δ_l , shrinkage Δ_{cs} and the additional short-term deflection $\Delta_{i,add}$.

The results from the proposed Alternative Approach are compared to recorded experimental flat slab deflections in Chapter 5 to evaluate the effectiveness of the method to predict actual deflection behaviour. It is also compared in Chapter 5 to the deflection prediction methods from the design standards.

3.9 CONCLUDING SUMMARY

It was observed that the crack development of a flexural member is estimated mathematically and that the influence of tension stiffening is of great importance and needs to be considered. It was observed that significant differences occur between the predicted deflection behaviour and the actual deflection behaviour. The differences between the calculated span/depth ratios from the various design standards were also observed. It was shown that limitations for the methods from the various design standards could be quantified, in terms of the percentage tension reinforcement (ρ), the stiffening ratio (I_g/I_{cr}) and the M_a/M_{cr} range, by which the prediction accuracy of the approach is evaluated.

Branson (1977) used an empirical approach to derive the effect of a partially cracked section for a flexural member. The method is however, limited to a section with a percentage tension reinforcement larger than or equal to 1.0%, a I_g/I_{cr} ratio of less than 3.0 and a M_a/M_{cr} ratio of

between 2.0 and 3.0. For lightly reinforced members, which fall outside these limits, the approach by Branson underestimated deflections by roughly 45% - 50%. The ACI 318 (2002) and the SABS 0100-1 (2000) use Branson's approach, and therefore does not predict deflections for lightly reinforced members with sufficient accuracy.

Bischoff (2005) re-evaluated Branson's approach by including a tension stiffening factor. Bischoff's approach presents a far better approximation of the experimental response for a flexural member undergoing deformation. The limits presented by Branson's method are irrelevant for Bischoff's approach. The predicted behaviour according to Bischoff produce deflections very close the experimental results and are at most 10% overestimated or 10% underestimated in the extreme cases. The EC2 (2004) uses Bischoff's approach, thus most of the results indicate the EC2 method is the most accurate to use.

The curvature approach as presented by the BS 8110 (1997) wrongly assumes the effect of constant value of tension stiffening in the tension zone of the flexural member. This assumption produces a deformation response far beyond the actual response. The BS 8110 overestimates deflection for lightly reinforced member up to a 200% larger at a $M_a/M_{cr} = 1.1$ and underestimates the deflection by 60% at a $M_a/M_{cr} = 1.3$. The variability of the response relative to experimental data shows that the BS 8110 is the least appropriate method to use to predict deflection for members with a percentage tension reinforcement less than 1.0%, a M_a/M_{cr} ratio of less than 2.5 and an I_g/I_{cr} ratio of less than 3.0. It was further observed that the *Critical M_a/M_{cr} Ratio Range* is between 1.0 and 2.5. This ratio becomes less relevant as the percentage reinforcement (ρ) increases. Thus, when the percentage tension reinforcement is less than 1.0% and when the M_a/M_{cr} ratio falls within the range as stated, it might be expected that the predicted deflection according to the design standards, will not produce similar results. This difference is in the order of 6.0% when using either the ACI 318 (2002), the SABS 0100-1 (2000) or the EC2 (2004) for a section with a $\rho = 0.18\%$, but 16.36% if the BS 8110 (1997) is used.

As a reaction on to what was observed, an Alternative Approach is suggested by the author. The new approach is similar to the EC2 (2004) method, but with a few changes. The effectiveness of this Alternative Approach will be verified in Chapter 5.

4 MODELLING APPROACH

4.1 INTRODUCTION

The use of a finite element model is convenient to observe the behaviour of a structure. It is however, important to model the structure correctly. The elasto-plastic behaviour of a concrete flat slab structure is sophisticated and not easy to present accurately within a finite element framework. This Chapter discusses the capabilities of the finite element (FE) software required by the user to model time-dependent flat slab behaviour realistically. These capabilities include the modelling of tension stiffening, the influences of creep and in turn the concrete cracking.

The chapter starts by discussing which element is required to account for localised behaviour of the flat slab system. A composite layered element is suggested, but the limitations of such an element are discussed. The chapter continues by incorporating the element type with the linear and nonlinear analysis. Due to the limitations with the application of the suggested element type, and the incompatibility of this element within the framework of the chosen finite element software, a new simple alternative finite modelling approach is suggested for evaluation. This new alternative uses property modifications to simulate the time-dependent effects using a simple shell element and a linear analysis.

This chapter concludes by discussing the procedure to implement the alternative finite element model.

4.2 MODELLING OF CONCRETE MATERIAL PROPERTIES

This section discusses which aspects should be taken into account when evaluating whether a chosen finite element modelling software sufficiently models the behaviour of a lightly reinforced concrete member. Firstly, the material properties that need to be incorporated in the finite element model are discussed (local behaviour) and secondly, the global behaviour of the structure is discussed.

Mathematically Simulating Reinforced Concrete Material Properties

Finite element modelling is a popular and inexpensive way to simulate the behaviour of structural members. When attempting to realistically simulate the actual behaviour of a structure, much attention and care should be invested to allocate the correct material properties. The allocated values and the equations used in the analysis should mimic the actual material behaviour.

In a study by Bailey, Toh, and Chan (2008), the authors suggested a specific element to model the reinforced concrete section of a member which is thin in relation to its span. The authors suggested an eight-node quadrilateral isoparametric curved layered shell element type (CQ40L). Each element would be divided into layers, having a reinforcement layer between several concrete layers as demonstrated in Figure 4-1.

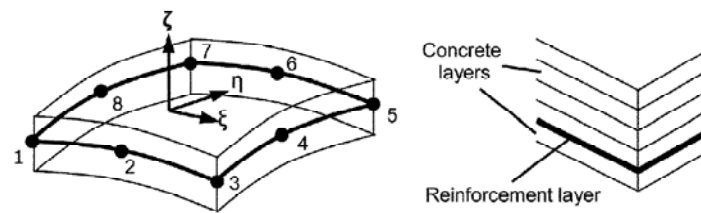


Figure 4-1: CQ40L layered shell element as suggested by Bailey, Toh and Chan (2008).

The reinforcement layer is determined using the equivalent cross-sectional area relative to the area provided by the reinforcement bars. Refer to the work by Bailey, Toh and Chan (2008) with reference to the main assumptions on using the composite layered shell element.

The CQ40L element is a more complex form of a normal plate or shell element. The plate/shell element is the most general type of plate element in that it is a two-dimensional membrane and bending element. It is the only plate element that permits out of plane displacements associated with bending behaviour. This includes the analysis of flat plates and general two-dimensional shells (Strand7 Application Programming Interface Manual – Edition 6a). By choosing an element type to simulate the composite material such as that of reinforced concrete, it is important to allocate the correct nonlinear material properties to the different layers and to be sure that all the layers work together to simulate the correct material behaviour.

Mathematically Simulating Flat Slab Behaviour

In order to simulate the simplified nonlinear (elasto-plastic) behaviour of reinforced concrete, the stress-strain curves for both the concrete and reinforcement steel are required. Both the compressive and tensile behaviour of the stress-strain curve of concrete is required. This is essential to simulate the effects of tension stiffening (tensile strength of concrete between cracks) of the concrete accurately. An example of such stress-strain curves for both concrete and reinforcement are presented by Maaddawy, Soudki and Topper (2005).

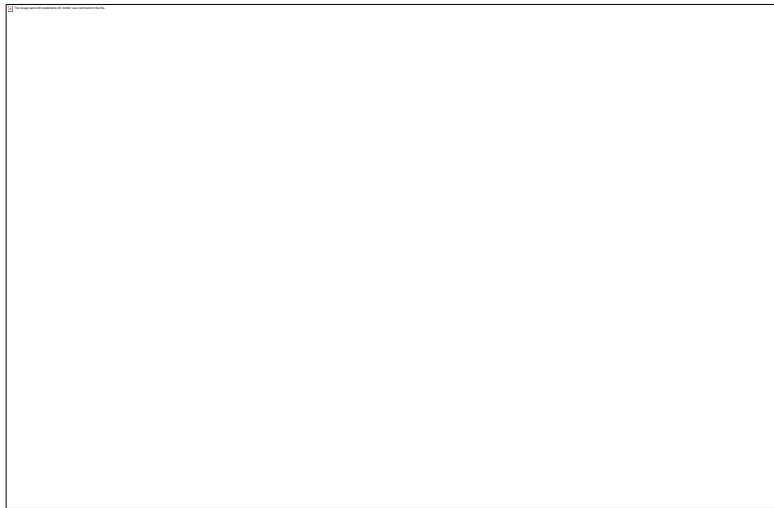


Figure 4-2: Material stress-strain curves for both the (a) concrete and the (b) reinforcement (Maaddawy, Soudki and Topper, 2005).

The time-dependent behaviour of the modulus of elasticity for concrete is also required to include and simulate the effects of creep on the member. As the interactive behaviour of the different material properties are identified, more questions arise. These include:

- What are the material limits for concrete and reinforcement?
- Does the finite element software realistically include the effects of tension stiffening?
- What are the value and behaviour of the shear between the layers of the CQ40L element or how is this value determined?
- If a slab system consists of a mesh of CQ40L elements, how does the element represent localised cracking as different areas undergo time-dependent cracking?
- Is the effect of time-dependent cracking influenced by the element size?

The above topics are vital to simulate the behaviour of lightly reinforced concrete flat slabs accurately and realistically. The use of a nonlinear analysis is inevitable in order to simulate behaviour beyond the point of cracking. In finite element analysis, the nonlinear behaviour is normally categorised into three types, namely geometric, material and boundary nonlinearity (Strand 7 Application Programming Interface Manual – Edition 6a). In order to simulate concrete cracking material nonlinearity will suffice.

In a material nonlinear analysis, stresses are calculated based on the material model provided. Depending on its ability to return to the original shape when external loading is removed, a material model is categorised as either elastic or elasto-plastic. For an elastic material, such as rubber, stress can be calculated purely based on its current deformation, as it always returns to its original shape with no remaining stress or strain when the external loading is removed. For an elasto-plastic material, the stress history is required to determine the stress level. Once the material has yielded during the loading process, residual stress and strains will remain even after external loading is completely removed. Structures made of materials which have significant different mechanical properties in tension and compression, such as concrete, should be modelled using a nonlinear analysis (Strand7 Application Programming interface Manual – Edition 6a).

The failure criteria required when performing a material nonlinear analysis with a composite layered element becomes complex due to the large amount of variables that need to be considered. These variables include:

- The stress-strain curve as it changes with time for concrete.
- The effect of bond between the reinforcement and concrete, the localised failure (due to cracking) and the localised strength of the concrete between cracks.
- The three-dimensional behaviour of the flat slab system, especially when the slab has a much longer span in the one direction forcing cracks to develop more prominently in that direction.

The software used to model a flat slab system should incorporate the effect of all the interactive variables. If these variables are modelled without certainty the resulting behaviour presented by the analysed model will not present actual slab behaviour.

4.3 NONLINEAR MODEL FOR A REINFORCED FLAT SLAB

The possibility exists to use a composite layered element to model a structure, as presented by the Strand7 software (Strand 7 Application Programming Interface Manual – Edition 6a). It is possible to identify the material limits and direction in which the properties attributes are relevant. However, at present this feature is only available in a linear analysis in the Strand7 software (Hill, 2009), thus only demonstrating the linear behaviour of the material. For every layer the material properties may be allocated, such as the modulus of elasticity and shear modulus. Figure 4-3 illustrates this process. The figures represent a beam section over a support with tension reinforcement at the top of the section.

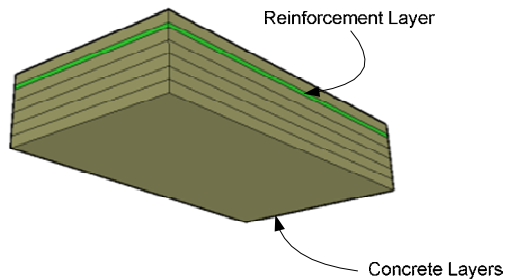


Figure 4-3: Three-dimensional representation of a composite layered element for a continuous beam section (Strand 7, 2005).

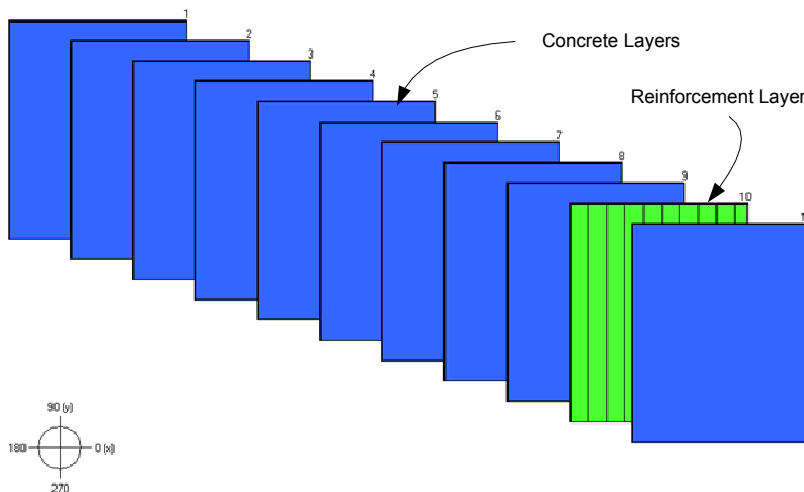


Figure 4-4: Properties for every layer depending on whether the layer is concrete (quasi-isotropic) or reinforcement (unidirectional) (Strand 7, 2005).

The use of the composite layered element to find the short-term deflection (ignoring long-term effects) for a structure using a linear solver is quite sufficient while the applied moment is less than the cracking moment. When the applied moment is larger than the cracking moment, significant tension stiffening and cracking occurs which would influence the deflection. The composite layered element in a linear elastic analysis does not take these effects into account and produces an under-predicted deflection. Using the same element within a nonlinear analysis to find the time-dependent deflections that occur when the structure is cracked while considering the effects of creep and shrinkage, is not yet possible within the scope of the Strand 7 software (Hill, 2009). The software only allows the time-dependent properties of shrinkage and creep to be applied to elements of a uniform material.

The restriction on the use of the composite layered element with the nonlinear solver raises many uncertainties, which is problematic since the aim of this study is to use a suitable finite element model to realistically model the elasto-plastic behaviour of a lightly reinforced structure beyond the point of cracking. As a result, the element type and method of analysis was reconsidered. A new model was suggested to account for the time-dependent properties and gradual cracking. Section 4.4 discusses the assumption for an alternative approximate linear model by which to model the elasto-plastic behaviour of a lightly reinforced structure to obtain a deflection prediction. The new model is merely a proposal to allow a designer to model an approximation of the nonlinear behaviour of a flat slab structure.

4.4 LINEAR MODEL FOR A REINFORCED FLAT SLAB

The complexity of the nonlinear model presents many uncertainties which led to the development of a more simple approach. A linear model using a simple uniform shell element was considered. When assuming such a model to simulate nonlinear time-dependent behaviour, the global behaviour of the structure takes priority while the localized material behaviour takes a secondary priority. When using such a modelling approach, the effects of cracking and creep need to be taken into account using a material property modification.

One of the uncertainties surrounding the use of a composite layered element is the aspect of tension stiffening. The occurrence of tension stiffening for a member in flexure requires the concrete to carry no tensile stress at the cracks, and the reinforcement to carry all the tensile stress while the concrete between the cracks, carry some tensile stress, reducing the amount of tension carried by the reinforcement. The way in which the composite layer represents this behaviour is questionable using a nonlinear solver and is non-existent using a linear solver. Thus a more simple approach is to use a uniform shell element with a reduced stiffness. The shell element is only an approximation, since it ignores the effects of reinforcement and thus, tension stiffening. A modification of the element properties for the shell element is introduced to represent global flat slab behaviour.

The deflections are dependent on the moment distribution and the stiffness of the member. Taking these two factors as the priority variables, it is required to simulate the desired global behaviour of a flat slab, using the following approximation. The reduced modulus of elasticity or cracked modulus of elasticity, E_{cr} is calculated as a function of the effective moment of inertia, I_e , of the uncracked moment of inertia, I_u and the effective modulus of elasticity, E_{eff} at the time of loading. It is too complex to alter the uncracked moment of inertia I_u within the linear approximation of the finite element framework, being dependent on the dimensions of the model. Therefore, altering the stiffness EI using a reduced modulus of elasticity is a less complex approach. In this way, if a uniform eight-node shell element is used in the model, the loads are applied for the specific loading stage to obtain the moment distribution. Then, by altering the stiffness of the model with a cracked modulus of elasticity, the desired flat slab behaviour may be obtained. The basic relationship required when calculating the E_{cr} is shown in Equation 4-1.

$$I_u E_{cr} = I_e E_{eff,t} \quad (4-1)$$

where I_u is the uncracked moment of inertia and I_e is the effective moment of inertia for the Section. The time-dependent modulus of elasticity, $E_{eff,t}$ is the effective modulus of elasticity due to creep which is dependent on the number of days after loading.

The graphical interpretation of this approximation is presented in Figure 4-5. $I_u E_{cr}$ is used to simulate cracking within the flat slab model.

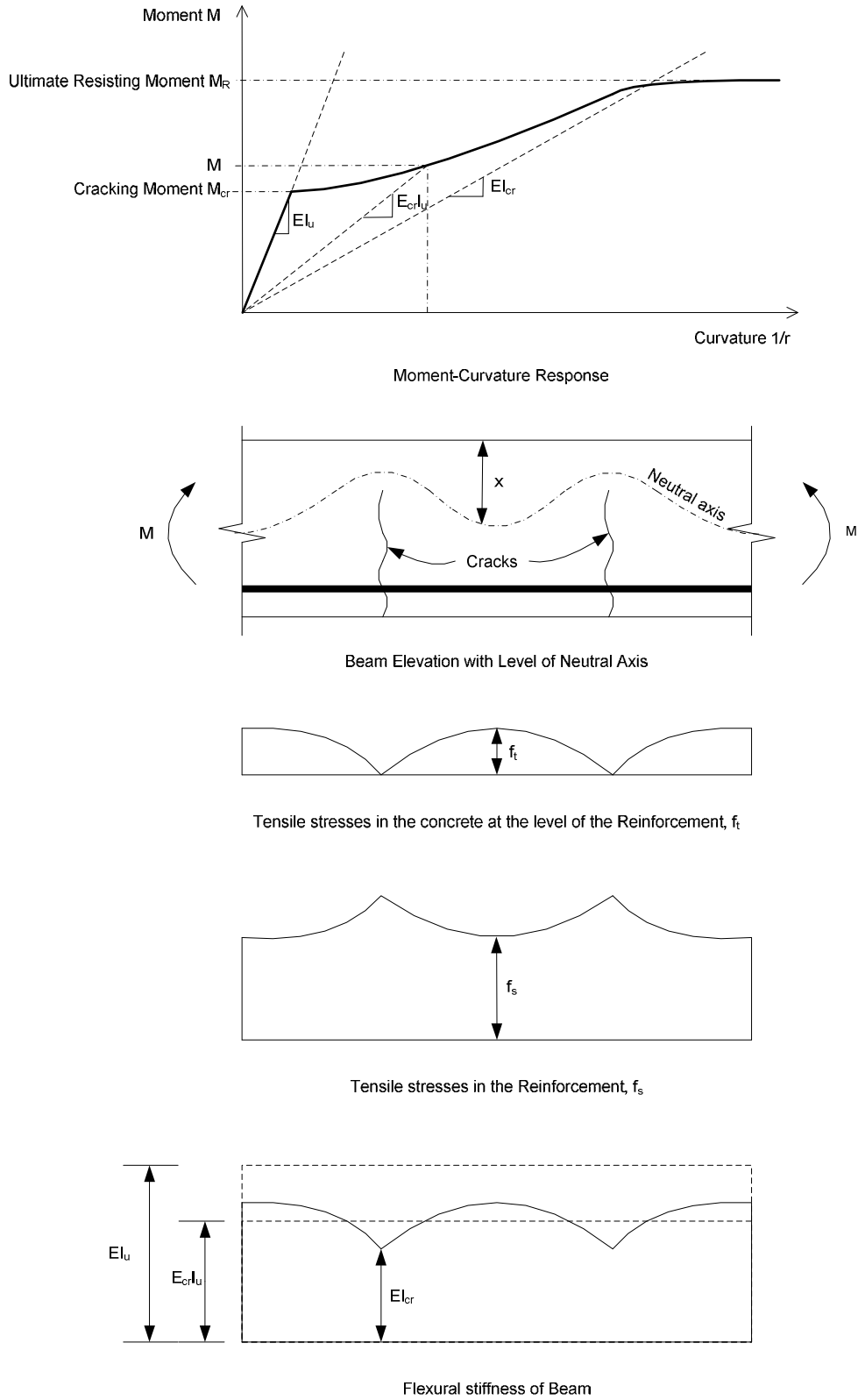


Figure 4-5: Approximation for the cracked modulus of elasticity for beams in flexure (Robbets and Marshall, 2008).

Figure 4-6 presents a three-dimensional model of a flat slab with indicated coloured areas where E_{cr} is assigned. By first applying the applied load on the linear elastic model, the actual moments due to that loading stage may be obtained. The moments are then compared to the cracking moment calculated for the individual column and middle strips. When the obtained moment is larger than the cracking moment along a length of the moment diagram for the column or middle strip, it is evident that cracking occurs and the calculated E_{cr} value may be allocated to the shells over that length. The coloured areas in Figure 4-6 represent these cracked areas for a slab. The example shows that cracking is expected over column C4, C5 and C6.

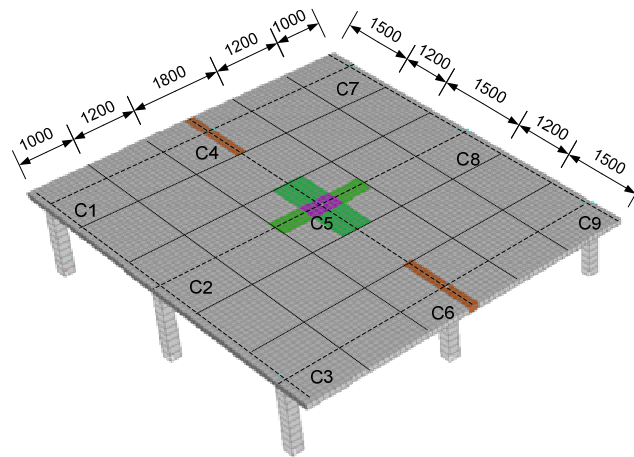


Figure 4-6: Three-dimensional flat slab model with allocated areas where the E_{cr} is applied.

For this finite element model approximation it is assumed that slab behaviour may be approximated as several wide beam strips. The allocated column and middle strips, similar to how the required reinforcement is calculated for flat slab design. Even though cracking does not follow an orderly pattern as presented in Figure 4-6, it is assumed that the indicated areas adequately reduce the stiffness in these areas to reduce member stiffness.

Adopting such an approach simplifies much of the complex localised behaviour that presented modelling difficulties. The analysis time is also reduced when using a simple linear elastic solver which takes a few minutes to complete. This approximation of flat slab behaviour is also applicable to less sophisticated finite element software available.

This simple model is, however, dependent on available recorded data on material properties over structure's life, such as the time-dependent creep properties and the actual loading history. Without a good approximation of actual properties, this model will not produce realistic results.

The next section discusses how such a cracked finite element model is composed and altered to include areas of a reduction in stiffness.

4.5 FINAL FINITE ELEMENT MODEL

In this section a step-by-step procedure is presented with which to build the proposed linear model which incorporates cracking. It should be stressed that this is only an approximation to the nonlinear behaviour of reinforced concrete used for a flat slab structure. The aim of this model was to present a simple model that could be used by designers in practice to time-effectively approximate nonlinear flat slab behaviour realistically. There are no references presented for this model, since the concept was introduced by the author.

The basic process by which the finite element model resembles a flat slab which includes uncracked and partially cracked sections is explained below. The process is explained using a series of steps. This step-wise approach is essential in order to simulate time-dependent cracking. Following Section 3.6, the effect of pattern loading is ignored and it is assumed that slabs are loaded equally with the applicable service loads.

The following steps are used:

Step 1: Calculate the Properties for the Critical Span

The critical span relates to the span carrying the largest bending moments. For a two-way continuous slab, this is usually the first interior panels and the corner panels. This critical span may also be identified as the span carrying the most loads in a slab system with a uniform layout.

Divide the critical span into the column and middle strips and calculate the uncracked properties (I_u and x_u) and the cracking moment, M_{cr} using the Equations presented in Section 2.3.3.

Step 2: Simplify the Loading History and identify the zones of Cracking

Simplify the loading history and compile an approximate loading history with distinct loading stages. Complete the model setup with the aim of obtaining the moment distribution for every loading stage. Use the modulus of elasticity at the point in time of first loading.

The finite element model is compiled using beam elements for the columns and shell elements for the slab. The correct interface between the beam and the shell elements is essential to obtain the appropriate moment transfer between the beam (columns) and shell (slab) elements. Figure 4-7 illustrates the application of rigid links between the beam (columns) and shell (slab) elements.

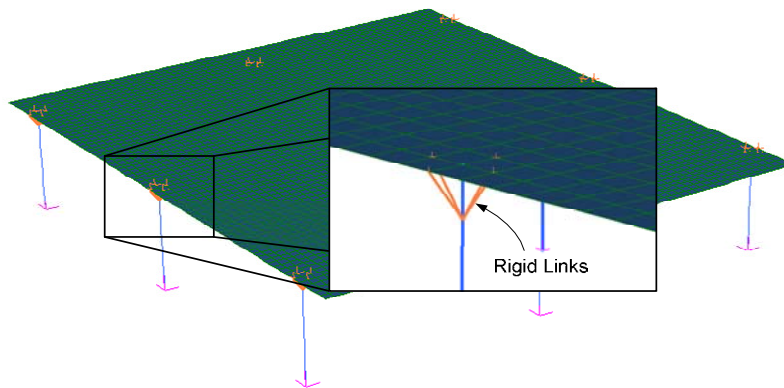


Figure 4-7: Rigid Links between beams and slab elements.

Then, identify the areas along the column and middle strips where the bending moments (for the loading stage) are considered larger than the cracking moment.

Step 3: Calculate E_{cr} for the Loading Stage and Apply to Model

Calculate E_{cr} for the loading stage using Equation 4-1 and apply the property change to the shell element property values for the areas that were identified as having a moment larger than the cracking moment. Take note that E_{cr} must be allocated as either an isotropic or orthotropic property

depending on the direction of the moment distribution in the two-dimensional plane of the flat slab model. E_{cr} may only be allocated to an area with the applied moment larger than the cracking moment in the specific direction of the column or middle strip. It is important to note the orthogonal direction of cracking for each of the column and middle strips. Figure 4-8 illustrates the importance of the middle and column strip directions.

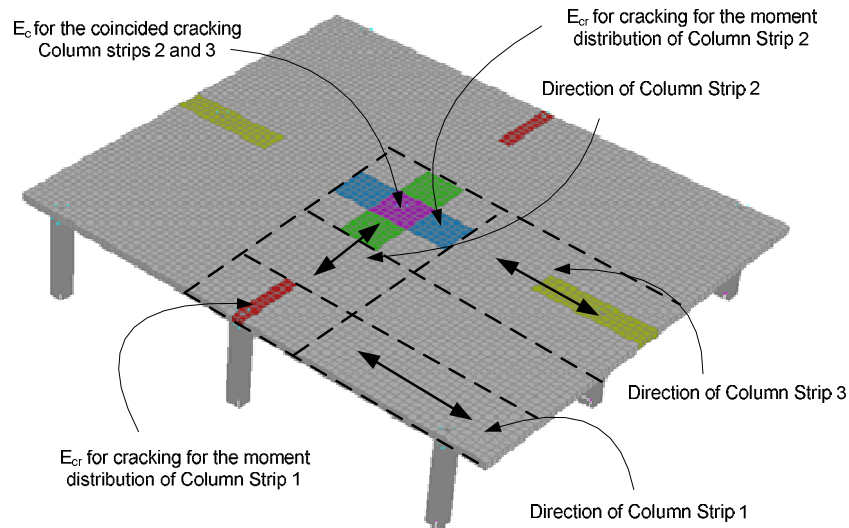


Figure 4-8: Example of areas for a cracked modulus of elasticity for a slab.

In the direction of Column Strip 1, a certain area of shells undergo cracking, thus E_{cr} is allocated to the shell properties in the direction of Column Strip 1 (orthotropic property). The modulus of elasticity in the orthogonal direction of Column Strip 1 remains $E_{eff,t}$. The similar principle is applied for Column Strip 2. If the cracked sections (applied moment larger than the cracking moment) for column strips or middle strips coincide, the material is assumed to be isotropic as can be seen in the area where Column Strip 2 and 3 overlap. The calculated value of E_{cr} in that location is the same, thus assuming an isotropic E_{cr} value is appropriate. The use of isotropy for areas of overlap cracking is to ensure that no singular matrices develop during the finite element analysis process.

Step 4: Obtain Mid-Panel Deflections

After applying the changes to the specific shells and allocating the correct $E_{eff,t}$ to the remainder of the shell properties, the linear analysis may be performed. The resulting deflections obtained from the model represents the predicted deflection taking the effects of cracking and creep into account.

It is assumed that the behaviour of the slab may be approximated using a series of wide beams in two directions. These wide beams are presented in the design standards as column and middle strips. Approximating flat slab behaviour with column and middle strips is a simplified method of design and used to allocate reinforcement to the appropriate areas in a flat slab design. A similar approach is used for the simplified finite element model. The amount of cracking is evaluated for each column and middle strip. Evaluating cracking in regularly shaped strips produces a resulting crack pattern regular in shape, which does not reflect the actual circular crack pattern as observed in practice. Nevertheless, the regular shaped crack pattern is assumed to sufficiently reduce the stiffness of the cracked areas to produce a more slender slab structure. The column and middle strips occur in orthogonal directions. It is important to allocate the reduced property stiffnesses in each direction, thus the finite element software is required to incorporate orthogonal and isotropic properties for a model.

A more accurate approach would be repeat Steps 3 and 4 and perform an iterative process to obtain the best possible approximation of the cracked modulus of elasticity. In such a way the moment distribution for the column and middle strips would change, as the stiffness converges. However, this was not done. It was thought the model would become too impractical and time-consuming contradicting the purpose for which the model was suggested. The model is proposed to present an alternative finite element model by which to approximate the nonlinear behaviour of reinforced concrete structure. This model should be simple to apply to allow designers in practice the opportunity to apply in practice.

The results from the approximate finite element model are compared with experimental slab specimens in Chapter 5. The experimental slabs have equal length spans and a symmetrical reinforcement layout. It is therefore proposed that the model is only valid for regular slabs, being tested only for such slabs in Chapter 5.

4.6 CONCLUDING SUMMARY

A composite layered element was introduced to model the reinforced concrete material used to flat slab structures. The introduction of this element into the software framework may be problematic

since the time-dependent effects are not incorporated realistically. The issue of cracking, tension stiffening and creep, requires accurate definitions of the element behaviour and material properties. Due to uncertainty and incompatibility of nonlinear material behaviour of the element within the chosen finite element software, a simpler approximate model was formulated. The approximate model focuses on modelling the global behaviour of the flat slab structure and not the localised material behaviour and respective influences.

The simple model is presented in a step-by-step process using a model compiled with uniform shell and beam elements, thus the model may be analysed with a linear elastic analysis. The effects of the time-dependent influences are incorporated using a material property modification of the shell elements. By modifying the material properties of the shells numerically, where the modified values include the effect of time, the predicted deflections can be calculated more realistic specific to that point in time. The effectiveness of the alternative finite element model to predict the deflections for a flat slab structure is evaluated in Chapter 5.